Seismic Intensities of Earthquakes of Conterminous United States—Their Prediction and Interpretation

GEOLOGICAL SURVEY PROFESSIONAL PAPER 1223

Seismic Intensities of Earthquakes of Conterminous United States—Their Prediction and Interpretation

By J. F. EVERNDEN, W. M. KOHLER, *and* G. D. CLOW

GEOLOGICAL SURVEY PROFESSIONAL PAPER 1223

Description of a model for computing intensity patterns for earthquakes. Demonstration and explanation of systematic variations of attenuation and earthquake parameters throughout the conterminous United States

UNITED STATES GOVERNMENT PRINTING OFFICE, WASHINGTON:1981

UNITED STATES DEPARTMENT OF THE INTERIOR

JAMES G. WATT, *Secretary*

GEOLOGICAL SURVEY

Doyle G. Frederick, *Acting Director*

Library of Congress catalog-card No. 81-600089

For sale by the Superintendent of Documents, U.S. Government Printing Office
Washington, D.C. 20402

CONTENTS

ILLUSTRATIONS

[Plates are in pocket]

TABLES

SEISMIC INTENSITIES OF EARTHQUAKES OF CONTERMINOUS UNITED STATES— THEIR PREDICTION AND INTERPRETATION

By J. F. EVERNDEN, W. M. KOHLER, and G. D. CLOW

ABSTRACT

We elaborate and expand our descriptions of the procedures given in previous papers for calculating intensities of earthquakes of the conterminous United States. We discuss the contrast between Modified Mercalli (M/M) intensities and Rossi-Forel (R/F) intensities and stress the necessity for taking account of this contrast when interpreting intensity data. Two new techniques, one graphical and one statistical and both based on our usual mathematical model, are described and used to analyze several earthquakes. Further examples of the interpretability of observed intensity values in terms of location of fault, fault length and orientation, k value, and depth of focus are presented. In addition, we present a scheme for estimating expected replacement value of damage to wood-frame construction as the result of any hypothesized California earthquake. This scheme is shown to agree with published values of losses from the San Fernando earthquake. It is applied to numerous potential earthquakes in California and provides a means for estimating the approximate relative impact of these several earthquakes.

In a reevaluation of an earlier analysis, the statewide intensity values for the Kern County earthquake of 1952 are more accurately predicted, the predictions in this paper taking account both of variations in attenuation within California and of different definitions of R/F and M/M intensity units. Available intensity data of the Fort Tejon earthquake of 1857 are almost perfectly predicted by the model. Location of the Lompoc earthquake of 1927 was on the Hosgri fault, the intensity data allowing no other conclusion.

By use of published intensity data and seismic moments, we have established the relation between length of break and moment for all attenuation (k) regions of the conterminous United States, determining that there is nearly a thousandfold increase in moment for a given length of break (2L) for earthquakes in regions of k=1 relative to earthquakes that occur in regaions where k=1¾. We also show that energy in the frequency pass-band relative to intensity measurements (approximately 2–4 Hz) is a function only of length of break and not of k value. These two observations, illustrating drastic heterogeneity in stress storage in the vicinity of essentially all earthquakes, are shown to be consistent with a model of earthquakes that is based on the following assumptions: all fault zones are very similar and comparatively weak; high-frequency energy derives from breakage of asperities, while all fault breaks of a given 2L have similar asperity strengths and distribution; low-frequency energy derives from large volume relaxation; and the basic difference between fault zones as a function of k is that the weak fault zone is surrounded by a more and more rigid crust as k value decreases. The theory of weak inclusions as developed by Eshelby serves as the basis of this quantitative explanation.

Estimates of replacement value for wood-frame construction (and for total construction by scaling from the San Fernando earthquake) indicate that the potential California earthquakes that would cause the greatest losses due to shaking are repeats of San Francisco 1906 and Hayward 1836. These earthquakes would cause losses nearly three and two times greater, respectively, than the expected loss from a repeat of Fort Tejon 1857. The total loss or replacement value for damage to buildings from a repeat of the Fort Tejon earthquake of 1857 was calculated by means of our simple model to be $1.2 billion (1977 dollars and prices). Only about half of this loss or replacement value is related to wood-frame construction. Earthquakes causing losses one half as great as those for a repeat of Fort Tejon 1857 are a repeat of Long Beach 1933 and a 20-km break on the Whittier fault. The hypothetical 31-km break on the Malibu Coast fault and the 32-km break on the Santa Monica fault are calculated to cause losses amounting to 60 percent and 190 percent, respectively, of losses caused by a repeat of Fort Tejon.

INTRODUCTION

Two recent papers (Evernden and others, 1973, and Evernden, 1975) presented a procedure for estimating Rossi-Forel intensity patterns for earthquakes throughout the conterminous United States. Evernden (1975) showed that the major factor controlling intensity patterns was the regional attenuation factor, k, which is a measure of crust/mantle attenuation properties; somewhat surprisingly, this factor correlates with maximum length of permissible fault break. Depth of focus is of secondary importance but does play a role in determining peak intensities in the epicentral region.

This report describes and illustrates a computer program for predicting intensities of any hypothetical earthquake at any hypothetical location in the conterminous United States. The program takes account of changes in k value in the calculation of intensities for earthquakes in regions of k equal to 1½ or less. Two new techniques, one graphical and one statistical and both based on our usual mathematical model, are described and used in analysis of several earthquakes. In addition, further examples of the interpretive power of the program in conjunction with observed isoseismal patterns are presented. Several examples of prediction are given, including detailed predictions for a repeat of the 1857 Fort Tejon and 1933 Long Beach earthquakes. Finally, a scheme for calculating expected dollar loss

from any earthquake is described, along with its application to numerous potential earthquakes in California.

ROSSI-FOREL INTENSITIES VERSUS MODIFIED MERCALLI INTENSITIES

In 1931, the U.S. Coast and Geodetic Survey (USCGS) changed from Rossi-Forel (R/F) intensities to Modified Mercalli (M/M) intensities in their annual reports of intensity data of United States earthquakes (see section entitled "Details of Rossi-Forel and Modified Mercalli Intensity Scales"). From our point of view, this change was an unfortunate one for two reasons. First, it confused the literature. The two scales are distinctly different, but there is a tendency to ignore their significant differences and to treat all intensity maps as being on the same scale. Second, the R/F intensity units scale better with physical measurements and agree with nearly all other scales in their stepwise structure, but the M/M units do neither. Evernden, Hibbard, and Schneider (1973) pointed out that intensity predictions based on a model supposing a doubling of peak acceleration for a unit increase of intensity (ignoring high-frequency g values at short epicentral distances) correlated better with R/F intensities than with M/M intensities. In addition, Medvedev (1961) showed that intensity values defined by twofold steps in peak response of a pendulum instrument designed for accentuating periods near 4 Hz (the range of periods of relevance in normal intensity observations) achieved excellent agreement with R/F intensities (as well as with numerous other intensity scales) but clearly disagreed with M/M values. We believe that a return to the R/F scale would be very desirable. R/F intensity X should be converted to a shaking intensity and followed by intensity values of XI and XII representing ground failure. What we most certainly do not need is a new intensity scale, a step that would create additional confusion in the U.S. literature and in reading of the U.S. literature by others.

Continual introduction of more restrictive building codes for wood-frame structures in California will require redefinition of intensity zones. When homes could be thrown off their foundations, intensity R/F IX–X could be reported; if all wood-frame homes are bolted or strapped to their foundations, intensity IX may disappear. Recent years have seen the introduction of building styles that, though meeting codes, are poor earthquake risks. Further proliferation of such styles may create a sufficient number of seismically vulnerable areas for high intensities to continue to be reported in California.

Figure 10 (Long Beach earthquake) and figure 15 (Kern County earthquake) and the table on page 26 (Seattle earthquake) illustrate the impact on intensity maps caused by the change from R/F to M/M intensities. Because the scales are equal at X (shaking intensity) and nearly one intensity unit different at R/F VIII (Neumann, 1931 and later volumes of "United States Earthquakes"), nearly 2.5 M/M intensities are included within 1.5 R/F units, and M/M IX is virtually eliminated as an observed quantity (R/F 9.5 is seldom reached). The absence of intensity IX values for Long Beach, Kern County, and Seattle earthquakes was noted in all reports for these earthquakes but with no recognition that the reason was the change in reporting units, not something to do with the earthquakes.

Given that, in a study such as this, one must convert M/M values to R/F or vice versa, the literature allows two or three schemes:

(1) Follow Medvedev (1961) and assume IV, V, and VI are identical for R/F and M/M. Since 2L (the length of fault break) values are generally set by sizes of V, VI, and VII boundaries, such a scheme would predict the same 2L values for M/M and R/F. However, trouble in predicting higher intensities might well appear because Medvedev places M/M VII, VIII, and IX as equivalent to R/F VII and VIII. Also, Medvedev's presentation of the comparison of these scales differs significantly from that resulting from reading of the scales and from that given by Neumann (1931). Medvedev (1968) uses an RF/MM relation quite similar to that suggested in (3) below.

(2) Interpret symbolism such as IV–V in Neumann (1931) as meaning IV ½. Then, M/M, IV, V, VI, VII, VIII, IX, and X are equivalent to R/F IV ½, V ½, VI ½, VII ¾, VIII ¾, IX ½, and X, respectively. With this scheme, and setting 2L by V, VI, and VII boundaries, 2L values are greater for the same radii of M/M V, VI, and VII than of R/F V, VI, and VII. The Kern County earthquake was analyzed in this manner. Treatment of the published isoseismal values of this earthquake as R/F leads to a predicted 2L of about 30 km, whereas proper use of the M/M values leads to a predicted 2L of about 60 km. See discussion below of Kern County earthquake.

(3) Assume that the scaling law between M/M and R/F values is a continuous function and use the following table of relative values in a scheme of linear interpolation:

R/F	1	3	5	7.75	8.75	9.5	10
R/F–M/M	0	0	0.5	0.75	0.75	0.5	0

This scheme will lead to nearly the same answers for 2L as (2) and assumes a smooth rather than stepwise relation of R/F values and M/M values. We have implemented this scheme as an option in our program, and examples of its use are given below (Long Beach, Bryson, and Seattle earthquakes).

PRESENTLY AVAILABLE MODELS FOR PREDICTING SEISMIC INTENSITIES

CALIFORNIA

The program described in Evernden (1975) for predicting intensities of California earthquakes has not been extended, other than to add the capability to predict M/M intensities. (See section entitled "Mathematical Details of Model for Predicting Intensities.") For an earthquake near the boundary between k regions of 1¾ and 1½, a special, as yet unprogrammed, type of calculation must be made. See the reanalysis given below of the Kern County earthquake (July 21, 1952) for an example of such a study. In the analysis of the Fort Tejon earthquake (January 9, 1857), this problem was avoided by using only the intensity data obtained in the region of k equal to 1¾.

A major addition to calculational capability has resulted from digitization on a ½-minute by ½-minute grid of the geologic map of California for all of western and nearly all of central California (fig. 1). The data used were the sheets of the Geologic Map of California (Olaf P. Jenkins edition) published at the scale of 1:250,000. All geologic rock units indicated on those maps were grouped into 10 seismic response units (table 1). For purposes of predicting expected intensity values, these 10 groups were assigned relative R/F intensity values (table 2) on the basis of experience in the San Francisco Bay area, using procedures originally developed by Borcherdt (1970).

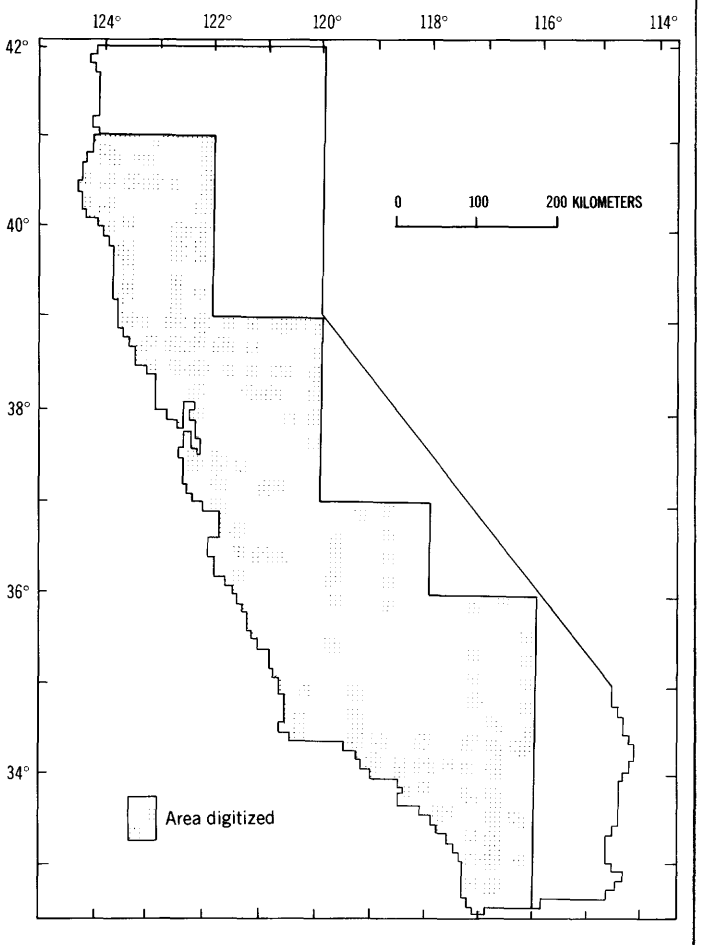

FIGURE 1.—Area of California for which geology has been digitized on a ½-minute by ½-minute grid.

TABLE 1.—*Correlation of geologic and ground-condition data units in California*

[½-minute by ½-minute grid. Source: State Geologic Maps, scale 1:250,000]

Geologic map units	Ground-condition unit
Granitic and metamorphic rocks (Kjfv, gr, bi, ub, JT_{RV}, m, mV, PpV, PmV, Cv, Dv, pS, pSv, pCc, pCgr, pC, epC, TI)	A
Paleozoic sedimentary rocks (Ms, PP, Pm, C, CP, CM, D, S, pSs, O, E)	B
Early Mesozoic sedimentary rocks (Jk, Ju, JmE, Tr, Kjf)	C
Cretaceous through Eocene sedimentary rocks (Ec, E, Epc, Ep, K, Ku, KE)	D
Undivided Tertiary sedimentary rocks (QTc, Tc, TE, Tm)	E
Oligocene through middle Pliocene sedimentary rocks (PmEc, PmE, Mc, Muc, Mu, Mmc, Mm, ME, Φe, Φ)	F
"Plio-Pleistocene" sedimentary rocks (Qc, OP, Pc, Puc, Pu)	G
Tertiary volcanic rocks (Pv, Mv, Olv, Ev, QTv, Tv)	H
Quaternary volcanic rocks (Qrv, Qpv)	I
Quaternary sedimentary deposits (Qs, QaE, Qsc, Qf, Qb, Qst, QE, Qq, Qt, Qm)	J

TABLE 2.—*Correlation of ground-condition units of California and assigned relative intensity values*

½-minute by ½-minute grid	
Ground-condition unit	Relative intensity
A	−3.0
B	−2.6
C	−2.2
D	−1.8
E	−1.7
F	−1.5
G	−1.0
H	−2.7
I	−2.7
J	0.

6-minute by 6-minute grid	
Ground-condition unit	Relative grid
A. Granite	−2.50
B. Coast Ranges	−1.75
C. Coastal marine sedimentary rocks	−0.80
D. Alluvium	0.

The most critical point to note relative to predictions given later is that all alluvial terrains (J of table 1) are treated in all predictions as being thick and saturated with water to zero depth. This assumption is certainly untrue in many cases, particularly today. For older earthquakes, the condition of full saturation was probably true in nearly all alluviated valleys and areas such as the Los Angeles basin, so comparison of observations and prediction for these events should be made on the basis of full saturation. Where the water table has been lowered by about 10 m, there is a drop of at least one intensity unit relative to that occurring when the water table is at the surface (Medvedev, 1962). Therefore, any use of the maps of this report for prediction of expected intensities and damage estimation should allow for this factor. One should ascertain actual depth to water table at all sites of concern, then lower the intensity values for alluvium shown on the figure by one unit if the water table is at a depth of 10 m and 1½ units if the water table is at a depth of 30 m or more. Also, corrections for type and thickness of alluvium should be made. Work is progressing on this important aspect of predicting intensities.

For studies concerned with predictions on a statewide or regional basis, the 6-minute by 6-minute grid described in Evernden (1975) was used (table 2).

CONTERMINOUS UNITED STATES

Since rates of decrease of intensity are so low in many areas of the United States (Evernden, 1975), the capability to predict intensities across changes in k values is a necessary aspect of a generally applicable program. This capability has been introduced into the program, there being now the capability to predict across multiple k boundaries. The logic used depends upon the fault break appearing as essentially a point source at adequate distance of the k boundary from the center of the break; this condition is fulfilled at four times the fault length or greater. Because potential fault lengths are 60–80 km in regions where k = 1½, about 20 km in regions where k = 1¼, and 5 km or less in regions of k = 1, this distance requirement is easily met in nearly all situations of interest in these regions. In regions where k = 1¾ or where the earthquake is too near the k boundary to be treated as a point source, an as yet unprogrammed technique is followed (see discussion of the Kern County earthquake of July 21, 1952).

Plate 2 indicates the pattern of k values now incorporated in the program, the figure actually giving 4k values. Stepwise changes in k values are almost certainly erroneous, but no more sophisticated model seems warranted at this time.

A few additional comments on this plate are appropriate. Milne and Davenport (1969) studied attenuation rates of intensity and acceleration in eastern Canada and Northeast United States, using data of the 1925 St. Lawrence, 1929 Grand Banks, 1935 Timiskaming, 1939 St. Lawrence, and 1944 Cornwall-Massena earthquakes. They found a k value of very nearly 1.0 as appropriate for this general region, a value in agreement with that used by us.

The map shows a region of 4k = 5 intruding along the St. Lawrence River into the great area of 4k = 4 that includes most of the Eastern United States. This region of 4k = 5 is established on the basis of analysis of several earthquakes (Evernden, 1975). Peter Basham of the Dominion Observatory, Ottawa, Canada has indicated (oral commun., 1978) that analyses conducted by the group at Dominion Observatory confirm the existence of this zone. They have analyzed data of some small events along the St. Lawrence River and have established the boundary between the zone of 4k = 4 north of the St. Lawrence and the zone of 4k = 5 along the St. Lawrence. Thus, nearly all major seismic activity in the eastern part of the continent can be related to the region of 4k = 5. All activity along the St. Lawrence and the Cape Ann and Charleston earthquakes are certainly in such regions, and the possibility exists that the New Madrid earthquake was also in such a region (Evernden, 1975). The detailed placement of 4k boundaries on figure 2 has a degree of uncertainty about it. Along and east of the Mississippi embayment, the 4/5 boundary is placed along the inland limit of Tertiary subsidence. Westward, the location of the zone of 4k = 5 between zones of 4 and 6 is pure conjecture, and its extent northward into Canada is even less certain.

The Geological Map of the United States published in the National Atlas of the United States of America (p. 74 and 75) was used for the complementary geologic base. Digitization was on a 25-km by 25-km grid. Table 3 indicates the seismic units that correspond to the geologic units of the geologic map, plate 2 shows the United States mapped in terms of these seismic units, and table 4 gives tentative relative intensity values for these units.

In the study of an earthquake, three maps are printed routinely. The first map presents the ground-condition data in terms of seismic response units. The second map indicates predicted R/F or M/M intensities on saturated alluvium. For earthquakes in California and using the ½-minute by ½-minute grid, either a contoured or digitized version of this map can be presented. The third map presents predicted R/F or M/M intensities in accordance with the ground-condition data of the first map. The third map is always printed

in digitized form. A variety of map formats can be produced, several of which are illustrated in following figures.

It is important to remember that the depth sensitivity of the intensity values is controlled by a factor C (Evernden, 1975), which is an unknown function of depth and, therefore, does not have a value equal to depth. For earthquakes of normal depth in western California, the C value that yields intensity values in best agreement with observations is 25. In general, it appears that C is about equal to depth of focus plus 15 to 20.

Through no basically new modes of calculating event parameters from intensity data have been designed, we have developed two new techniques for making such calculations. The first technique was stimulated by Hanks' use of A_{VI} (area within intensity VI contour on published intensity maps) values (Hanks and others 1975). When we tried to use such A_{VI} values for estimating event parameters, we found that they commonly yielded invalid estimates of 2L and values of 2L in disagreement with estimates based on use of all intensity data. The errors were greatest for small values of A_{VI} (less than 10^{14} cm^2). Therefore, we designed a technique that tried to avoid the problem of small A_{VI} values, used all intensity contours, and was useful with published intensity maps.

We do not use intensity areas from these maps. Rather, we use the maximum distance of each contour from the epicenter (for long faults, we use maximum distances both perpendicular and parallel to the fault). The logic behind this procedure is the recognition that ground condition can seriously perturb contour values, particularly for small-area contours. We assume that the maximum dimension of any intensity contour i (R_i) is the best estimate we can make from the contours of the maximum distance that any given intensity was felt on saturated ground. In estimating 2L, we also use the reported local magnitude (M_L) and the maximum recorded intensity (I(MX), corrected for ground condition if necessary). We interpret the "Limit of Detection" (L.O.D.) contour as intensity 3.0 if there is an intensity IV contour and as intensity 3.0–3.5 if there is no intensity IV contour. This usage of the L.O.D. contour derives from analysis of numerous intensity maps.

These several values for each earthquake [R_i values, I(MX), and (M_L)] are plotted on a figure for the appropriate k value. See figure 2 as an example of such an analysis. We then make a somewhat subjective interpretation of the data (that is, ignoring high-intensity radius if it disagrees badly with other data), selecting the 2L value that seems to give the best fit to all data. The 2L estimate obtained in this simple manner has always been within a factor of two of that obtained by detailed station-by-station analysis. When the R_i, I(MX), and M_L values yield a consistent estimate of 2L, the agreement with detailed analysis is improved.

Because of the satisfactory agreement between the detailed calculations and those by the technique just described, all analysis of earthquakes of the Eastern United States will be by the latter technique.

The second new technique of analysis was developed to satisfy requests that we generate a statistical approach to analysis of intensity data. The approach we have followed is to use observed station values of intensity as the input data (corrected for ground condition) and to calculate fault centers, fault lengths, and fault orientations that minimize several fitting criteria, all calculations of intensity being as in our regular calculations.

The observational data are treated singly in some criteria and are grouped into bandwidths of observed intensity value in other criteria. When all data are considered in a criterion, either all points are treated separately or bandwidth values are weighted according to the inverse of the bandwidth. Thus, for the Lompoc

TABLE 3.—*Correlation of geologic and ground-condition units, conterminous United States*

[Source: National Atlas of the United States]

Units of geologic map	Ground-condition unit
Sedimentary rocks	
Quaternary	A
Upper Tertiary	B
Lower Tertiary	C
Cretaceous	D
Jurassic and Triassic	E
Upper Paleozoic	F
Middle Paleozoic	G
Lower Paleozoic	H
Younger Precambrian	I
Older Precambrian	J
Volcanic rocks	
Quaternary and Tertiary volcanic rocks	K
Intrusive rocks	
All ages	L

TABLE 4.—*Correlation of ground-condition units and assigned relative intensity values, conterminous United States*

Ground-Condition unit	Relative intensity
A	0
B	−1.00
C	−1.50
D	−2.00
E	−2.25
F	−2.50
G	−2.75
H	−2.75
I	−2.75
J	−3.00
K	−3.00
L	−3.00

earthquake, Byerly (1930) reported intensity values as IX, VIII, VI–VII, and IV–V, that is, bandwidths of 1, 1, 2, and 2.

The several criteria we have investigated are:

(a) H − L, called (H − L) in tables;

(b) $\Sigma_I |H - L|_I$, called $|H - L|$ in tables;

(c) $1/n\Sigma_i$ (Obs − Calc)$_i$, called (O − C) in tables;

(d) $1/n\Sigma_i |\text{Obs} - \text{Calc}|_i$, called $|O - C|$ in tables;

(e) $1/n\Sigma_i$ (Obs − Calc)$_i^2$, called R.M.S. in tables;

(f) On plot of (Obs − Calc)$_i$ versus Obs$_i$, calculate absolute value of area between line Obs − Calc = O, regression line (Obs − Calc)$_i$ = a+b(Obs)$_i$, and lines Obs = 3.5 and Obs = 9.5. The actual parameter used is width of the rectangle of equivalent area and length on the Obs − axis. This parameter is called CP in the tables. This criterion seeks a minimum of residuals against a prescribed and reasonable pattern of residuals rather than merely seeking the conventional minimum of (e). Also, it allows estimates of probability of nonminimum values. Criteria (e) and (f) should yield nearly the same estimate of event parameters.

In the above formulae,

H = number of stations having calculated intensities greater than band of observed value,

L = number of stations having calculated intensities less than band of observed value,

I = band value,

Obs$_i$ = observed intensity at station i, all Obs values having the central value of each band,

Calc$_i$ = calculated intensity at station i.

n = number of observing stations.

These quantities are calculated for a network of potentially possible sets of source parameters. The calculations begin with a defined fault line (straight or curved), either as observed (Hosgri fault for Lompoc earthquake, Newport-Inglewood fault for Long Beach earthquake) or as assumed (extension of Hosgri fault south of Point Sal). The coordinates S (slip) and T (translation) are measured parallel and perpendicular to the great circle best fitting the fault trace. We select a reference center of break on the basis of an initial analysis of the intensity data. We then select a pattern of S, T, and 2L values as test solutions. If deemed appropriate, we vary the C value (depth parameter), k value, and orientation of the modeled fault (rotate an angle Φ counter-clockwise through assumed center of fault after slip and translation).

With observed data well distributed in all quadrants and at all distances around an epicenter and with accurate corrections for ground condition, the several criteria should yield minima with nearly the same event parameters. If data are too limited at short ranges, the CP criterion can fail when using four-quadrant data. When observations well distributed in distance are limited to about a 120° quadrant including axis of fault and its perpendicular, the CP criterion will yield an excellent minimum, especially when combined with independent geologic data, and will be very sensitive to the best k value. We reserve further discussion of this mode of analysis until we discuss the several quakes analyzed by this technique.

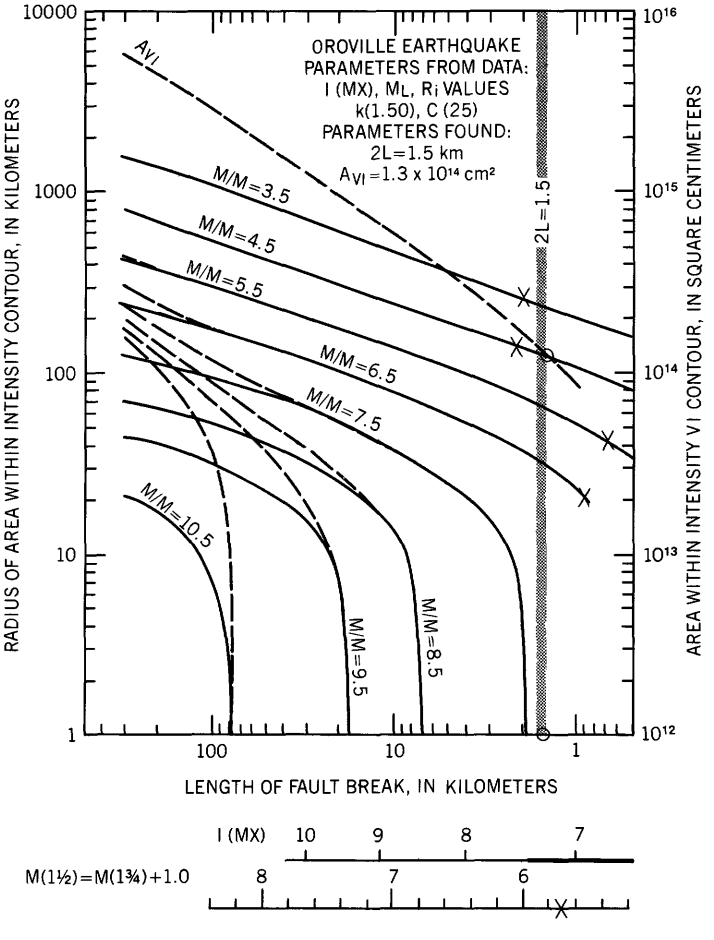

FIGURE 2.—Analysis of intensity data of Oroville, Calif., earthquake August 1, 1975.

EXAMPLES OF OBSERVED VERSUS PREDICTED INTENSITIES

SANTA BARBARA EARTHQUAKE OF JUNE 29, 1925 (ROSSI-FOREL INTENSITIES; BYERLY, 1925)

Known parameters:

(1) k = 1¾ (epicenter in western California)

(2) C = 25 (normal depth for California earthquakes)

(3) Location of faulting (defined by observed intensities)

Unknown parameter:

(4) 2L

Location of the fault break and its length are constrained by the observed intensities. In a region where k = 1¾, intensity values of IX or greater extend only a comparatively few kilometers laterally from the fault break, particularly when fault breaks are in the range of 30 km. Therefore, the pattern of published isoseismals (fig. 3) requires a break length of 30–40 km and a location of the break near or just onshore.

Fault lengths of both 30 km and 40 km were investigated; figure 3 illustrates predicted intensities for 2L = 40 km. The observed and reported intensity values are in good agreement, and the reported values are assumed to be relevant to saturated alluvium because nearly all reporting localities were on alluvium. The detailed shape of the intensity VIII contour from Byerly (1925) is quite certainly the result of trying to include within one contour line all VIII observations, even though these are distributed on both sides of the Santa Ynez Mountains. The solid or predicted intensity lines on figure 3 are based on saturated alluvium and do not indicate geologic factors. If these are taken into account, the predicted shape of the intensity 8 contour, if the presence of the Santa Ynez Mountains is ignored, is as reported by Byerly (fig. 4). Figure 5 indicates the detailed pattern of predicted intensities when using a ½-minute by ½-minute geologic grid.

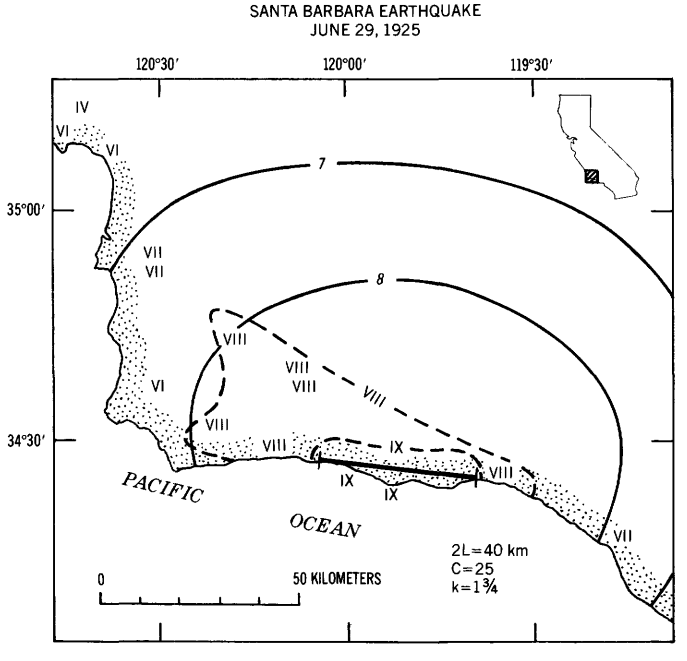

FIGURE 3.—Reported and predicted R/F intensity values for Santa Barbara earthquake, June 29, 1925 (2L = 40, C = 25, k = 1¾). Reported values are in Roman numerals.

Byerly (1925) acquired intensity data only along or near the present route of Highway 101, that is, along or near the road extending from Ventura through Santa Barbara to Santa Maria and San Luis Obispo. Thus, no observations were collected for the entire northeast quadrant. The absence of values in this area does not indicate low intensities but lack of data.

Note on figure 3 that the predicted area of intensity VI reaches only as far to the northwest as was observed. Shortening of the fault by a factor of 2 (to 2L = 20) would yield predicted intensities that are too low for stations north of the mountains. A comparison of predicted versus observed intensities versus length of 2L is given in table 5.

Even for 2L = 40, predicted values may be slightly too low. Attempts to estimate 2L by size of the reported IX area are complicated by the fact that there may not have been reports at the full range of actual IX-level shaking. The reported length of the IX area is 42 km, but a 2L of 40 km predicts a IX-length of 74 km and a 2L of 30 km predicts a IX-length of 55 km. These values would suggest a 2L of 20 or less, which would markedly disagree with the data of table 5. The seemingly most reasonable conclusion is that the length of the IX region for saturated alluvium is not expressed by Byerly's (1925) contouring and that the individual station reports at greater distances provide the best basis for estimating the fault length (2L). Thus, we conclude that a 2L of 30 to 40 km is in near agreement with observations, and an estimate of 2L = 40 is favored.

MONTEREY BAY EARTHQUAKE OF OCTOBER 22, 1926 (ROSSI-FOREL INTENSITIES; MITCHELL, 1928)

Known parameters:

(1) k = 1¾ (western California)

(2) C = 25 (normal depth)

(3) Location of fault break (aftershocks-main epicenter)

(4) 2L = 20–40 (maximum length of 40 by aftershocks)

The parameters of this earthquake can be set quite well without recourse to intensity data. However, an apparent discrepancy between 2L values based on aftershocks and on intensity values can be shown. The epicenter of the main shock is well controlled and is just offshore from Monterey. Aftershock locations, based on S-P times at Berkeley, were placed as far north as the coastline west of Santa Cruz (Mitchell, 1928)/(fig. 6). If the aftershock zone is deemed a measure of length of faulting at time of the main earthquake, a 2L of 44 km results. For comparison, we calculated predicted intensity values for 2L values of 22 and 44 km, both fault breaks extending northward from the epicenter of the main event (see table 6 and fig. 7). Table 6 presents observed and predicted R/F intensities for 2L values of 22 and 44 at various sites. The stations are arranged by increasing latitude, and the two modeled fault breaks are indicated in proper latitudinal relation to the stations.

TABLE 5.—*Observed and predicted intensities, Santa Barbara earthquake*

Site	Observed intensity	Predicted intensity[1]	
		2L = 40 km	2L = 30 km
San Luis Obispo	IV	4(6)	4(5–6)
Pismo	VI	5(6)	5(5)
Arroyo Grande	VII	6(6)	6(6)
Nipomo	VII	5–6(6)	5–6(6)
Santa Maria	VII	6–7(7)	6(6–7)
Orcutt	VII	7(7)	6–7(6–7)
Los Alamos	VIII	7(7–8)	6–7(7)
Lompoc	VI	7(7)	6(6)
Los Olivos	VIII	8(8)	8(8)
Gaviota	VIII	7–8(8–9)	7(8)
Goleta	IX	8(9)	8(9)
Ventura	VII	7–8(7–8)	7(7)
Santa Barbara	X	8(9)	8(9)

[1]First number incorporates ground condition as on 6-minute by 6-minute grid. Second number is for saturated alluvium.

Both models show excellent agreement between predicted and observed intensities for stations south of the breaks. For stations at the same latitude or more northerly latitudes, the intensities predicted by a 2L of 44 are clearly too high. Average observed intensity for these 14 stations is 5.2, average predicted intensity for 2L of 22 is 5.6, and average predicted intensity for 2L of 44 is 6.3. Our conclusions are that a fault break of 22 km is an appropriate length to use for modeling the high-frequency source of the main event and that this source was the southern portion of the aftershock zone. One might, of course, suggest use of a 2L of 44 km with the energy density reduced below the normal value (Evernden, 1975). Intensities to the north would still be predicted as too high.

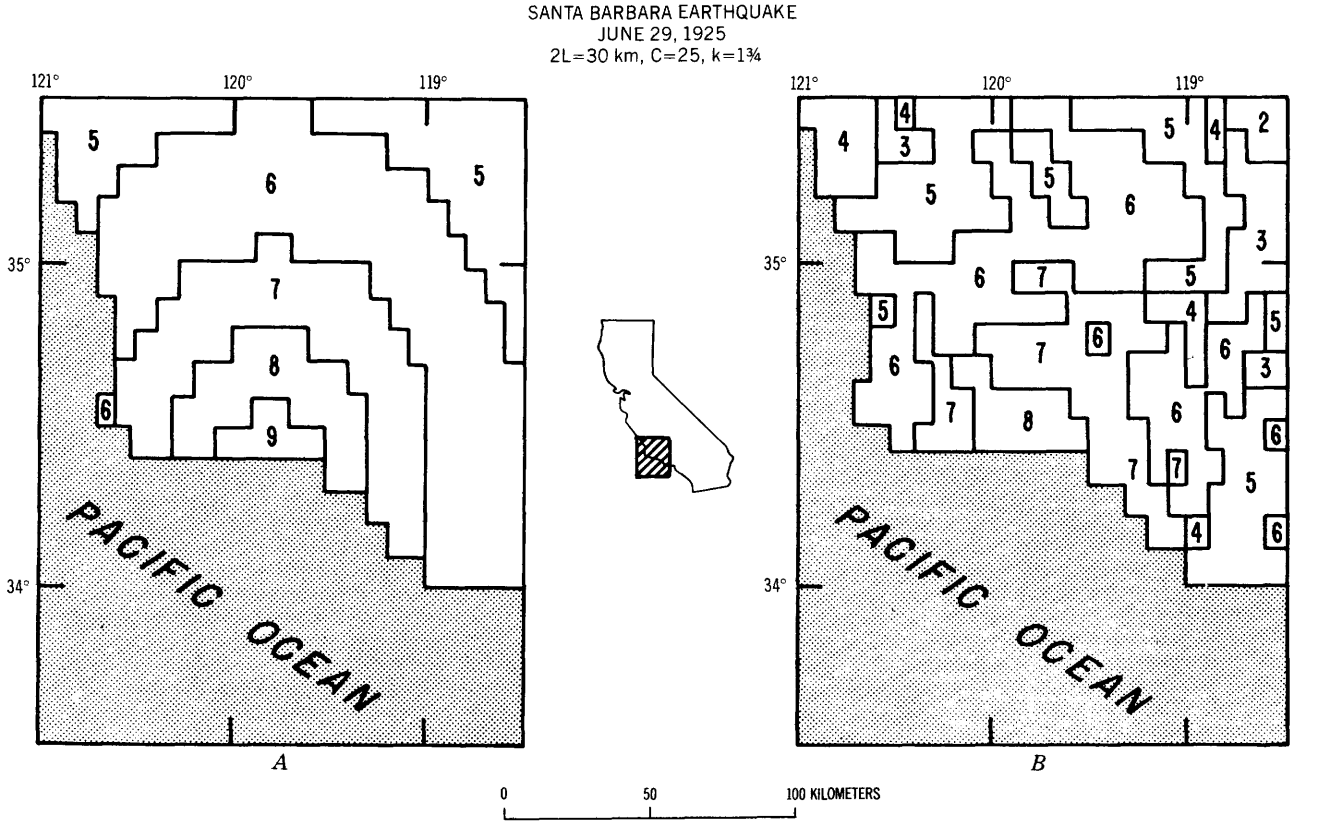

FIGURE 4.—Predicted R/F intensity values, 6-minute by 6-minute grid, Santa Barbara earthquake, June 29, 1925 (2L = 40, C = 25, k = 1¾). *A*, Saturated alluvium. *B*, 6-minute by 6-minute ground-condition units (table 2).

A point of possible significance is the prediction of too-high intensities for San Jose, Morgan Hill, and Palo Alto. In the presently used codification of geologic maps, all Quaternary deposits are treated as of equivalent physical properties and of appreciable depth with the water table at the surface. This is a gross simplification that will lead to prediction of excessively high intensities in regions of thin and (or) unsaturated and

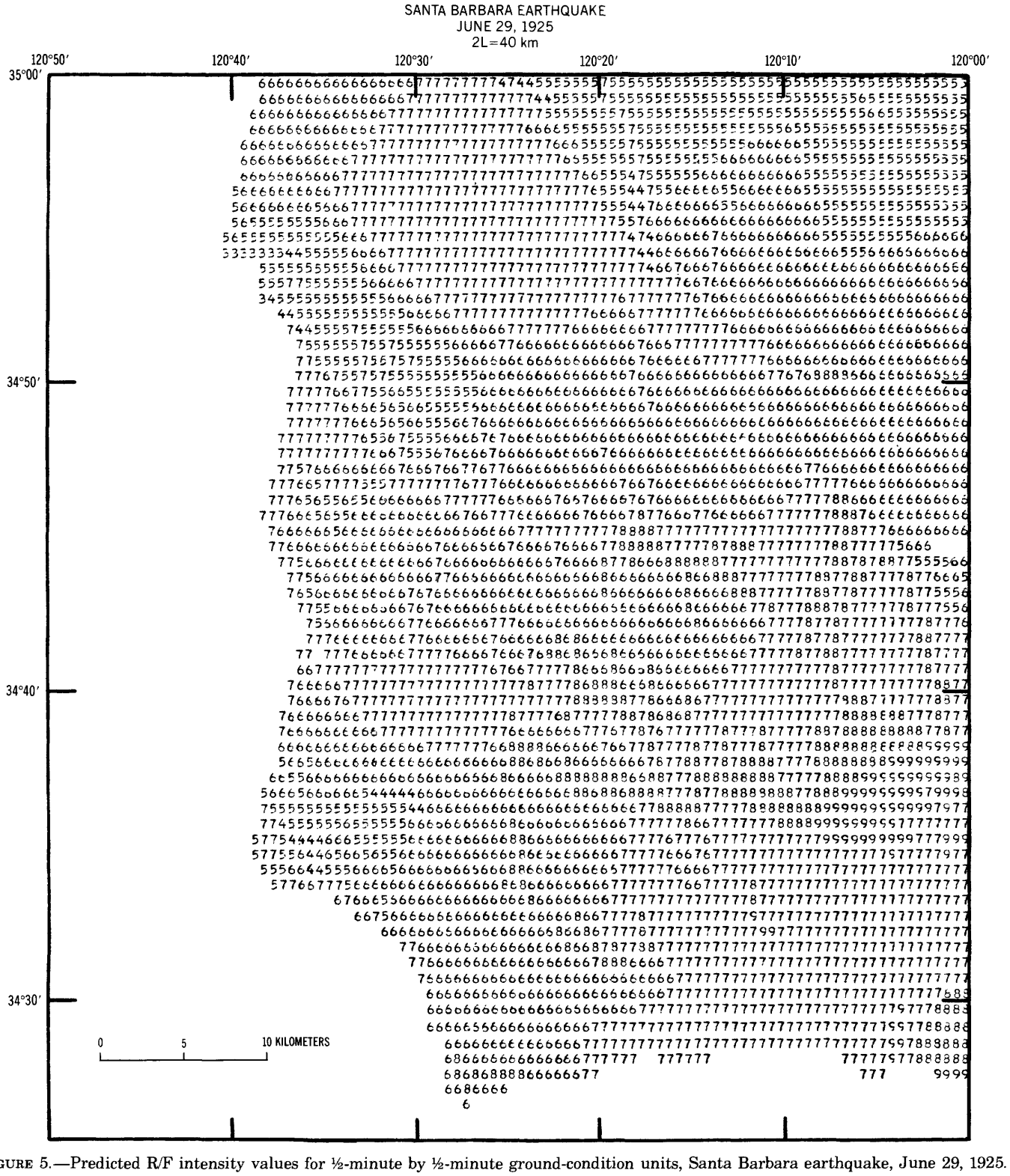

FIGURE 5.—Predicted R/F intensity values for ½-minute by ½-minute ground-condition units, Santa Barbara earthquake, June 29, 1925. Computer plot of south half of Santa Maria sheet of Geologic map of California. 2L = 40.

(or) physically different materials. Thus, for the sand-covered areas of much of western San Francisco, the use of a formulation that assigns all Quaternary materials the same ground condition leads to predicted intensities for the 1906 San Francisco earthquake that are much too high (9+ predicted, 7+ observed). In this case, thin unsaturated sand on bedrock (Franciscan Formation) reacted as essentially bedrock. Without details of local geology, we chose in this paper to predict the worst case while advising everyone of that fact and suggesting more refined work in local areas so that improved estimates of expected intensity values in areas of Quaternary deposits can be made.

Palo Alto circa 1926 was nearly entirely on ground now characterized as Older Bay Mud. It is stronger than Young Bay Mud. In Evernden, Hibbard, and Schneider (1973), the Young Bay Mud (F) was assigned relative intensity of (+½), while Older Bay Mud (E) was assigned a value of (−½).

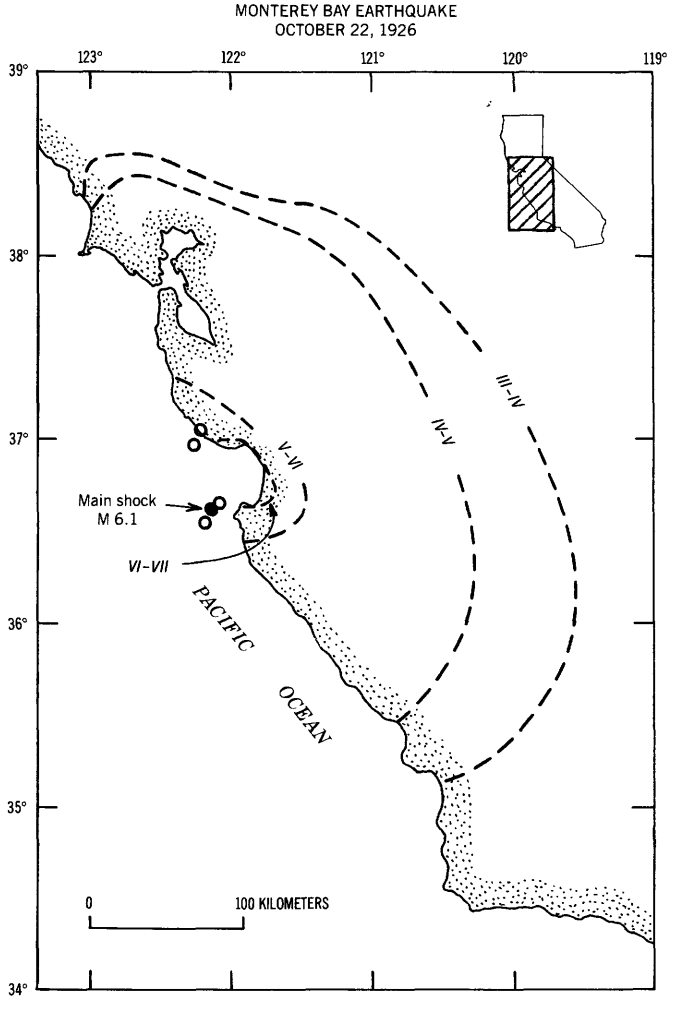

FIGURE 6.—Location of main shock, aftershocks, and isoseismals, Monterey Bay earthquake, October 22, 1926.

Morgan Hill and San Jose are located in the Santa Clara Valley on thick valley alluvium. If the ground were saturated, these areas would be expected to reach nearly the intensity values predicted for our standardized Quaternary (J of table 2). However, by the time of the 1926 earthquake, the water table in the San Jose area had been lowered by several tens of meters. It may be relevant to point out that predicted intensities for San Jose resulting from the San Francisco 1906 earthquake were correct but those for 1926 were too high. The predictions for San Jose and Morgan Hill for the Monterey Bay earthquake are probably too high because the present model fails to incorporate depth to water table in its predictions.

Thus, any predictions for a coming earthquake based on our present modeling of Quaternary deposits should be lowered by at least one intensity unit for parts of the Santa Clara Valley in which the water table has been lowered 10 m or more. One of the most effective ways to protect a community from high intensities (VIII+) might be to lower the water table several tens of meters. Shaking intensities of greater than R/F VII–VIII are probably impossible under such conditions.

SAN JOSE EARTHQUAKE OF JULY 1, 1911 (ROSSI-FOREL INTENSITIES; TEMPLETON, 1911)

Known parameters:

(1) k = 1¾ (western California)
(2) C = 25 (normal depth)
(3) Location (Wood, 1911)
(4) 2L = 5–11 (aftershocks)

TABLE 6.—*Observed and predicted R/F intensity values, Monterey Bay earthquake*

Site	Observed Intensity	Predicted intensity 2L=22	Predicted intensity 2L=44
Santa Maria	III	3–4	4
Lompoc	II–III	3	3
San Luis Obispo	IV	3	3
Paso Robles	IV–V	4	5
King City	V–VI	5–6	6
Carmel	VI	6	6
Monterey	VI+	6–7	6–8
Salinas	VI–VII	7	8
Hollister	IV–V	6	7
Watsonville	V–VI	7	8
Soquel	VI–VII	7	8
Santa Cruz	VII+	7–8	8
Saratoga	V	5	7
San Jose	V	6	7
Morgan Hill	V	6	6
Palo Alto	V	6	7
San Leandro	V	5	5
Berkeley	V	5	6
Walnut Creek	V	4–5	5
Novato	V	5	5
Petaluma	V	4–5	4–5
Santa Rosa	IV	4	5
Martinez-Concord	V/IV–V	5	5
Stockton	IV–V	5	5
Merced	IV	4+	5
San Francisco (downtown)	5		5

This earthquake is of interest because it is one of the very few earthquakes of approximately magnitude 6 that has occurred in central California since 1906. The location of this earthquake is as suggested by Wood (1911). To quote from him (p. 39) "Examination of the map and its explanatory table shows clearly that the circles of origin-distance for a majority of the shocks (and also, in the main, those most reliably determined having Mt. Hamilton at center) intersect the projected course of the Hayward fault at frequent intervals all the way from a point due south of Mt. Hamilton to a point due north of Gilroy, a distance of about 12 km along the course of the fault." Though more recent geologic mapping has led to the interpretation that the region considered by Wood to contain an extension of the Hayward fault actually contains an extension of the Calaveras fault, his basic mode of estimating fault length is still valid because the Calaveras fault in this part of its course lies exactly where Wood considered the Hayward fault to be. We modeled this earthquake

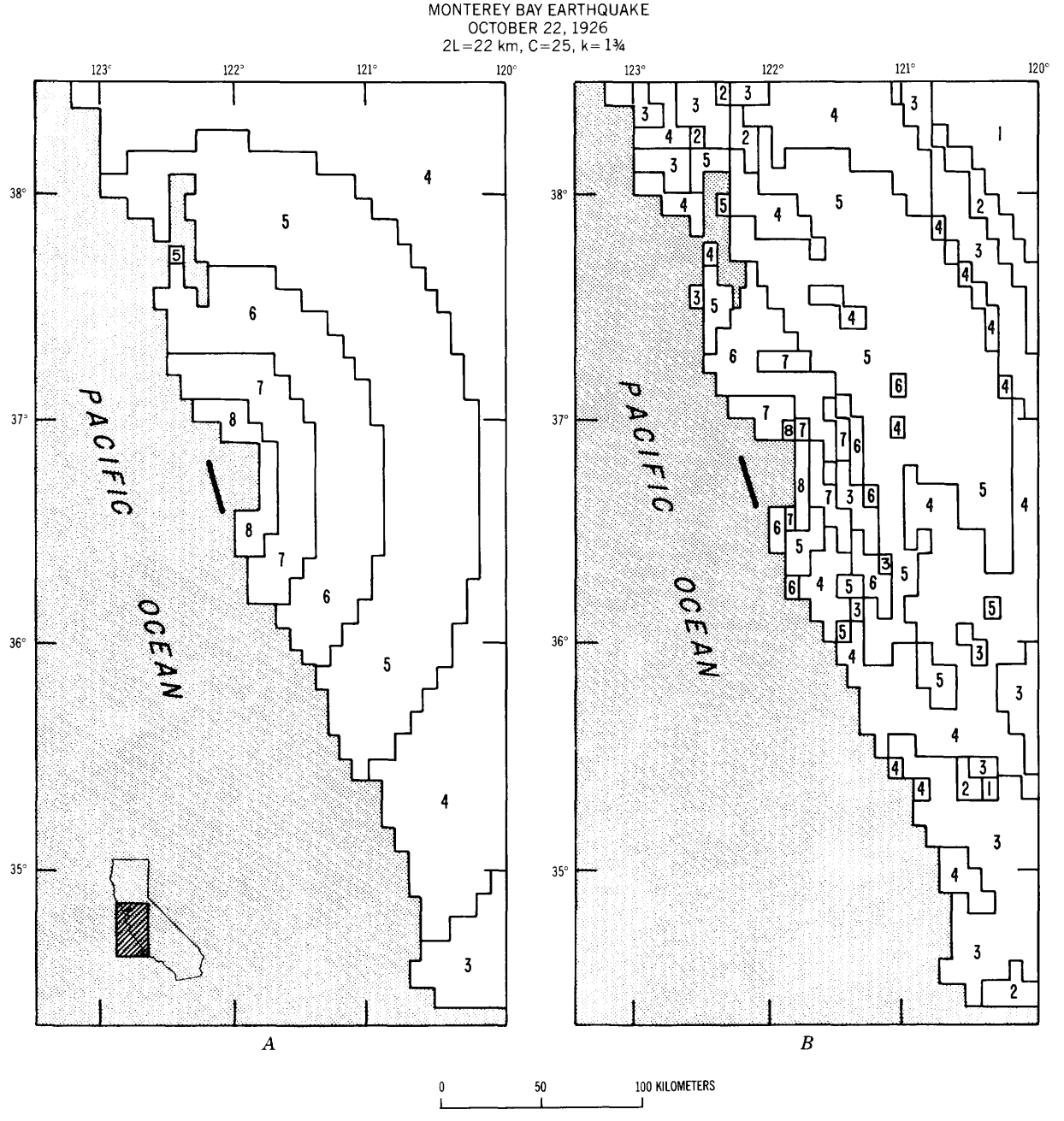

FIGURE 7.—Predicted R/F intensities for Monterey Bay earthquake of October 22, 1926 (2L = 22, C = 25, k = 1¾). *A*, Saturated alluvium. *B*, 6-minute by 6-minute ground condition.

using two different values of 2L, a value of 11 to agree with the aftershock zone, and a value of 5½ as half of that zone; we chose to use the south half of the aftershock zone. Table 7 gives a comparison of observed and predicted intensity values for 2L values of 11 and 5½. The major unexplainable discrepancy between reported and predicted values is the area of San Francisco, for which Templeton gives a value of VI–VII; the model predicts only V on saturated alluvium. The reported San Francisco intensity is inconsistent with the entire pattern of other observed values. In order for intensity VII to be predicted at San Francisco, this earthquake would have required a 2L of 75, a totally inadmissable value in view of the absence of surface breakage and of the inconsistency of such a length with all other intensity data. In addition, McAdie (1911) reported "There was * * * no damage of any consequence in San Francisco." "Few objects were overturned * * *". The VI-VII value assigned by Templeton must be in error.

Gilroy, Watsonville, and Santa Cruz are all predicted to have experienced higher intensities than reported, the predicted intensities (table 7) having been derived from the assumption that these communities are situated on saturated alluvium. The explanation for these too-high predictions may be that the appropriate ground condition for these sites is less sensitive than saturated alluvium.

Both San Jose and Morgan Hill experienced intensities as predicted for saturated alluvium, in contrast to the prediction for the Monterey Bay earthquake, thus supporting the conjecture made earlier about the effect of lowering of the water table in the Santa Clara Valley between 1906 and 1926.

The observed data appear to agree better with a 2L of 5½ than with one of 11, and averaging of observed and predicted values would suggest a 2L nearer 5½ than 11.

TABLE 7.—*Observed and predicted R/F intensities, San Jose earthquake*

Site	Observed intensity	Predicted intensity	
		2L=5½	2L=11
Modesto	4	5	6
Sacramento	4	4	4
Santa Rosa	4	3–4	4
Monterey	4	3–5	3–5
Berkeley	5	5	5
Hayward	5	5	5–6
Stockton	5	5	5
Watsonville	5	[1]6–7(Al)	7(Al)
Santa Cruz	6	6–7(Al)	7–8(Al)
Belmont	5	5	6
Pleasanton	5–6	5	5
Livermore	5	5	5–6
Oakland	6	5	5–6
Redwood City	6	5	6
Palo Alto	6	6	6
Calaveras Valley	6	6	6
San Martin	6	6	7
Gilroy	6	7–8(Al)	8
Boulder Creek	6	5–6	6
Pescadero	6–7	5	6
San Francisco	6–7	5(Al)	5(Al)
Morgan Hill	7	7	8
Los Gatos	7	7	7
Saratoga	7	6–7	7
Santa Clara	7	6–7	7
San Jose	7	7	7
Coyote	8+	8	8

[1](Al) signifies that predicted intensity values entered in table are based on saturated alluvium. Discussion of the discrepancies between observation and prediction for these stations is included in the text.

FORT TEJON EARTHQUAKE OF JANUARY 9, 1857 (MODIFIED MERCALLI INTENSITIES; AGNEW AND SIEH, 1978)

Known parameters:

(1) k = 1¾ (region of concern south and west of San Andreas fault)
(2) C = 25 (normal depth)
(3) Location of faulting (San Andreas fault)
(4) 2L = 320 (surface breakage—Cholame to Cajon Pass)

This earthquake has been reanalyzed (Evernden and others, 1973) using the model of Evernden (1975) and using a k value of 1¾. The most interesting aspect of this study is that, thanks to the labors of Agnew and Sieh (1978), there is now available a compilation of numerous intensity observations for this earthquake. Intensity values experienced at numerous sites in California can now be compared with predicted values. Table 8 indicates Rossi-Forel intensity values estimated by us using the data of Agnew and Sieh (they chose to use M/M intensities) and R/F intensity values predicted on saturated alluvium for a fault break ex-

TABLE 8.—*Observed and predicted R/F intensities, Fort Tejon earthquake*

Site	Observed intensity	Predicted intensity
San Diego	V–VI	5
San Bernardino	VII–VIII	8
San Gabriel Valley	VIII	8
Los Angeles (downtown)	VII+	7 (high)
San Fernando Valley	VIII–	8
34.6°N. 117.4°W.	VIII–	8
34.1°N. 119.0°W.	VIII–	7
Ventura	VIII+	8
Santa Barbara	VII	7
San Andreas fault	=IX	≥9
Fort Tejon	VIII–IX	9
34.0°N. 118.7°W.	VIII+	9
35.4°N. 119.0°W.	VIII+	9
35.9°N. 119.3°W.	VI–VII	7
36.2°N. 119.3°W	VII+	7
Visalia	VII–VIII	6
36.7°N. 121.3°W.	VII	6
Monterey	IV–V+	4–6
Santa Cruz	III–V+	3–5
San Francisco	V+	4
Stockton	IV	5
Sacramento	V+	[1]4
		[2]5–6

[1]All path k=1¾.
[2]Part of path k=1½)

tending along the San Andreas fault from lat 34°18.3′ N., long 117°3.15′ W. to lat 35°55.0′ N., long 120°27.9′ W.

Agreement between prediction and observation is excellent, there being virtually no sites at which observed and predicted R/F intensities differ by as much as one (1) intensity unit.

The data for the 1857 earthquake substantiate the prediction that the peak intensity to be expected in the Los Angeles area from a great earthquake on the San Andreas fault is R/F VII/VIII, San Fernando Valley and eastern Los Angeles experiencing possibly VII. These intensities presume a zero depth to water table. The marked lowering of the water table in much of this area in the intervening 120 years should result in peak intensities VI/VII in most alluviated areas of the San Fernando Valley and Los Angeles.

We have modeled this earthquake in detail using the ½-minute by ½-minute grid. Plate 1 indicates geology of the area and also indicates predicted R/F intensities with ground-condition corrections of table 2 applied and assuming zero depth to water table in alluviated areas (J regions of plate 1). This plate is as published by Blume and others (1978); they used our predictions in constructing it.

As pointed out by Algermissen (1973) and substantiated by Blume and others (1978) and this study, a repeat of the great 1857 Fort Tejon earthquake will not be a disaster of the magnitude sometimes imagined. San Fernando Valley will suffer less from an 1857 repeat than it did from the San Fernando 1971 earthquake. The remoteness of the San Andreas fault from heavily urbanized areas in southern California and the high rates of attenuation in the region will result in a repeat of the 1857 earthquake having a surprisingly small impact on the area as a whole. This conclusion is supported by results given in a later section in which predictions of losses for numerous potential California earthquakes are given.

A fact worth mentioning here is a basic disagreement of the general near-fault patterns of predicted intensity shown on plate 1 and previously presented for the San Francisco 1906 earthquake (Evernden and others, 1973) with the reported pattern shown by Lawson (1908, maps 21–23) for the San Francisco earthquake. Lawson shows narrow zones of all intensities as the fault is approached, irrespective of ground condition and any ideas of attenuation as linked with depth of focus. No model incorporating legitimate values of attenuation and depth of focus can predict such patterns as shown by Lawson. In addition, there is total absence of data within Lawson (1908) to support the near-fault intensity contouring on his maps. In fact, the data of his study specifically refute his contouring. Apparently, Lawson worked under the assumption that all intensities must occur between VI and X–XI, even though intensities VI through IX are largely defined by shaking criteria whereas X and IX are defined by ground rupture. It is perfectly possible to have severfeet of displacement associated with shaking intensities on only VII—VIII. It is our belief that Lawson's near-fault contouring is almost totally a derivative of misconception and is quite erroneous. No modeling of expected intensities for a repeat of 1906 or any other earthquake should incorporate near-fault patterns of intensity as shown by Lawson.

LONG BEACH EARTHQUAKE OF MARCH 10, 1933 (MODIFIED MERCALLI INTENSITIES; NEUMANN, 1935)

Known parameters:

(1) k = 1¾ (western California)
(2) C = 25 (normal depth)
(3) Location of faulting (aftershocks)
(4) 2L = 22-44 (S and P travel times, aftershocks)

This is an interesting earthquake for a variety of reasons, a principal one being that it was the first major earthquake to be reported by the U.S.G.S. in Modified Mercalli units of intensity. Thus, it is the first significant earthquake without reports of intensity IX in the epicentral region. It is certain that, if this earthquake had been reported in units of Rossi-Forel intensity, a clearly defined region of intensity IX would have been defined, and this earthquake would have been accorded greater status in the hierarchy of historical California earthquakes.

Two possible models for this earthquake seem appropriate. The first is to make 2L equal to the aftershock zone, that is, about 40 km, as reported in Hileman, Allen, and Nordquist (1973). The second is to follow Benioff (1938) and use a 2L of about 27 km, an estimate based on comparison of S-P arrivals at southern California stations, the solution being restrained to lie along the Newport-Inglewood fault as indicated by the aftershocks. In our initial studies, we used 2L values of 22 and 44 km with the south end of both models being at the epicenter (k of 1.750). Table 9 gives observed and predicted Modified Mercalli intensities for both 2L values. Assuming that all sites in alluvial plains or on beaches behaved as for saturated alluvium, a 2L value of 22 is indicated as appropriate. If the 6-minute by 6-minute ground condition is used, the values in square brackets are predicted for San Clemente, El Toro, and San Diego; these values are in better agreement with observed values. As to the appropriateness of the assumption of saturated ground near Long Beach, Wood (1933) points to the correlation between "bad natural ground" and "deep water-soaked

alluvium." The general over-prediction of intensities in the VII zone when using a 2L of 44 would seem to imply too great a 2L because most of these sites were on alluvium. However, if pumping had lowered the water table to a 10-m depth, a 2L of 44 would be a better value. We conclude, on the basis of information in hand, that a 2L of 22 is more likely than a 2L of 44. Estimating the losses to be expected from a repeat of this earthquake depends strongly on knowledge of the depth to the water table in 1931 and today.

Wood (1933) comments on the absence of intensity IX values as being an indication of the small size of this earthquake. However, figure 8 makes clear that the change in definition of intensity units as of 1931 was the real reason for the absence of reported intensity IX values for the Long Beach earthquake.

TABLE 9.—*Observed and predicted Modified Mercalli intensities, Long Beach earthquake*
[All values for saturated alluvium]

Site	Observed intensity	Predicted intensities	
		2L=22	2L=44
Anaheim	8	7/8	8
Bellflower	8	7	8
Costa Mesa	8	8	8
Cypress	8	7	8
Garden Grove	8	8	8
Huntington Beach	8	8	8
Newport Beach	8	8	8
Santa Ana	8	8	8
Seal Beach	8	8	8
Signal Hill	8	8	8
South Gate	8	7	8
Willowbrook	8	7	8
Torrance	7	7	8
Redondo Beach	7	7	8
Norwalk	7	7	8
Manhattan Beach	7	7	7
East Los Angeles	7	7	8
Lomita	7	7	8
Laguna Beach	7	7	8
Huntington Beach	7	7	8
Artesia	7	7	8
Fullerton	7	7	8
Alhambra	6	6	7/6
Beverly Hills	6	6	6
Covina	6	6	7
Culver City	6	6	6
Fillmore	6	5	5/6
Gardena	6	7/6	8/7
Glendale	6	6	6
Montebello	6	7/6	8
Oxnard	6	5	5/6
Pasadena	6	6	7
Placentia	6	7	7
Pomona	6	6	7
Santa Monica	6	6	7
Simi	6	5	6
Ventura	6	5	5
Whittier	6	7	8
San Clemente	5	7/6 [5][1]	7
Escondido	5	5	—
Moreno	5	5	—
El Toro	5	7/6 [6][1]	—
Cardiff-by-the-Sea	4	5	—
Carlsbad	4	5	—
Santa Maria	3	3/4	—
San Diego	3	5 [3][1]	—

[1][ ] 6-minute by 6-minute ground condition.

As an example of the further refinement in estimation of event parameters apparently possible by use of the statistical model described earlier, we analyze the data of the 45 reporting stations via the several criteria mentioned earlier. We consider the earthquake to have been on the Newport-Inglewood fault, so the only parameters evaluated are length of break (2L), position on the fault line (S), and the appropriate k value, there being the possibility that actual k values in any given area of western California are slightly different from the 1¾ value routinely used for this region.

Table 10 presents the results of these calculations (A through D are for k = 1.750, and E, F, and G are for k = 1.825). Table 10A, presenting values of (H-L) and $|H-L|$, indicates (H-L) to have a zero value at about 2L = 22 for S = −8 and 2L = 25 km for S = −12. We include within the dashed line the most likely 2L/S values. Table 10B presents (Obs-Calc) values, the minimum value being at 2L = 22, S = −8. The $s.d._{(Obs-Calc)}$ is such that a great range of 2L/S values are permissible at 95 percent confidence (area within dashed lines). Table 10C gives |Obs-Calc| values, the minimum value being at 2L = 22, S = −12, with a large range of 2L/S values permissible at 95 percent confidence. Table 10D presents CP values, the minimum being at 2L = 22, S = −4 with 2L = 22 and $4 \geq S \geq -8$ as well as 2L = 24, $-4 \geq S \geq -12$ acceptable at 95 percent confidence. The only area of overlap of all criteria at 95 percent confidence is 2L = 24, $-8 \geq S \geq -12$.

The solution 2L = 24, S = −10 has its south and north termini at latitudes 33°38.9′ N. and 33°48.8′ N., respectively. These are to be compared with the reported latitude 33°37′ N. of the Long Beach earthquake with the aftershocks extending srom 33°35′–37′ N. to 33°51′–53′ N.

With the best solution for k = 1.750, there was a slight tendency for mean (O-C) values in each intensity band to be function of O values and thus of distance, implying a slightly incorrect value of k. Therefore, we redid the analysis using a k value of 1.825; tables 10E and F show these results. The best solution via (H - L) and |H - L| (table 10E) is 2L = 34–38 and S = −8. Table 10F, based on CP values, gives as a best solution 2L = 34, S = −4. Given the calculated CP and $s.d._{CP}$ values for these coordinates (CP=.079, $s.d._{CP}$=.012), all solutions based on k = 1.750 are rejected at 99 percent probability. At k = 1.825, solutions within the 95 percent confidence area have 2L = 32–36 and $4 \geq S \geq -12$. Table 10G gives an abbreviated listing of R.M.S., CP, and (H - L)/|H - L| values, indicating essential agreement as to the best event parameters. The following table compares predicted location of fault break for 2L = 34, S = −4 and −6 (CP solution and average of H - L and CP solutions) and observational data.

	Latitude south end	*Latitude north end*
Solution 2L = 34, S = −4	33°39.3′ N	33°53.4′ N
Solution 2L = 34, S = −6	33°38.5′ N	33°52.5′ N
Main shock epicenter	33°37′ N	—
Aftershocks	33°35′–37′ N	33°51′–53′ N

The marked decrease in CP value, the better fit to the aftershock zone, and the elimination of the dependency of residuals upon distance suggest that the solution based on k=1.825 is superior to that based on k=1.750.

BRYSON EARTHQUAKE OF 21 NOVEMBER 1952 (MODIFIED MERCALLI INTENSITIES; MURPHY AND CLOUD, 1954)

Known parameters:

(1) k = 1¾ (western California)

(2) C = 25 (normal depth)

Unknown parameters:

(3) Location of epicenter

(4) 2L

This earthquake is of interest for two reasons. First, it is the only historical earthquake of significant magnitude that has occurred between the Lompoc and Monterey Bay earthquakes, though it was located on a different fault than either of these. Second, the reported intensities are apparently anomalous at first glance because intensities of VI and VII were reported to significant distances but no intensity VIII was reported. Even though the reported values were Modified Mercalli rather than Rossi-Forel, the reported intensity pattern appears anomalous. However, there is a logical explanation. Table 11 presents observed and predicted M/M intensities for two different models (2L = 20 and 40 km) of this earthquake. The fault break is distributed equally on either side of the calculated epicenter. The NOAA epicenter (Murphy and Cloud, 1954) is lat 35.8° N., long 121.2° W. Recently, the location of this event was recalculated (W. V. Savage, oral commun., 1979), the result being lat 35°47.9′ N., long 121°11.4′ W., while Bolt and Miller (1975) gave the location as lat 35°44′ N., long 121°12′ W. and assigned it a "b" quality. These locations agree with the NOAA epicenter but have an uncertainty of 10–15 km in the northeast-southwest direction.

All predicted intensity values in table 11 are for ground condition according to the 6-minute by 6-minute California grid. Some entries show the estimated alluvium value included in square brackets. Entries designated (Al) indicate either that the assumed ground condition is saturated alluvium on the 6-minute by 6-minute grid, although this assumption may be inappropriate (predicted greater than observed; San Simeon, for example), or that the peak value pre-

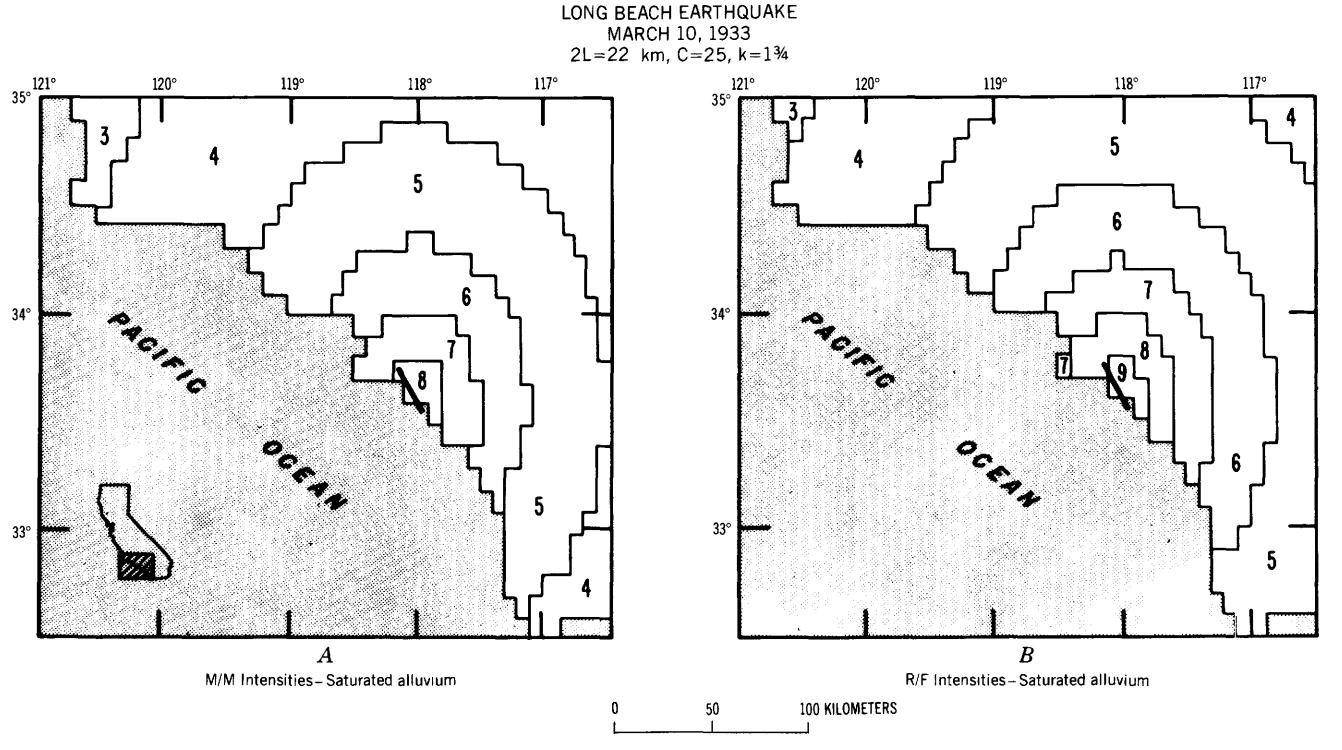

FIGURE 8.—Predicted M/M (*A*) and R/F (*B*) intensities for the Long Beach, Calif., earthquake of March 10, 1933 (2L = 22, C = 25, k = 1¾).

TABLE 10.—*Calculated parameters for the Long Beach earthquake*

A
Reference Fault: Newport-Inglewood
Reference Coords: 33°48.0′ N 118°10.7′W
k = 1.750 T = 0 C = 25
Bands Used: VIII, VII, VI, V, IV, III
Upper Values: (H - L) Lower Values: |H - L|

S \ 2L	12	16	20	24	28	32
8	−14	−7	−1	2	6	9
	16	17	17	16	16	19
4	−16	−7	−1	3	7	10
	16	17	13	15	17	16
0	−20	−8	−1	3	7	10
	20	16	13	16	15	15
−4	−22	−11	−2	4	9	13
	22	15	14	14	11	13
−8	−21	−14	−6	2	8	12
	21	18	16	12	10	12
−12	−22	−15	−11	−2	6	11
	22	19	15	12	10	11
−16	−22	−15	−12	−7	1	7
	24	17	16	15	13	13

2L = 22, S = −8: (H - L) = 0, |H - L| = 12

B
Reference Fault: Newport-Inglewood
Reference Coords: 33°48.0′ N 118° 10.7′ W
k = 1.750 T = 0 C = 25
Bands Used: VIII, VII, VI, V IV, III
Upper Values: (O − C) Lower Values: $s.d._{(O-C)}$

S \ 2L	12	16	20	24	28	32
8	.402	.209	.067	−.068	−.176	−.275
			(.100)			
4	.400	.206	.062	−.073	−.178	−.276
			(.092)	(.092)		
0	.410	.216	0.69	−.066	−.173	−.272
			(.085)	(.085)		
−4	.432	.238	.090	−.047	−.154	−.253
			(.080)	(.080)		
−8	.468	.272	.124	−.015	−.127	−.225
			(.076)	(.077)		
−12	.512	.316	.167	.028	−.087	−.187
−16	.565	.370	.219	.079	−.033	−.139

2L = 23, S = −8: (O − C) = 0, $s.d._{(O-C)}$ = .076

C
Reference Fault: Newport-Inglewood
Reference Coords: 33°48.0′ N 118° 10.7′ W
k = 1.750 T = 0 C = 25
Bands Used: VIII, VII, VI, V, IV, III
Upper Values: |O − C| Lower Values: $s.d._{|O-C|}$

S \ 2L	12	16	20	24	28	32
8	.644	.578	.549	.537	.547	.574
4	.602	.542	.513	.503	.512	.536
0	.570	.509	.483	.472	.481	.505
−4	.550	.478	.456	.452	.455	.473
−8	.549	.463	.432	.430	.442	.460
−12	.566	.462	.422	.415	.435	.459
			(.048)	(.043)		
−16	.609	.483	.433	.417	.428	.461

2L = 22, S = −12: O − C = .412, $s.d._{O-C}$ = .041

TABLE 10.—*Calculated parameters for the Long Beach earthquake*—Continued

D
Reference Fault: Newport-Inglewood
Reference Coords: 33°48.0′ N 118° 10.7′ W
k = 1.750 T = 0 C = 25
Bands Used: VIII, VII, VI, V, IV, III
Upper Values: CP Lower Values: $s.d._{CP}$

S \ 2L	12	16	20	24	28	32
8	.292	.180	.154	.191	.264	.355
		(.041)	(.013)	(.048)		
4	.298	.163	.130	.167	.252	.343
		(.046)	(.012)	(.052)		
0	.317	.161	.118	.148	.237	.329
		(.051)	(.013)	(.049)		
−4	.340	.173	.114	.130	.216	.308
			(.017)			
−8	.373	.197	.121	.124	.191	.283
−12	.405	.228	.145	.126	.170	.256
−16	.439	.267	.180	.149	.167	.226

2L = 22, S = −4: CP = .110, $s.d._{CP}$ = .013

E
Reference Fault: Newport-Inglewood
Reference Coords: 33°48.0′ N 118° 10.7′ W
k = 1.825 T = 0 C = 25
Bands Used: VIII, VII, VI, V, IV, III
Upper Values: (H - L) Lower Values: |H - L|

S \ 2L	20	24	28	32	36	40
12	−16	−8	−6	−3	0	3
	18	16	18	17	16	17
8	−15	−10	−4	−2	−1	2
	17	16	18	16	15	14
4	−15	−10	−5	−1	0	4
	17	16	17	15	14	16
0	−20	−10	−7	0	3	4
	20	16	15	14	15	14
−4	−22	−14	−7	−3	4	6
	22	16	15	15	12	12
−8	−21	−17	−11	−2	1	5
	21	19	17	14	11	11
−12	−21	−18	−13	−9	−1	1
	21	18	17	15	13	11

F
Reference Fault: Newport-Inglewood
Reference Center: 33°48.0′N 118°10.7′W
k = 1.825 T = 0 C = 25
Bands Used: VIII, VII, VI, V, IV, III
Upper Values: CP Lower Values: $s.d._{CP}$

S \ 2L	20	24	28	32	36	40
8	.312	.214	163	143	147	175
4	.327	.200	.124	.093	.104	.156
				(.020)		
0	.345	.217	.124	.085	.091	.146
				(.031)	(.024)	
−4	.370	.240	.139	.085	.083	.130
				(.024)	(.016)	
−8	.399	.268	.162	.099	.086	.118
				(.039)	(.010)	(.044)
−12	.430	.299	.192	.125	.099	.115
				(.042)	(.016)	(.026)

2L = 34, S = −4: CP = .079, $s.d._{CP}$ = .012

TABLE 10.—*Calculated parameters for the Long Beach earthquake*—Continued

G
Reference Fault: Newport-Inglewood
Reference Coords: 33°48.0′ N 118°10.7′ W
Bands Used: VIII, VII, VI, V, IV, III

A. k = 1.7500

2L	S	CP	RMS	(H-L)/|H-L|
20	−4	.114±.017	.537	−2/14
20	−8	.121	.521	−6/16
20	−12	.145	.527	
20	−16	.180	.557	
24	−4	.130	.533	
24	−8	.124	.510	2/12
24	−12	.126	.504	−2/12

B. k = 1.8125

2L	S	CP	RMS	(H-L)/H-L
32	0	.085	.578	0/14
32	−4	.085	.549	−3/15
32	−8	.095	.537	
32	−12	.125	.541	
36	0	.091	.572	
36	−4	.083	.544	4/12
36	−8	.086	.527	1/12
36	−12	.099	.528	0/13

TABLE 11.—*Observed and predicted M/M intensities, Bryson earthquake*
[Values for 6-minute by 6-minute ground condition]

Site	Observed intensity	Predicted intensity	
		2L=20	2L=40
Bradley	7	7	7
10 miles NW of Bradley	7	7	7
Bryson	7	7	7
Arroyo Grande	6	5	6
Atascadero	6	5	6
Cambria	6	6(Al)	7(Al)
Carmel Valley	6	5	5[6(Al)]
Cayucos	6	5/6	6
Chualar	6	5	6
Guadalupe	6	5	5
Harmony	6	5	6
King City	6	6	7
Lockwood	6	6	7
Morro Bay	6	6	6
Oceano	6	5	6
Parkfield	6	5	6
Paso Robles	6	6	6
Pismo Beach	6	5	5
Salinas	6	5	5
San Ardo	6	5/6	6
San Luis Obispo	6	5[6(Al)]	5[6(Al)]
San Simeon	6	7(Al)	7(Al)
Santa Margarita	6	5	5[6(Al)]
Templeton	6	6	7
Avenal	5	5	6
Ben Lomond	5	4	4
Big Sur	5	5	5
Buellton	5	4	5
Buttonwillow	5	4	5
Casmalia	5	5	5
Cholame	5	5	5
Coalinga	5	5	5
Corcoran	5	4	5
Dos Palos	5	4	5
Hollister	5	5	5
Kettleman City	5	4	5
Lompoc	5	4	4[5(Al)]
Foot Hills	5	4	5
Maricopa	5	4	4(Al)
Monterey	5	5	5(Al)
Nipomo	5	4/4	5
Orcutt	5	5	5
San Miguel	5	6(Al)	7(Al)
Santa Cruz	5	4/5	5
Santa Maria	5	4/5	5

dicted by model is below the reported value (predicted less than observed; Maricopa, for example).

It appears from the table that 2L values of 20 and 40 bracket the best estimate of 2L, the suggestion being that 40 is somewhat too long because a few sites for which intensity 7 was predicted actually reported 6. Averaging all the predicted values indicates a 2L of 40 km to be nearly correct.

In addition to the studies above, we investigated the Bryson intensity data by use of our statistical programs. Though there were a greater number of reporting stations, their nonuniform distribution created a problem in use of CP. The virtual absence of stations in a 180° quadrant centered northwestward from Bryson for a distance of 75 km (that is, to intensity of about 5.5) resulted in very poor control on S when solving for CP values. Tables 12 A–C indicate marked disagreement between R.M.S. and CP estimates of the event's parameters, the CP criterion actually having its

TABLE 12.—*Calculated parameers for the Bryson earthquake*

A
Reference Fault: Nacimiento
Reference Center: 35°47.9′N 121°11.4′W
k = 1.750 2L = 30 C = 25
Bands Used: VIII, VII, VI, V, IV, III
Upper Values: CP Lower Values: RMS

S \ T	−15	−10	−5	0	5	10	15
10	.457	.408	.364	.328	.298	.377	.266
5	.411	.361	.316	.279	.249	.227	.218
0	.366	.313	.268	.231	.201	.184	.176
−5	.324 [.466]	.271 [.447]	.225 [.439]	.189 [.455]	.159	.141	.135
−10	.284 [.461]	.230 [.441]	.186 [.432]	.147 [.437]	.121 [.455]	.105	.102
−15	.246 [.468]	.192 [.449]	.148 [.439]	.112 [.442]	.084 [.459]	.071 [.489]	.073 [.530]
−20	.211 [.487]	.157 [.471]	.114 [.462]	.078 [.464]	.055 [.478]	.047 [.504]	.055 [.540]

Values in box are for parameter values having CP_T minima. See table 13 and text.

B
Reference Fault: Nacimiento
Reference Center: 35°47.9′N 121°11.4′W
k = 1.750 2L = 35 C = 25
Bands Used: VIII, VII, VI, V IV, III
Upper Values: CP Lower Values: RMS

S \ T	−15	−10	−5	0	5	10	15
5	.268 [.433]	.218 [.422]	.175 [.420]	.144 [.434]	.123	.113	.116
0	.225 [.422]	.173 [.409]	.132 [.409]	.103 [.423]	.087	.081	.087
−5	.185 [.425]	.134 [.414]	.094 [.412]	.067 [.423]	.054	.057	.069
−10	.147	.098 [.431]	.059 [.429]	.041 [.440]	.042 [.463]	.055	.067
−15	.115	.066 [.461]	.037 [.460]	.037 [.469]	.063 [.488]	.080	.089
−20							

Values in box are for parameter values having CP_T minima. See table 13 and text.

TABLE 12.—*Calculated paramaters for the Bryson earthquake*—Continued

C
Reference Fault: Nacimiento
Reference Center: 35°47.9'N 121°11.4'W
k = 1.750 2L = 40 C = 25
Bands Used: VIII, VII, VI, V, IV, III
Upper Values: CP Lower Values: RMS

S \ T	−15	−10	−5	0	5	10	15
10	.293	.248	.209	.182	.165	.158	.160
5	.247 [.424]	.202 [.418]	.165 [.424]	.138	.125	.122	.129
0	.204 [.407]	.157 [.401]	.123 [.407]	.103 [.429]	.095	.096	.106
−5	.162 [.398]	.119 [.405]	.088 [.425]	.074 [.455]	.075	.085	.099
−10	.126 [.415]	.086 [.410]	.064 [.415]	.066	.086	.107	.118
−15	.096 [.439]	.062 [.436]	.061 [.441]	.095 [.457]	.124	.143	.153
−20	.074 [.473]	.058 [.473]	.094 [.479]	.129	.157	.175	.182

Values in box are for parameter values having CP_T minima. See table 13 and text.

minimum on tables B and C at S ≤ −20, an unacceptable location because the seismological data place a constraint of a very few kilometers on the northwest-southeast position of the epicenter.

The problem with the estimate of S is that data to the north effectively cover such a short range of intensity that, given the noise level in the data, a CP minimum is found (that is, artifically low mean (Obs − Calc) value as a function of O) by moving the calculated fault south of its correct location. A technique for suppressing this effect is to multiply calculated Obs − Calc values by the cosines of the angles between the northward direction of the fault and the radials from the center of the fault to the stations before calculating a CP-type number. The quantity derived from this operation, called CP_S, is used to find the best S value as a function of 2L and k.

The same effect that yields a poor value for S may also yield a poor estimate of T. Therefore, we calculated CP_T values after the CP_S values, CP_T differing from CP in that all (Obs − Calc) values for stations west of the fault are multiplied by (−1) prior to calculation of a CP-type number. We did not use a sine function because such a procedure suppresses the influence of near-station intensity values on the 2L estimate and thus on T.

Table 13 gives CP_T and R.M.S. values for 2L, S pairs having small CP_S values for T=0. R.M.S. values, of course, are as they were in tables 12 A–C. Use of CP_S and CP_T does effectively suppress the effects of poor station distribution in the intensity data, giving small CP values for k values of 1.6825 and 1.7500 over small ranges of event parameter values while also giving best estimates very near those suggested by the R.M.S. values. We interpret the great range of equally acceptable 2L, S, T sets for k = 1.8125 as an indication of smearing of the analysis by use of an incorrect parameter value.

We conclude that the event's location probably was near the Nacimiento fault as given by all published locations, but we cannot certainly rule out a location 15 km to the southwest, in the zone of active faults crossing San Simeon Point southeast to northwest.

Therefore, the intensity data indicate that this earthquake was as large or larger than the Santa Barbara or Long Beach earthquakes, both of which had significant areas experiencing Modified Mercalli intensity VIII. The explanation, of course, lies in the facts of

TABLE 13.—*Calculated parameters for the Bryson earthquake*

Reference Fault: Nacimiento
Reference Center: 35°47.9'N. 121°11.4'W.
Bands Used: VIII, VII, VI, V, IV, III

A. k = 1.6875

2L	S	T	CP_S	CP_T	RMS
12	−15	0	.037	.044	.558
16	−15	5	.008	.088	.470
16	−15	0	.001	.008±.056	.473
20	−10	−5	.027	.037±.017	.434
20	−10	0	.030	.075	.444
24	−10	−5	.013	.054±.008	.420
24	−10	−10	.015	.103	.412
28	−5	−5	.027	.085	.432
28	−5	−10	.028	.100	.416
28	−15	−15	.035	.155	.411

B. k = 1.7500

2L	S	T	CP_S	CP_T	RMS
30	−10	0	.029	.051	.451
30	−10	−5	.026	.046	.443
35	−10	−5	.015	.029±.019	.413
40	−5	−5	.022	.042	.409
40	−5	−10	.023	.081	.401
45	−5	−10	.015	.079	.398
45	−5	−15	.004	.120	.395
50	0	−15	.034	.120	.398

C. k = 1.8125

Minimum CP_T at 55, −5, −5 of .014±.049. There results a great range of 2L values that give CP_T values of less than .014 + .049(1.64) = .105. Table is for low RMS values.

2L	S	T	CP_S	CP_T	RMS
60	−5	−5		.019	.396
60	−5	−10		.071	.391
65	0	−5		.042	.396
65	0	−10		.060	.388
65	0	−15		.119	.394
70	0	−5		.056	.400
70	0	−10		.058	.385
70	0	−15		.096	.385
75	0	−10		.061	.391
75	0	−15		.082	.385
75	0	−20		.129	.391
80	5	−15		.086	.393
80	5	−20		.129	.395

Wide range of equally acceptable parameters interpreted as meaning incorrect k value with consequent smearing of analysis.

geology. The epicentral region of the Bryson earthquake is in a remote, nearly unpopulated region with only very small stream valleys and occasional ranches. Although an area of 2,700 km^2 was predicted to experience M/M VIII on saturated alluvium, the nearly total absence of such material in the epicentral region led to peak reported intensities of VII. The contrasting M/M intensities for the Bryson earthquake as predicted for saturated alluvium and as predicted when incorporating the 6-minute by 6-minute ground condition are shown in figure 9.

According to table 1 of Evernden (1975), a 2L of 40 km in western California leads to a predicted magnitude value of 6.85 as compared to a reported value of 6± for this earthquake (Coffman and van Hake, 1973).

KERN COUNTY EARTHQUAKE OF 1952, (MODIFIED MERCALLI INTENSITIES; MURPHY AND CLOUD, 1954)

Known parameters:

(1) Location (main shock and aftershocks)

(2) 2L = 30–60 (observed fracturing and aftershocks)

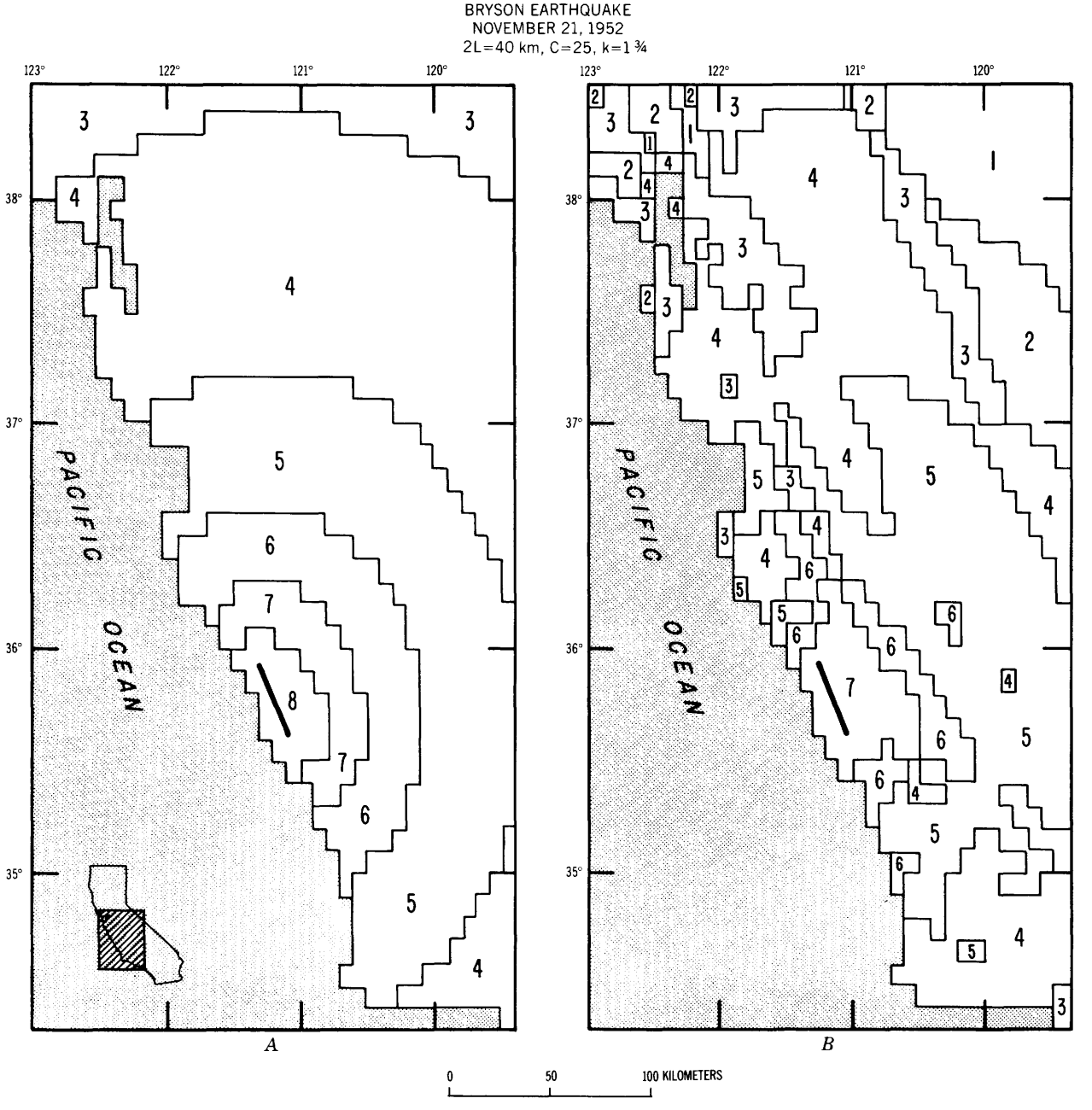

FIGURE 9.—Predicted M/M intensities, Bryson, Calif., earthquake (2L = 40, C = 25, k = 1¾). *A*, Saturated alluvium. *B*, 6-minute by 6-minute ground condition.

Unknown parameters:

(3) k

(4) C

This earthquake was studied in the first paper of this series (Evernden and others, 1973) with unsatisfactory results. In particular, the model used failed to predict the northward extent of intensities V and VI along the east side of the Sierra Nevada. When that paper was written, the existence of gross regional differences in attenuation had not yet been appreciated. The location of this earthquake near the boundary between regions of k = 1¾ and k = 1½ should lead to pronounced perturbation of observations from predictions based on a uniform k model.

In order to construct a predicted intensity map for this earthquake, the following steps were taken:

(1) Define the line through California that separates regions having k values of 1½ and 1¾. Through the Central Valley, the boundary (shown as a heavy solid line in figures 10 and 11) is assumed to be along the contact between granite and the Franciscan assemblage buried under the Tertiary sedimentary rocks in the middle of the valley. By trying several models, it was concluded that the White Wolf fault, focus of the Kern County earthquake, is in the region of k = 1½ and the k boundary is to the west of the fault (see fig. 10). The boundary is assumed to then swing sharply eastward, essentially paralleling the Garlock fault. It is assumed that a k value of 1½ applies all the way to Needles, Calif., that nearly all the path to San Diego has a k value of 1¾, and that the position of the k boundary is uncertain along some intermediate southeast azimuths.

(2) Calculate expected intensities for different fault lengths (30 and 60 km) and a k value of 1½. Compare with observations in regions having k values of 1½. Select appropriate 2L value.

(3) From the boundary between 1½ and 1¾, propagate intensities predicted for k of 1½ into regions of k of 1¾ according to predictions for attenuation in k of 1¾. This was actually done by: (a) noting that predicted I values along the k boundary near the epicenter were on the average about 1½ intensity units lower for k of 1¾ than for k of 1½ when assuming uniform models of 1¾ and 1½; (b) thus, increasing all I values predicted by uniform k 1¾ model by 1½ units in regions of k = 1¾; (c) adjusting the misjoin of the predicted intensities in the two k regions by assuming that values in k regions of 1½ were correct, intensity values in k regions of 1¾ were correct if ray directions made large angles with the k boundary, and I values in other k regions of 1¾ were obtained by interpolation. Figure 10 indicates the result of these several steps and the resultant predicted M/M intensities on saturated alluvium for 2L = 60 and C = 25. The figure also indicates the high intensity values reported in each region of predicted intensities, it being assumed that these reports of high intensities are correlative with presence of saturated alluvium or equivalent ground condition. There is excellent agreement between prediction and observation in both k regions. The much further northward extent of intensity V values east of the Sierra Nevada than along the coast of California is clearly predicted by this model. The predicted extent of intensities VII and VIII in regions of k of 1½ and 1¾ is confirmed by observations.

As pointed out above, the model used for figures 10 and 11 assumes a length of fault break of 60 km. A fault break of 30 km predicts too small an areal extent for intensity values of V through VIII.

Figure 11 indicates the difference in intensity between published contours (Murphy and Cloud, 1954) and those predicted when adjusted for 6-minute by 6-minute ground condition. The difference is small up the Central Valley. However, there are large differences throughout the Sierra Nevada. The published isoseismals of Murphy and Cloud (1954) ignore the granite and are based solely on scattered sedimentary sites in and east of the mountains. On the other hand, the predicted values based on the 6-minute by 6-minute grid give great regions of low intensity throughout the mountains. Thus, figure 10 predicts intensity IV for sites on saturated alluvial ground north and west of Lake Tahoe as observed, while figure 11 shows all of this as intensity II because the 6-minute by 6-minute grid sees only volcanic rocks and granite.

Though a model with parametrs of 2L = 60, C = 25, k = 1½ satisfactorily explains intensity values of VIII and less, it does seem to predict too-high intensities in the epicentral region. Thus, as shown in figure 12*A*, a C value of 25 causes a prediction of a large area of intensity X (shaking intensity) for saturated ground condition. Figure 12*B* indicates that a C value of 40 results in total elimination of predicted X and halving of the area of IX values, while figure 12*C* shows near elimination of IX values when incorporating 6-minute by 6-minute ground condition. We conclude that this earthquake occurred at significantly greater depth than is typical of western California earthquakes.

The absence of intensity IX values in the observed intensities for this earthquake, even though 8 feet of displacement was measured in a Southern Pacific Railroad tunnel, was simply a quirk of observation combined with the odd definitions of intensities VIII and IX on the Modified Mercalli scale. If M/M values are converted to R/F values, nearly all M/M VIII values become intensity IX, numerous M/M values of VII become VII to VIII, the result being to give a clearly

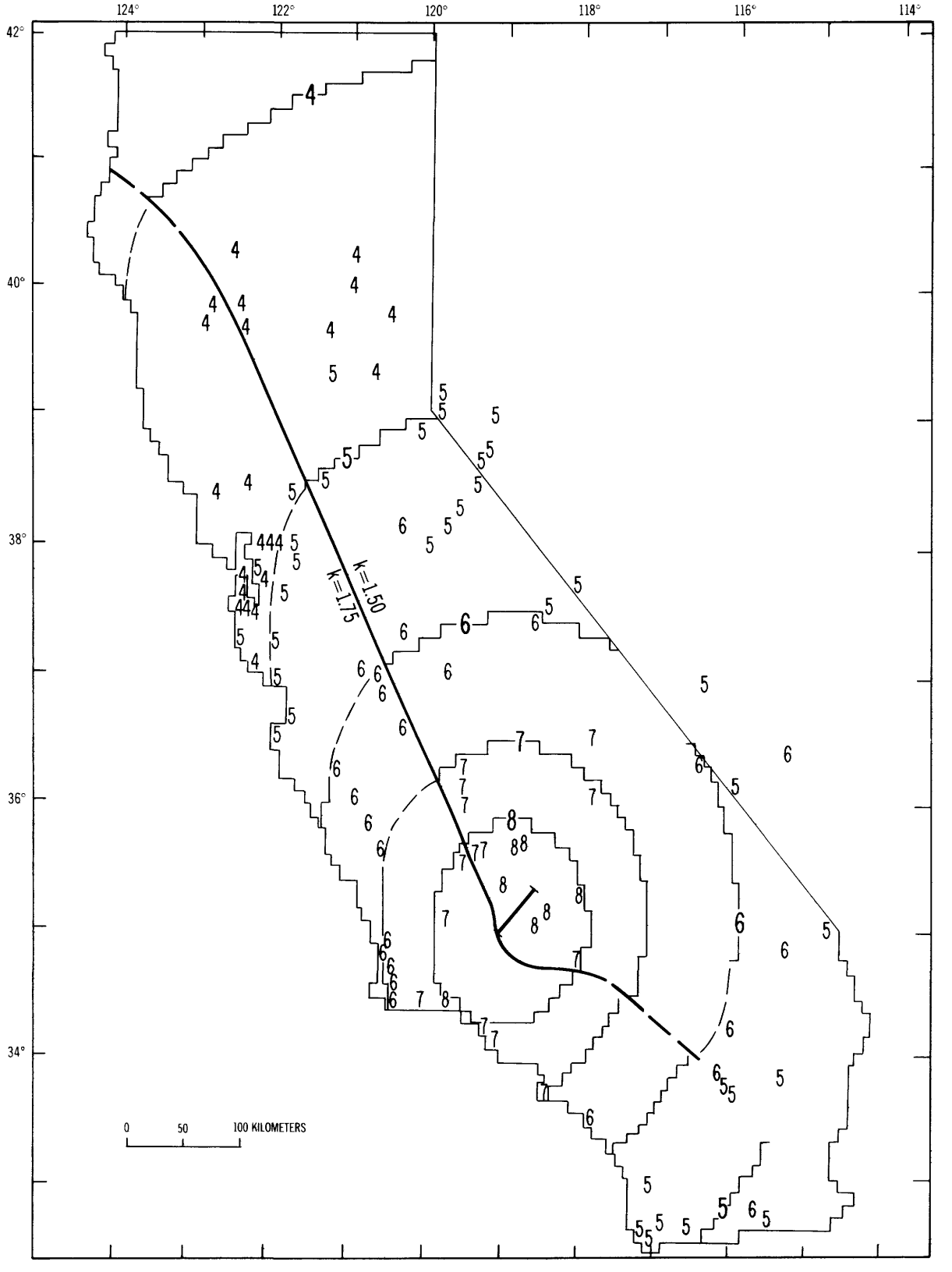

FIGURE 10.—Observed (spot values) and predicted (contours) M/M intensities for Kern County, Calif., earthquake of July 21, 1952 (2L = 60, C = 25).

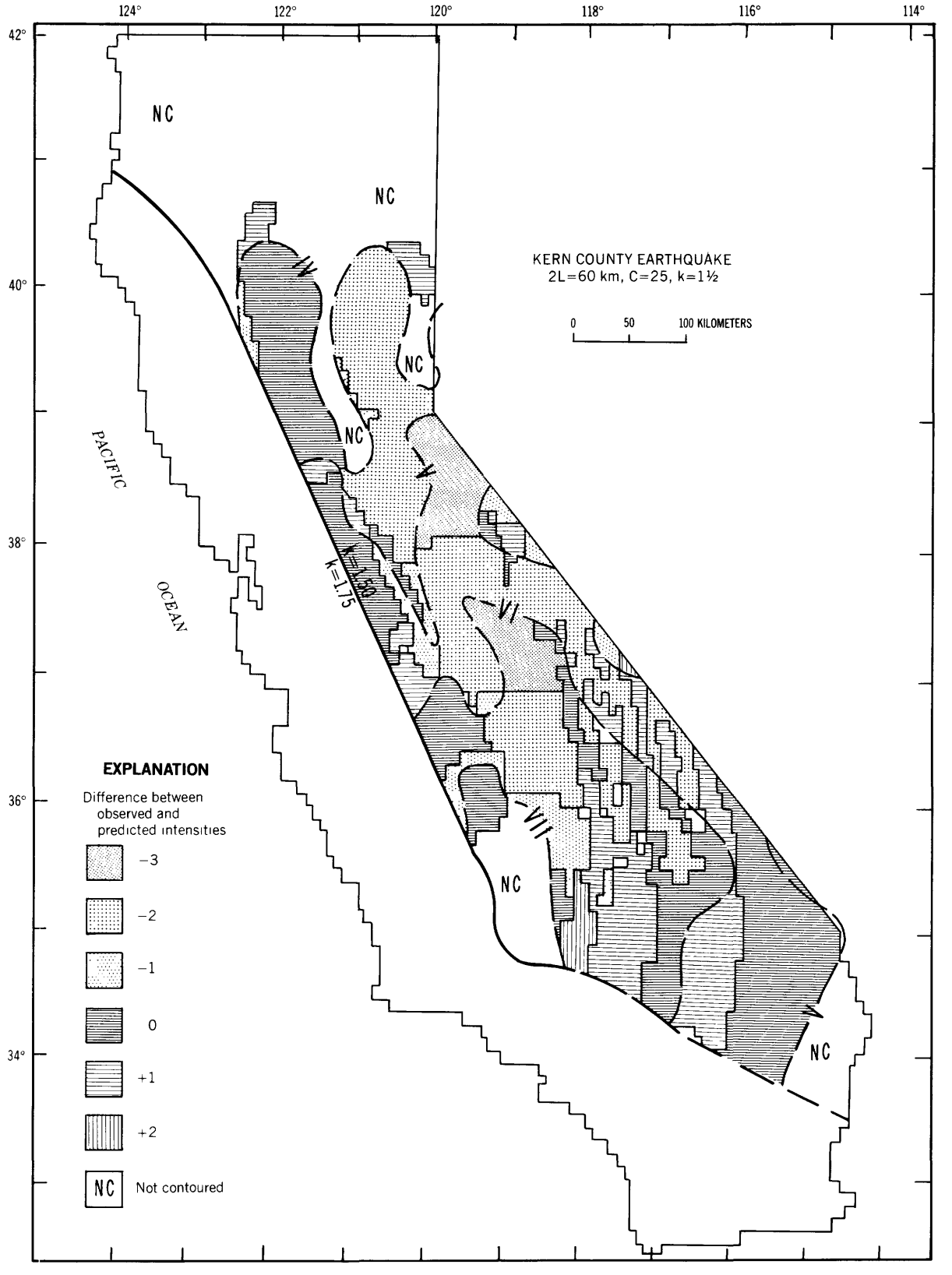

FIGURE 11.—Comparison of predicted and observed M/M intensities for Kern County earthquake of July 21, 1952 (2L = 60, C = 25, k = 1½). Contours of observed values from Murphy and Cloud (1954). Patterned areas indicate difference between observed and predicted intensity values.

defined area of intensity R/F IX for this earthquake. Figure 13 indicates the contrast in intensity maps that results when using Rossi-Forel and Modified Mercalli units. As noted earlier, there are sound reasons for abandoning the Modified Mercalli scale and reverting to the Rossi-Forel scale.

Our conclusion is that a model based on juxtaposition of zones of k equal to 1¾ and 1½ can satisfactorily explain the observations of intensity of the Kern County earthquake of 1952. In fact, we have been unable to explain the observations in any other way. The data of this earthquake constitute a beautiful confirmation of the existence of regions of varying k value, that is, of varying attenuation.

Another point that can be emphasized at this time is that these data are explained only by a model assuming a regional k value, combined with local ground condition responding to the energy delivered by the basement rocks. A model such as that used by Blume and associates (Blume and others, 1978) cannot accurately predict published intensity values from IX through IV. Their model must fail because it incorporates *local* ground condition as the ground condition controlling attenuation along the entire propagation path.

Finally, it should be noted that there is marked discrepancy between the magnitude value (7.1) associated with a 2L of 60 km for western California and the magnitude value (7.7) observed for this earthquake (Richter, 1955). This discrepancy between the observed magnitude and that predicted for such an earthquake in western California serves as confirmation of regional changes in attenuation and of the location of this earthquake in a region having a k value of 1½. This matter of interregional discrepancy between magnitude values and energy release was discussed in some detail in Evernden (1975, 1976) and is discussed further in a following section.

SEATTLE EARTHQUAKE OF 13 APRIL 1949 (MODIFIED MERCALLI INTENSITIES; MURPHY AND ULRICH, 1951)

Known parameters:

(1) k = 1½ (Evernden, 1975)

Unknown parameters:

(2) C value

(3) Location of epicenter

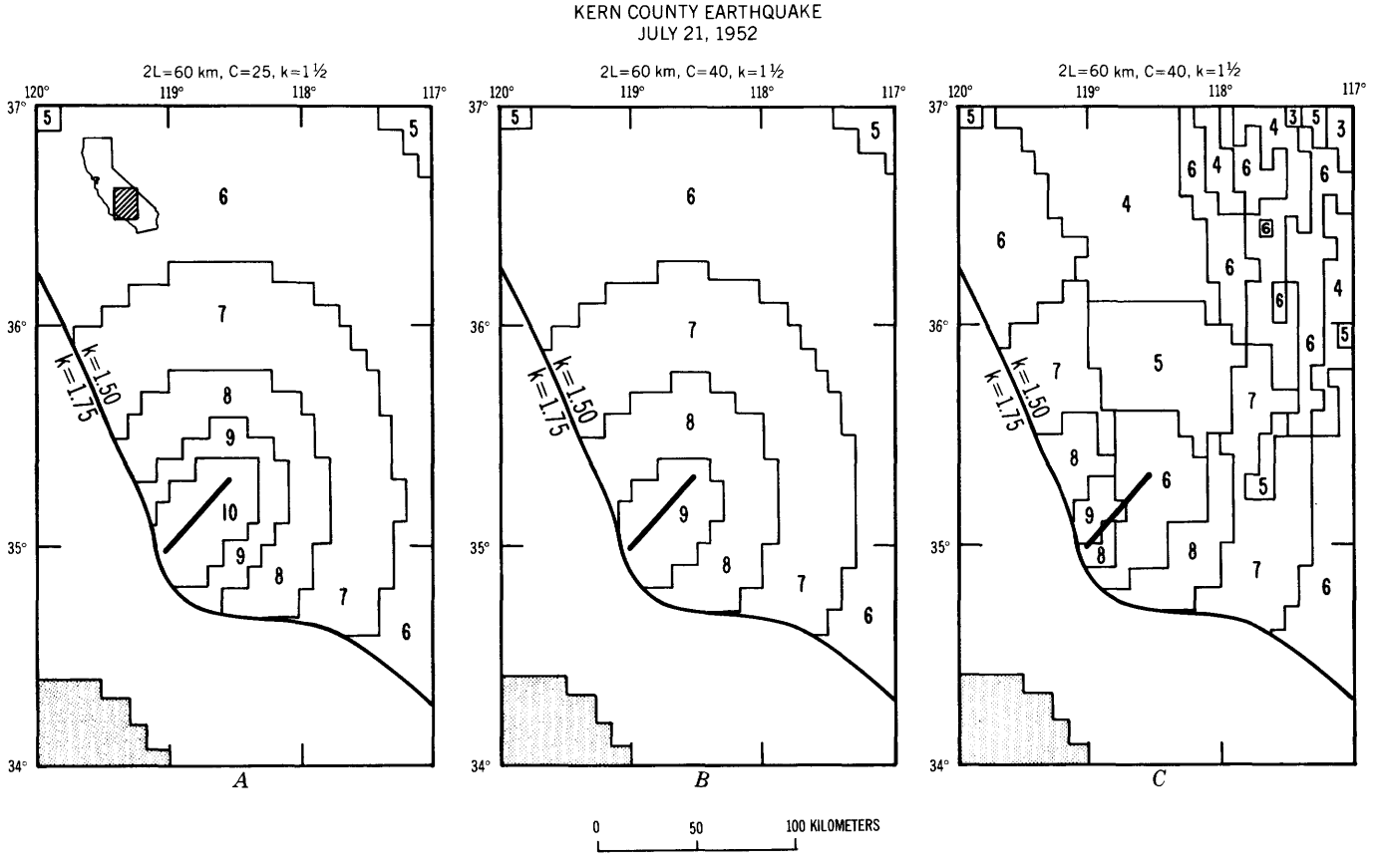

FIGURE 12.—Predicted M/M intensities for Kern County earthquake of July 21, 1952 (2L = 60, C = 25, k = 1½). *A*, C = 25 (saturated alluvium). *B*, C = 40 (saturated alluvium). *C*, C = 40 (6-minute by 6-minute ground condition).

(4) 2L value

This earthquake is the largest historical earthquake in the Seattle area. It is important to try to decide whether this is the maximum potential earthquake in the area. If not, can we estimate how large the maximum earthquake may be?

As for the Long Beach and Kern county earthquakes, use of the Modified Mercalli scale precluded reports of intensity IX for the Seattle earthquake.

As so many communities reported intensities for this earthquake, table 14 is limited to communities having population of 2,000 or greater in the 1960 census (National Atlas). It can be shown that a k value of 1.45 and a 2L of 40 km or a k value of 1.55 and a 2L of 100 km give very similar predictions and are nearly indistinguishable on the basis of available data. A recent study by Milne (1977), using observed accelerations in the Georgia Strait-Juan de Fuca Strait area for earthquakes of the region, found the appropriate attenuation factor (k value of the paper) to be 1.4, that is, in essential agreement with our analysis of the data of the Seattle earthquake. All calculations for table 14 were based on a k value of 1.50. All predicted intensity values not in parentheses are predicted for saturated alluvium. Intensity values in parentheses are predicted using the ground condition of the 25-km by 25-km grid of the United States map. Figures 14 and 15 present maps of predicted intensities (2L = 40 km and 2L = 100 km) for the northwestern United States for saturated alluvium and for the 25-km by 25-km

FIGURE 13.—Predicted Rossi-Forel and Modified Mercalli intensities for Kern County earthquake of July 21, 1952 (2L = 60, C = 25, k = 1½, 6-minute by 6-minute ground condition). *A*, Modified Mercalli. *B*, Rossi-Forel.

TABLE 14.—*Observed and predicted M/M intensities, Seattle earthquake*

[Population ≥ 2,000]

Sites	Observed intensity	Predicted intensity 2L=40	Predicted intensity 2L=100
Aberdeen	8	7	7
Auburn	8	7	8
Berkeley	8	7	8
Centralia	8	[2]7/8	8
Chehalis	8	8	8
Hoquiam	8	7	7
Kelso	8	7	8
Longview	8	7	8
Olympia	8	7	8
Puyallup	8	7	8
Richmond Beach	8	7	8
Seattle	8	7	8
Shelton	8	7	7
Tacoma	8	7/8	8
Tumwater	8	7	8
Arlington	7	7	7
Bremerton	7	7	7/8
Camas	7	7/6	7
Des Moines	7	7	7/8
Enumclaw	7	7	7/8
Everett	7	6/7	7
Kirkland	7	7	7
Seahurst	7	7	7/8
Vancouver	7	6/7	7
Astoria, Oreg.	7	7	7
Hillsboro, Oreg.	7	6	7
North Portland, Oreg.	7	6	7
Oregon City, Oreg.	7	6	7
Portland, Oreg.	7	6	7
Seaside, Oreg.	7	6	7
Anacortes	6	6	6
Bellingham	6	7	8(6)
Bryn Mawr	6	7	7(8/5)
Chelan	6	5	6
Mercer Island	6	7	8(8/5)
Montesano	6	7	7(6)
Omak	6	5	5/6
Port Townsend	6	6	7(5)
Prosser	6	6	6
Snohomish	6	6	7(7/4)
Spanaway	6	7	8
Baker, Oreg.	6	4	5
Beaverton, Oreg.	6	6	7(6)
Corvallis, Oreg.	6	5	6
Dallas, Oreg.	6	6	6
Forest Grove, Oreg.	6	6	7(6)
Gresham, Oreg.	6	6	7(6)
Lebanon, Oreg.	6	5	6
McMinnville, Oreg.	6	6	6/7(6)
Monmouth, Oreg.	6	6	6
Newberg, Oreg.	6	6	7(6)
Newport, Oreg.	6	5	6
Prineville, Oreg.	6	5	5/6
Redmond, Oreg.	6	5	6
Salem, Oreg.	6	6	6/7(5)
Silverton, Oreg.	6	6	6/7(5)
Tillamook, Oreg.	6	6	6/7(4/6)7.0
Toledo, Oreg.	6	5	6
Woodburn, Oreg.	6	6	7(6)
Bellevue	5	7	7(5/7)
Colfax	5	5	5
Colville	5	5	5
Ellensburg	5	6	6(4)
Marysville	5	6	6/7(4/7)
Pomeroy	5	5	5
Port Angeles	5	6	6(5)
Sedro-Woolley	5	6	6(5)
Spokane	5	4	5
Walla Walla	5	5	5
Wenatchee	5	6	6(4)
Yakima	5	6	6(4)
Albany, Oreg.	5	5	6(5)
Gresham, Oreg.	5	6	7(6)
Hood River, Oreg.	5	6	7(4)
La Grande, Oreg.	5	5	5
Milwaukie, Oreg.	5	6	7(4/6)
North Bend, Oreg.	5	5	5
The Dalles, Oreg.	5	6	6(4)
Eugene, Oreg.	4	5	5(5/3)
Saint Maries, Idaho	4	4	4/5
Sandpoint, Idaho	4	4	4

[1]Saturated alluvium—no parenthesis.
[2]Ground condition applied—parenthesis.

First value—correct square.
Second value—adjacent square.

ground condition. See the plates for correlation of latitude and longitude and of units of U.S. grid.

Note first that a 2L value of 40 km predicts intensity 7 at numerous sites where 8 was observed, 6 at 7, and 5 at 6, indicating that a 2L of 40 is certainly too short with a k of 1.50. For a 2L of 100 km, the suggestion is that too-high values are being predicted. Though the intensity values given in parentheses are invariably as low or lower than observed (implying that ground condition may be the explanation for the observed values being lower than the intensity values predicted for saturated alluvium), it still seems that too many predictions are high. We conclude that a 2L value of about 75 km is appropriate for this earthquake when using a k value of 1.50.

To obtain the intensity values of table 14 required use of a C value of 60, a larger value than used for any other U.S. earthquake. As C is linked to depth of focus, becoming larger as depth increases, the requirement for a value of 60 for C means that intensity data are sensitive to depth of focus in the range 10–70 km. Nuttli (1951) reported a depth of focus of 70 km for this earthquake. The data of his paper do not allow evaluaton of the accuracy of that depth estimate, and there are no short-range S-P data for establishment of time of origin and thus of depth. There seems to be no doubt, however, that the depth was in the range 40–70 km, so an unusual C value for a U.S. earthquake is in agreement with an unusual depth for a U.S. earthquake.

A few reported intensity values are not explainable, such as the one at Baker, Oreg., where a VI was reported even though a 2L of 100 predicts only a 5.1. In addition, the paucity of reports of intensity IV is surprising. Where IV was reported, it was predicted. However, there is a vast area where IV is predicted, extending well into Montana and the northern Sacramento Valley of California, and from which there are no reports in Murphy and Ulrich (1951). It may be that distance from the epicenter was so great (800–900 km) that people were not canvassed or that they failed to

associate shaking at intensity IV level with the Seattle earthquake.

The 2L of about 75 found when using k of 1½, when considered in light of the discussion in Evernden (1975), implies that this earthquake is essentially the largest that can occur in the Seattle area. The only possibility for more severe shaking is to have a comparable earthquake occur at a shallower depth. For illustration, we present below predicted intensities for an earthquake of 2L = 75 km at various depths (C values), the shallowest event having a C value equal to that found appropriate for earthquakes of western California. Intensities are as predicted for saturated alluvium, Y = distance parallel to fault from center of fault, X = distance from line of fault. The column headed "I(X = 0, Y = 0)" indicates predicted R/F and M/M intensities at the center of the break. The columns headed "X(km)(I = 8.5)" and "X(km) (I = 7.5)" indicate the perpendicular distances in kilometers from the center of the break to intensities 8.5 and 7.5 on both the R/F and M/M scales.

	I(X = Y = 0)		*X(km)(I = 8.5)*		*X(km)(I = 7.5)*	
C	*R/F*	*M/M*	*R/F*	*M/M*	*R/F*	*M/M*
25	10.5	10.5	74	48	132	68
40	9.7	9.4	62	27	128	60
60	9.0	8.3	43	--	120	51

It is clear that occurrence of an event like the one of April 13, 1949 at a depth of 5 to 10 km would be a drastically different experience for the Puget Sound area than was the actual event. The item for serious research in the Seattle area is determination of

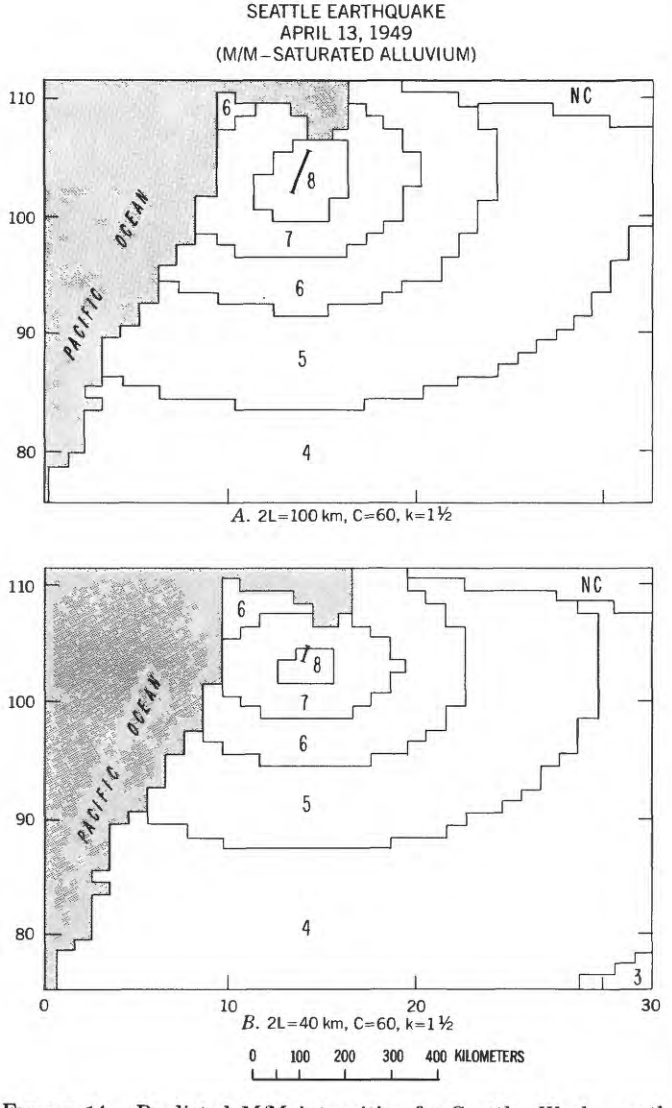

FIGURE 14.—Predicted M/M intensities for Seattle, Wash., earthquake of April 13, 1949, saturated alluvium. *A*, 2L = 100, C = 60, k = 1½. *B*, 2L = 40, C = 60, k = 1½. NC, not contoured.

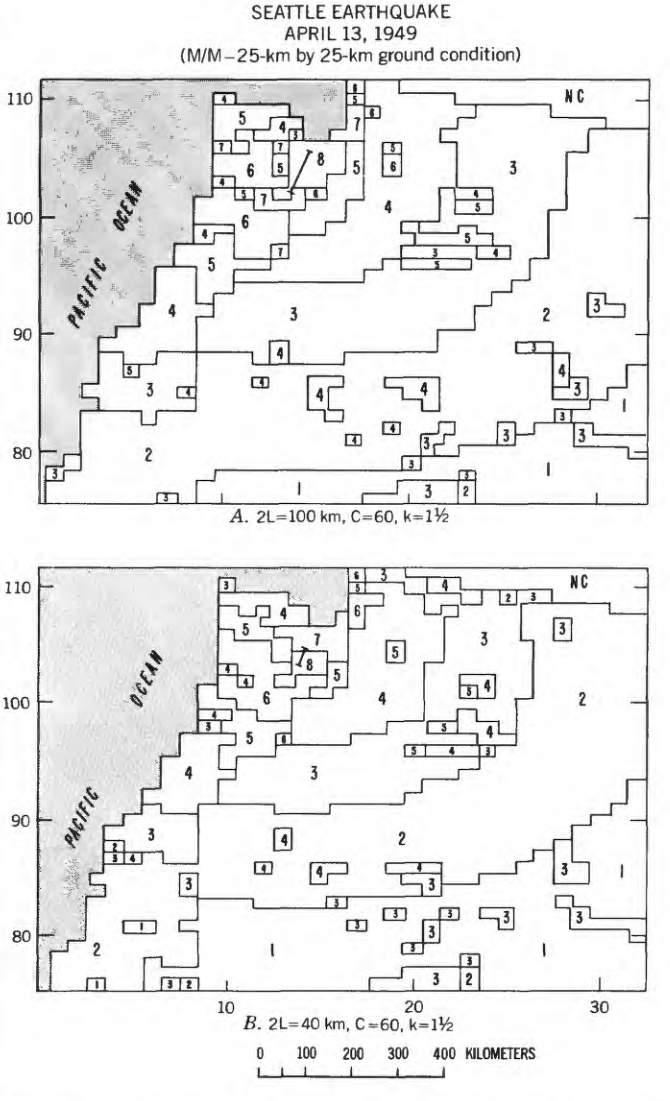

FIGURE 15.—Predicted M/M intensities for Seattle earthquake of April 13, 1949, 25-km by 25-km ground condition. *A*, 2L = 100, C = 60, k = 1½. *B*, 2L = 40, C = 60, k = 1½. NC, not contoured.

whether earthquakes comparable to 1949 can occur at shallower depths.

LOMPOC EARTHQUAKE OF NOVEMBER 4, 1927 (ROSSI-FOREL INTENSITIES; BYERLY, 1930)

Assumed parameters:
(1) k = 1¾ (western California)
(2) C = 25 (normal depth)
Unknown parameters:
(3) Location
(4) 2L

The location of this earthquake published by Byerly (1930) is far offshore. The purpose of the initial investigation of this earthquake was to ascertain whether the observed isoseismals were consistent with such an epicenter. Figure 16*A* gives observed intensities along with intensities predicted for a fault passing through Byerly's epicenter with a fault break of 600 km oriented parallel to the coast (that is, along the structural trend in this part of California). Figure 16*B* shows the results for a fault passing through Byerly's epicenter with a fault break of 600 km oriented east-west and reaching within 5 km of Point Arguello (no onshore faulting was observed). Figure 16*A* shows what is certainly an excessively long break, but it was used to illustrate the impossibility of reaching the observed intensities for such a location and orientation of faulting no matter what the length of break. Figure 16*B* illustrates that one way to attain high predicted onshore intensities is to have the end of a long fault near Point Arguello. However, this specific model has no credibility when considered in terms of the tectonics of the region. The predicted and observed intensities for this model have many similarities, but other models achieve better agreement with isoseismals and tectonic style.

Hanks (1978) calculated the epicenter on the basis of S and P data from stations in southern California (fig. 17). Three different fault models were put through this epicenter. The first (fig. 17*A*; 2L = 300 km parallel to shoreline) was to illustrate the inability of any fault through this epicenter and parallel to the San Andreas fault to explain the observed isoseismals. This model does not predict any onshore IX values. It gives VIII values in much of the region in which VIII was observed but, in so doing, it predicts VIII, VII, and VI values far north of where they were observed.

The second model based on Hanks' epicenter (fig. 17*B*) hypothesizes a 2L of 300 km oriented east-west with the fault break reaching within 5 km of shore. Though this fault does predict IX values as observed, it

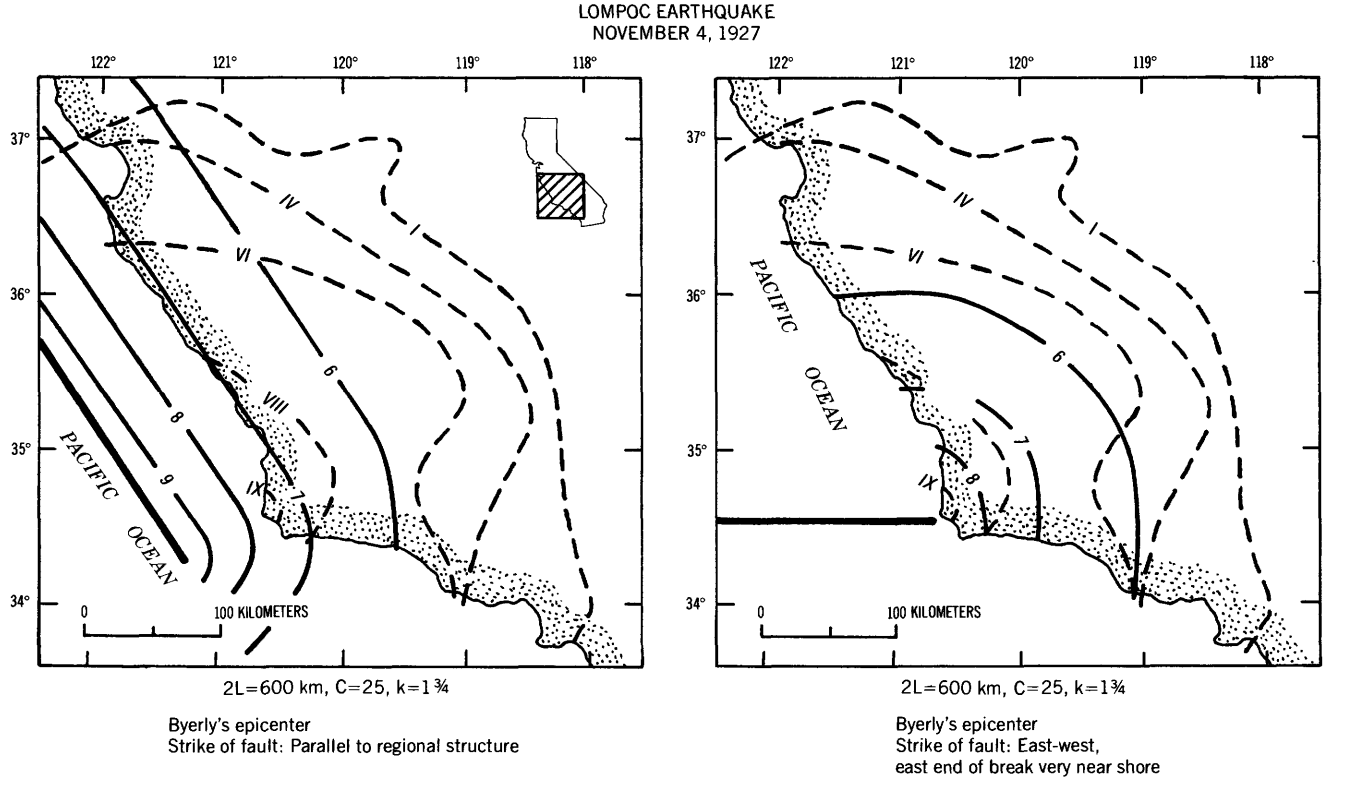

FIGURE 16.—Predicted (arabic numerals) and observed (roman numerals) R/F intensities for Lompoc, Calif., earthquake of November 4, 1927. *A*, Based on hypothetical fault through Byerly's epicenter (Byerly, 1930) and parallel to shoreline (2L = 600, C = 25, k = 1¾). *B*, Based on hypothetical fault through Byerly's epicenter and oriented east-west (2L = 600, C = 25, k = 1¾).

badly fails to predict VIII, VII and VI values.

The third model based on Hanks' epicenter (fig. 18) has a 2L of 80 km and an orientation as shown and as suggested by Hanks. Even when all observed VI values are treated as having been at sites on saturated alluvium, the predicted VI area is less than half that observed. There are no onshore IX values predicted, and the predicted VIII area is less than half that observed.

The basic failing of these models is placement of the fault too far offshore. Any tectonically credible orientation at such locations fails to generate sufficiently high intensities onshore. Even the tectonically incredible east-west faults fail in detail to predict observations. The actual fault break must have been near shore and must have been nearly parallel to the shoreline (no onshore fracturing), while the size of isoseismals requires a break length of several tens of kilometers.

Figure 19 presents the first effort to place the fault break so as to satisfy the isoseismals (2L = 125 km). A major point of this model and of all others that attempt to explain observations is placement of the south end of the break near Point Arguello in order to explain the observed IX values in this area. The main difference between this model and the one described below is its more northwesterly strike. The result is greater separation of faulting and shoreline northward and the resultant need for a greater fault length to explain onshore intensities. Though Figure 19 does indicate satisfactory agreement of observed and predicted VI values, the predicted area of VIII may be too small. Predicted areas of IV and V show great disagreement with reported observations.

Next, we model the fault break as suggested by Gawthrop (1978) along the Hosgri fault. The 2L length of 80 km was arrived at by trying several lengths between 50 and 125 km. Figure 20*A* shows intensities predicted for saturated alluvium, while Figure 20*B* shows intensities as predicted using the 6-minute by 6-minute ground-condition units. Figure 20*A* shows excellent agreement between observation and prediction for intensities VI and VIII.

Figure 20*B* indicates marked shrinkage of the area of predicted intensity VIII, probably because some areas of saturated alluvium were ignored by the 6-minute by 6-minute grid. All intensity IX values have disappeared for similar reasons. When the ½-minute by ½-minute grid is used, predicted intensity IX values extend from Point Arguello northward along the coast as far as they do on Figure 20*A*.

An apparent failing of the last two models is that they predict too large an area of intensity IX. Many of

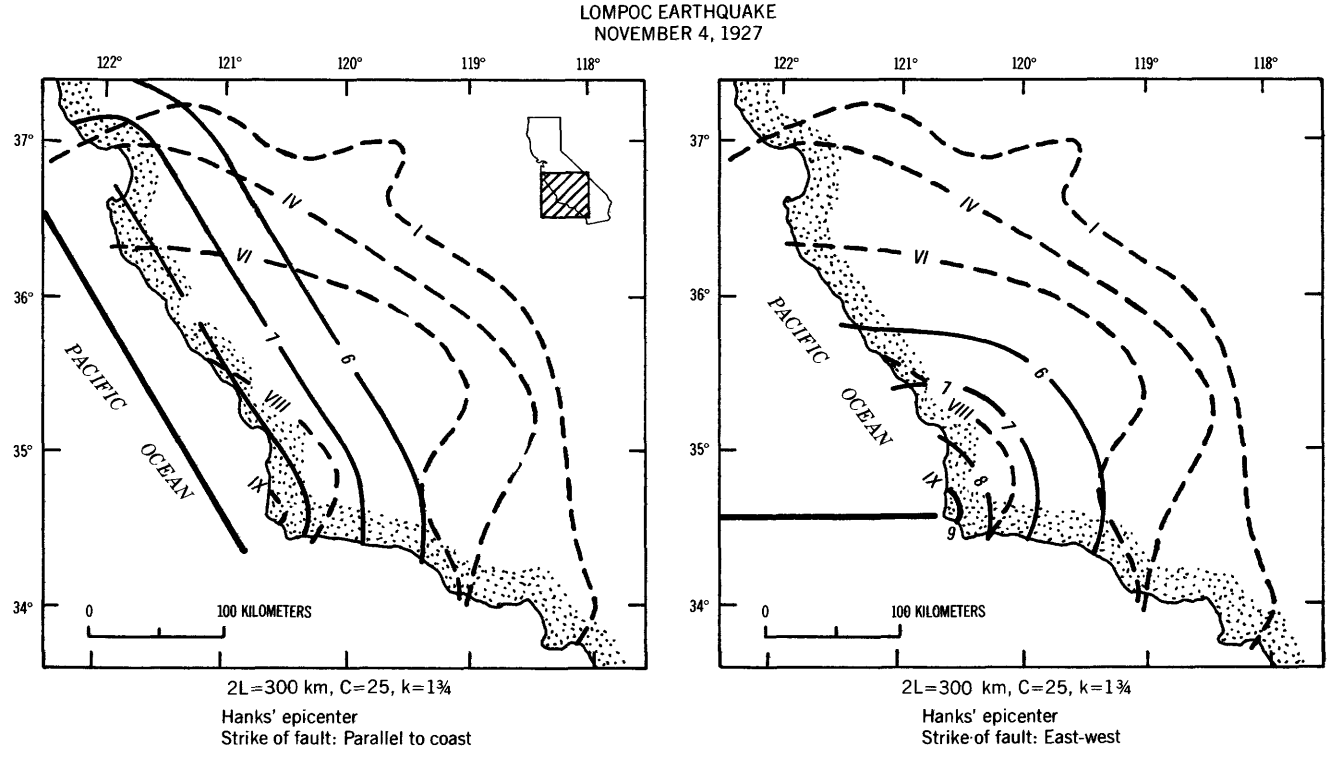

FIGURE 17.—Predicted and observed R/F intensities for Lompoc earthquake of November 4, 1927. *A*, Based on hypothetical fault through Hanks' epicenter and parallel to shoreline (2L = 300, C = 25, k = 1¾). *B*, Based on hypothetical fault through Hanks' epicenter and oriented east-west (2L = 300, C = 25, k = 1¾).

the IX values are predicted along the beach and in sand-dune areas where there probably were no people at the time of the earthquake and where our use of the J category for all alluvium is in error. The other areas of predicted IX at some distances from the shore are along streams and rivers. Flowing water is seldom seen in these rivers, and some may have no surface runoff for years at a time. Building sites have not been developed in these river courses, however, because when there is enough rain to produce surface runoff, flooding is common. The absence of dwellings suggests the likelihood that no basis for observations existed. Also, low water saturation and the physical characteristics of the alluvial materials (cobbles in sand) would imply intensities below those expected for saturated alluvium. Therefore, we do not believe that differences between observed and predicted IX values are a basis for rejecting either of the last two models.

This conclusion requires that at such stations as Betteravia (VIII vs. 8.9), Casmalia (VIII vs. 9.0), Lompoc (VIII vs. 8.8), and Oceano (VIII vs. 8.9), for all of which Byerly reported intensity VIII, and all of which are shown as alluvium on the ½-minute by ½-minute grid and thus are treated as on saturated alluvium in the calculations, predicted values were too high because the ground at these sites was somewhat less sensitive than saturated alluvium. The major remaining task relative to our program for predicting intensities is to identify and properly characterize various types of alluvium.

Hanks, on the basis of seismological arguments about S-P intervals and the consequent restraints on potential epicenters, suggested the shortening of the fault shown in figure 20*C*. The resultant predictions are in serious disagreement with observations, the predicted area of VI being half that observed, and the predicted area of VIII being a third or less of that observed.

As we did for several other earthquakes, we investigated the Lompoc earthquake by using site-intensity values. Table 15 lists sites for which Byerly reported Rossi-Forel intensities of VI or greater. The faults modeled (shown in figure 21) can be described as follows:

(A) Hosgri fault—70-km break

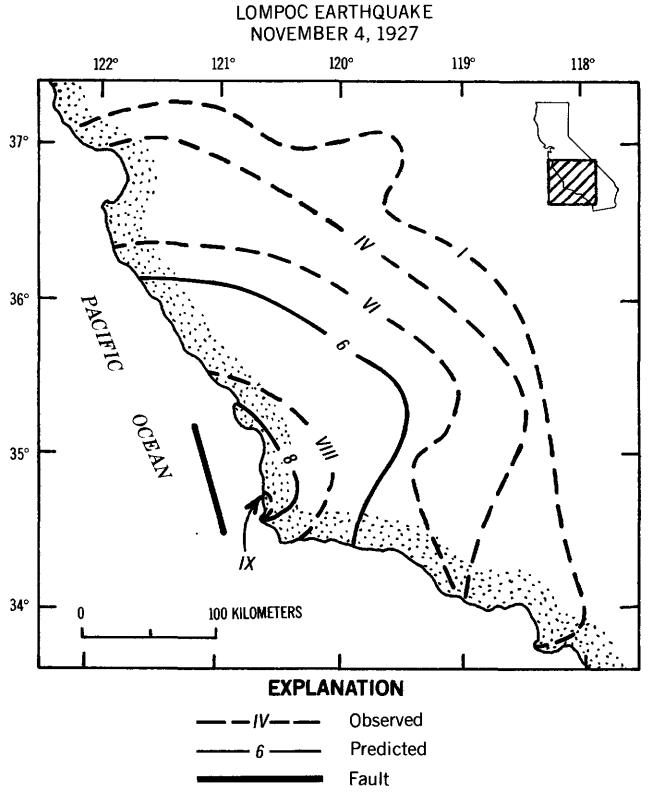

FIGURE 18.—Predicted and observed R/F intensities for Lompoc earthquake of November 4, 1927, based on hypothetical fault through Hanks' epicenter with length and orientation as suggested by Hanks (2L = 80, C = 25, k = 1¾).

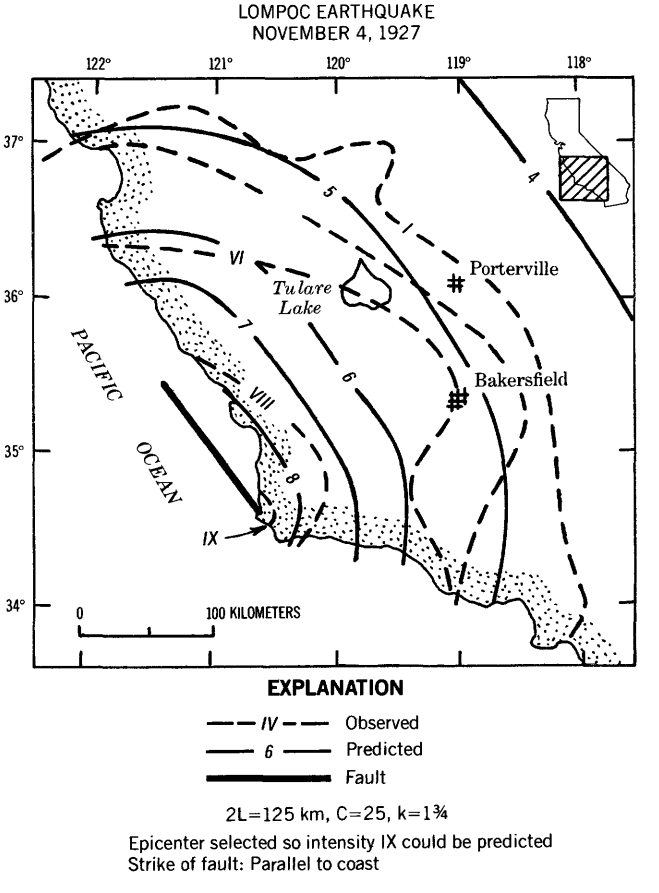

FIGURE 19.—Predicted and observed R/F intensities for Lompoc earthquake of November 4, 1927, based on hypothetical fault placed so as to yield isoseismals in agreement with observations (2L = 125, C = 25, k = 1¾). Intensities as predicted on saturated alluvium.

(B) Hosgri fault—52-km break (9 km off each end of (A))

(C) Hosgri fault—25-km break (center third of (A))

(D) Location suggested by Hanks—80-km break

The observed and predicted intensities for these several models are given in table 15. Two modes of analysis seem justified, the one chosen depending upon one's point of view: (A) The first is to select the model for which the average predicted intensity for stations within a given intensity bandwidth is equal to the central intensity value of that bandwidth. Under ideal conditions, the same model will achieve such agreement or near agreement for all bandwidths; (B) The second is to select as small an earthquake as possible such that no (or nearly no) observed intensities are greater than predicted intensities on saturated alluvium. A model in which more than a very few observed intensities are greater than those predicted on saturated alluvium is inadmissible because no perturbation of ground condition permissible within the model could explain such stations.

For analysis of mode A, consider table 16A. The headings of the last three columns indicate observed intensity and center intensity of each bandwidth. S/A and G/C indicate whether calculations of intensity were based on saturated alluvium (S/A) or ground condition (G/C) as on ½-minute by ½-minute ground-condition data. Using the latter values, table 16A indicates that fault D is systematically predicting av-

TABLE 15.—*Predicted and observed intensity values at specific sites, Lompoc earthquake of November 4, 1927*

Site	Population 1977	Fault A		Fault B		Fault C		Fault D	
		S/A	G/C	S/A	G/C	S/A	G/C	S/A	G/C
Intensity IX									
Surf	----	9.3	8.3	9.0	8.0	8.2	7.2	8.4	7.4
Honda	----	9.2	9.2	8.8	8.8	7.9	7.9	8.5	8.5
Intensity VIII									
Arlight	----	9.1	9.1	8.6	8.6	7.7	7.7	8.5	8.5
Arroyo Grande	7,500	8.7	7.7	8.6	7.6	8.1	7.1	7.9	6.9
Betteravia	400	8.9	8.9	8.7	8.7	8.3	8.3	8.0	8.0
Cambria	1,000	7.5	7.5	7.1	7.1	6.4	6.4	7.7	7.7
Casmalia	250	9.0	9.0	8.9	8.9	8.4	8.4	8.1	8.1
Cayucos	1,000	8.2	6.0	7.7	5.5	6.9	4.7	8.0	4.8
Conception	----	8.3	6.8	7.8	6.3	7.0	5.5	7.8	6.3
Guadalupe	3,100	9.0	9.0	8.9	8.9	8.5	8.5	8.1	8.1
Halcyon	----	8.7	7.7	8.6	7.6	8.1	7.1	7.9	6.9
Harriston	----	8.9	7.9	8.7	7.7	8.0	7.0	7.9	6.9
Huasna	----	8.8	7.3	7.8	6.3	7.4	5.9	7.3	5.8
Lompoc	25,300	8.8	8.8	8.5	8.5	7.7	7.7	7.9	7.9
Los Alamos	800	8.1	6.6	7.9	6.4	7.3	5.8	7.4	5.9
Los Olivos	200	7.6	7.6	7.3	7.3	6.7	6.7	6.9	6.9
Morro Bay	7,100	8.6	8.6	8.1	8.1	7.3	7.3	8.2	8.2
Nipomo	3,600	8.5	8.5	8.4	8.4	8.0	8.0	7.1	7.1
Pismo Beach	4,000	8.9	7.4	8.7	7.2	8.2	6.7	8.1	6.6
Oceano	2,600	8.9	8.9	8.7	8.7	8.3	8.3	8.1	8.1
San Luis Obispo	34,500	8.6	7.6	8.3	7.3	7.7	6.7	8.0	7.0
Santa Maria	32,700	8.5	8.5	8.4	8.4	8.0	8.0	7.7	7.7
Intensities VI and VII									
Adelaida	----	7.3	5.8	6.9	5.4	6.3	4.8	7.2	5.7
Atascadero	10,300	7.8	6.3	7.4	5.9	6.8	5.3	7.5	6.0
Bakersfield	69,500	5.3	5.3	5.2	5.2	4.7	4.7	5.1	5.1
Buellton	250	7.8	7.8	7.5	7.5	6.9	6.9	7.1	7.1
Buttonwillow	950	5.9	5.9	5.7	5.7	5.2	5.2	5.6	5.6
Carpinteria	7,000	6.0	6.0	5.8	5.8	5.3	5.3	5.8	5.8
Cholame	15	6.6	6.6	6.4	6.4	5.8	5.8	6.4	6.4
Creston	----	7.5	6.5	7.2	6.2	6.6	5.6	7.1	6.1
Gaviota	75	7.7	6.2	7.3	5.8	6.6	5.1	7.1	5.6
Goleta	5,000	6.7	6.7	6.4	6.4	5.8	5.8	6.3	6.3
Harmony	5	7.8	5.6	7.3	5.1	6.6	4.4	7.9	5.7
King City	3,400	5.8	5.8	5.5	5.5	4.9	4.9	5.9	5.9
Las Cruces	25	7.8	6.3	7.4	5.9	6.7	5.2	7.2	5.7
Naples	----	7.0	5.5	6.7	5.2	6.1	4.6	6.6	5.1
Oxnard	85,000	5.4	5.4	5.2	5.2	4.7	4.7	5.3	5.3
Paso Robles	7,200	7.3	7.3	7.0	7.0	6.3	6.3	7.1	7.1
Reward	----	6.2	6.2	6.1	6.1	5.6	5.6	5.9	5.9
Santa Barbara	70,200	6.4	6.4	6.1	6.1	5.6	5.6	6.1	6.1
Santa Ynez	350	7.4	7.4	7.2	7.2	6.6	6.6	6.9	6.9
Santa Margarita	1,000	8.1	6.6	7.8	6.3	7.1	5.6	7.6	6.1
Solvang	1,500	7.6	7.6	7.3	7.3	6.7	6.7	7.0	7.0
Taft	4,300	6.0	6.0	5.8	5.8	5.4	5.4	5.7	5.7
Templeton	900	7.6	7.6	7.2	7.2	6.6	6.6	7.4	7.4
Ventura	58,000	5.7	5.7	5.4	5.4	4.9	4.9	5.4	5.4
Wasioja	----	7.0	5.2	6.9	5.1	6.4	4.6	6.6	4.8

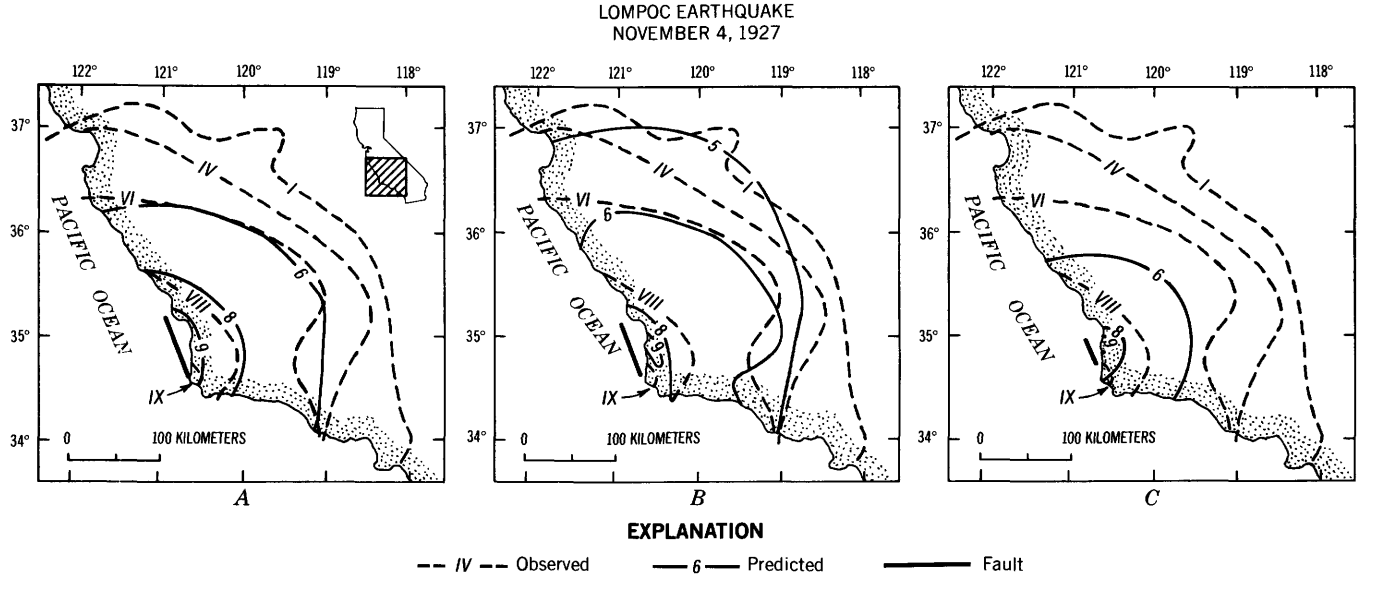

FIGURE 20.—Predicted and observed R/F intensities for Lompoc earthquake of November 4, 1927. *A*, Based on location of Hosgri fault with placement and length of break chosen so as to predict isoseismals in agreement with observations (2L = 80, C = 25, k = 1¾). Intensities as predicted on saturated alluvium. *B*, Same as *A*, but intensities as predicted using ground condition of 6-minute by 6-minute grid. *C*, Based on location of Hosgri fault with northward extent of break controlled by S-P arguments of Hanks (1978).

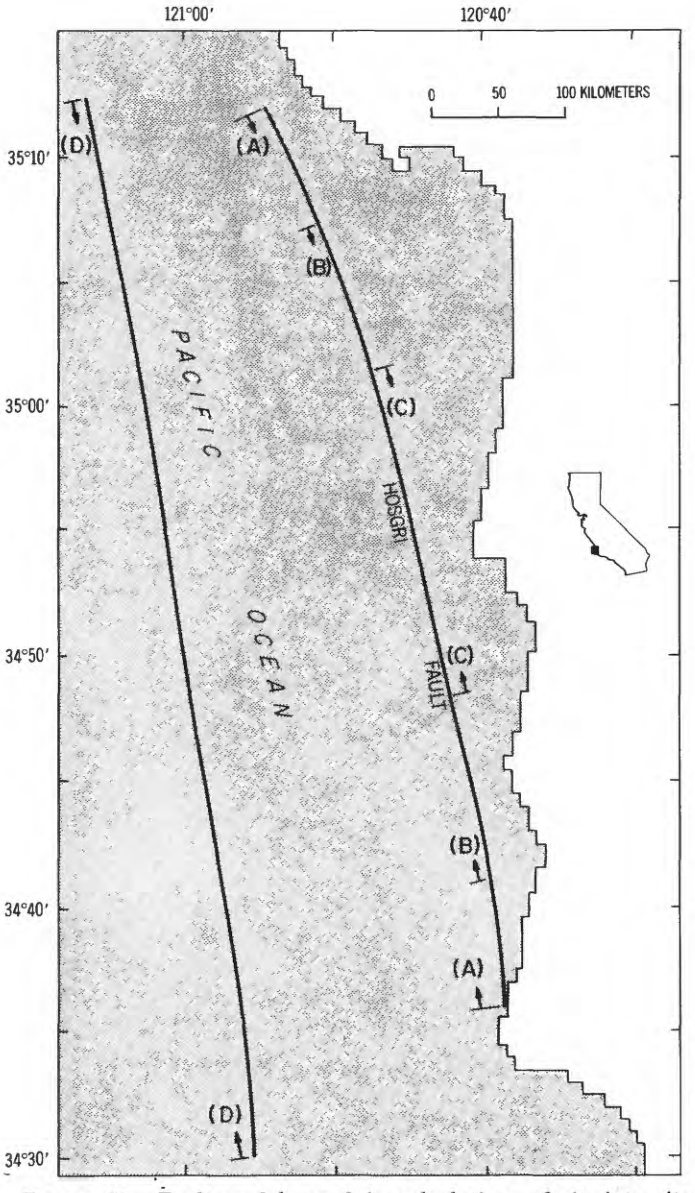

FIGURE 21.—Fault models used in calculations of site-intensity values (table 15) for Lompoc earthquake of November 4, 1927.

erage intensities that are too low. Any shorter fault break along this same line would show greater disagreement. As in the previous analysis, the intensity data appear to reject any location for the Lompoc earthquake as far at sea as that suggested by Hanks.

Fault A gives the best agreement of average predicted and central intensity value in each bandwidth; B and C yield values that are too low. From these data, too, a break of almost 70 km along the Hosgri fault is suggested.

For analysis of mode B, consider table 16B. The number following the intensity value in the headings is the number of reporting stations in each bandwidth. High predictions under S/A are deemed permissible, low predictions under S/A are not permissible. We might expect a nearly equal number of low and high predictions under G/C. With less certainty, fault D is again rejected because 1 of 2 and 3 of 20 stations were predicted low even when assuming S/A conditions. As in other modes of analysis, fault A satisfies the mode of interpretation best. There are no L values for VIII and IX and only 2 of 25 for VI–VII under S/A conditions, while there are similar H and L values under G/C conditions.

TABLE 16.—*Average predicted intensities for saturated alluvium and ½-minute by ½-minute ground-condition units, Lompoc earthquake, using two sets of intensity data*

A

Fault	2L (km)	IX (9.0) S/A	IX (9.0) G/C	VIII (8.0) S/A	VIII (8.0) G/C	VI–VIII (6.5) S/A	VI–VIII (6.5) G/C
A	70	9.25	8.75	8.58	7.95	6.83	6.27
B	52	8.90	8.40	8.31	7.68	5.49	6.03
C	25	8.05	7.55	7.70	7.07	- -	- -
D	80	8.45	7.95	7.86	6.23	6.55	5.99

B

Fault	2L	IX (2) S/A	IX (2) G/C	VIII (20) S/A	VIII (20) G/C	VI–VII (25) S/A	VI–VII (25) G/C
A	70	OH/OL	OH/1L	13H/OL	7H/4L	7H/2L	3H/4L
B	52	OH/OL	OH/1L	9H/2L	5H/8L	1H/2L	OH/7L
C	25	2L	2L	OH/7L	OH/12L		
D	80	OH/1L	OH/1L	OH/3L	OH/10L	2H/3L	OH/4L

H = Prediction above bandwidth
L = Prediction below bandwidth

Finally, we analyze the intensity data of the Lompoc earthquake via the previously described statistical model and present calculations of CP, $s.d._{CP}$, and R.M.S.

Table 17 presents calculations based on a k of 1.750, 2L values of 50, 60, 70, 80, 90, and 100 km, and S and T values of −30, −20, −10, 0, 10, and 20 km. For "observed" intensity values in calculations for these tables, we used the midpoint of each band defined by Byerly (1930)(IX, VIII, VII–VI, and V–IV.) As a matter of fact, nearly every point in band V–IV is certainly within the area of intensity V. Therefore, we redid all the calculations using an "observed" value in the (V–IV) band of 5.0 rather than 4.5 and obtained the results in table 18. Because of the possibility that a k value of 1.750 might be slightly in error, and because we were uncertain of the impact of such an error on the predicted fault parameters, we redid most of the calculations using a k value of 1.6750. The results of this procedure are shown in tables 19 and 20.

On all of these tables, we have marked the zone of geologically "acceptable" solutions, the definition of acceptability being that the fault break does not intersect land nor does the fault line extend into the Santa Barbara Channel. We consider any offshore position of the fault to be "acceptable." The reference fault line used is as shown on figure 21 with the following changes: (a) northward, the fault is extended according to published maps; (b) southward, it is extended arbitrarily along its general strike into the Santa Barbara Channel. This is done simply to provide the basis for calculations. The reference coordinates (S = 0,

T = 0) are at lat 34°55.0'N., long 120°44.3'W., that is, at the center of the Hosgri fault as shown on figure 21.

Table 17 indicates that a broad range of solutions yielding low values of CP and $s.d._{CP}$ are found when using k = 1.750. All 2L values are found to yield CP values of around 0.10 at some combination of 2L, T, and S, all minima on all tables being geologically unacceptable. The minimum CP at an acceptable site is 2L = 70, S = 0, T = 0 with an $s.d._{CP}$ = 0.019. In a partial search for a true minimum, a CP of 0.147 with $s.d._{CP}$ = 0.011 was found for 2L = 70, S = 0, T = 4. Thus, even 2L = 70, S = 0, T = −10 is strongly rejected (d = (0.329−0.177)/0.019=8.0), while a location 30 km offshore is clearly impossible. The only other acceptable coordinates having a low CP value are 2L = 60, S = 0, T = 0.

Table 18 (V–IV band treated as V band and termed MODIFIED on tables), shows a great reduction in CP values, implying that the change made in treatment of the (V–IV) band was appropriate. No low CP values are found for 2L = 50, but a long band of low CP values are found for all other 2L values, nearly all of them being geologically inadmissible. Geologically admissible low CP values are found for 2L = 90, S = 10, T = 0, and 2L = 80, S = 10, T = 0. The actual approximate minimum for 2L = 80 is at S = 10, T = 2, with CP = 0.029 and $s.d._{CP}$ = 0.038. Values of CP as high as 0.10 are rejected.

Table 19 gives calculations for k = 1.675 and band (V–IV) treated as (V–IV). The most significant result is that essentially all CP values are higher than for similar calculations when using k = 1.750. No CP values as low as 0.20 are found, while values below 0.10 were found in table 18. As expected, minima at each 2L move westward and the length of fault with the minimum CP gets shorter. However, the coordinates having minimum CP values are still near T = O. Thus, the smallest CP values at 2L = 60 are all at T = O. The smallest CP (0.206) at 2L = 50 is as S = −10, T = 0 while slightly lower values (0.186 and 0.163) are at geologically unacceptable locations (S = −, T = 10; S = −20, T = 10). Again, any location more than a few kilometers west of the minimum is rejected.

Table 20 shows calculations for k=1.675 and band (V–IV) treated as band (V). An interesting phenomenon here is the disappearance of the long line of similar CP minima that characterized nearly all values of 2L when using k = 1.750. No low CP minima are found for 2L = 80 and 70, while there is only a small region of CP minima for 2L = 60 (S = 0, T = 0; S = −10, T = 0; S = −20, T = 0), only points S = 0, T = 0 and S = −10, T = 0 being geologically acceptable. Low minima are found for 2L = 50 at geologically unacceptable coordinates.

This phenomenon, a line of minima on S versus T

TABLE 17.—*Calculated parameters for the Lompoc earthquake using midpoint of Byerly's (1930) "observed" intensity bands*

A

Reference fault: Hosgri Reference Center: 34°55.0'N 120°44.3'W
k = 1.750 2L = 50 C = 25
Bands Used: IX, VIII, VII–VI, V–IV
Upper Values: CP Lower Values: $s.d._{CP}$

S \ T	−30	−20	−10	0	10	20	30
30	.978	—	.660	.517	.420	.402	.470
	.920	—	.577	.421	.312	.293	.366
20						(.029)	(.022)
	.888	—	.524	.354	.230	.204	.281
10						(.030)	(.021)
	.884	—	.510	.329	.185	.140	.216
0						(.038)	(.022)
	.908	—	.537	.356	.198	.115	.181
−10					(.099)	(.058)	(.028)
	.957	—	.594	.412	.253	.145	.185
−20					(.106)	(.085)	(.039)
	1.026	.672	.495	.336	.219	.231	
−30							

B

Reference fault: Hosgri Reference Center: 34°55.0'N 120°44.3'W
k = 1.750 2L = 60 C = 25
Bands Used: IX, VIII, VII–VI, V–IV
Upper Values: CP Lower Values: $s.d._{CP}$

S \ T	−30	−20	−10	0	10	20	30
	.885	—	.574	.444	.368	.376	.457
30					(.021)	(.012)	(.012)
	.823	—	.484	.342	.264	.280	.367
20							
	.784	—	.420	.262	.179	.205	.294
10				(.037)			
	.772	—	.390	.214	.116	.150	.239
0				(.048)	(.014)	(.036)	(.027)
	.787	—	.399	.211	.085	.111	.203
−10				(.067)	(.029)	(.041)	(.030)
	.827	—	.446	.256	.105	.091	.184
−20					(.063)	(.015)	(.021)
	.887	—	.520	.337	.177	.119	.194
−30						(.037)	(.014)

C

Reference fault: Hosgri Reference Center: 34°55.0'N 120°44.3'W
k = 1.750 2L = 70 C = 25
Bands Used: IX, VIII, VII–VI, V–IV
Upper Values: CP Lower Values: $s.d._{CP}$

S \ T	−30	−20	−10	0	10	20	30
30	.824	—	.521	.405	.354	.386	.474
	.760	—	.431	.306	.268	.319	.407
20			(.033)	(.017)	(.020)		
	.720	—	.364	.228	.203	.280	.358
10			(.035)	(.016)	(.035)		
	.704	—	.329	.177	.159	.262	.323
0			(.042)	(.019)	(.052)		
	.713	—	.328	.159	.118	.230	.292
−10			(.51)	(.031)	(.054)	(.096)	
	.744	—	.359	.177	.087	.171	.252
−20				(.051)	(.020)	(.101)	(.064)
	.795	—	.419	.234	.105	.122	.219
−30					(.036)	(.035)	(.037)

TABLE 17.—*Calculated parameters for the Lompoc earthquake using midpoint of Byerly's (1930) "observed" intensity bands*—Continued

D

Reference fault: Hosgri Reference Center: 34°55.0'N 120°44.3'W
k = 1.750 2L = 80 C = 25
Bands Used: IX, VIII, VII–VI, V–IV
Upper Values: CP Lower Values: s.d.$_{CP}$

S \ T	−30	−20	−10	0	10	20	30
30	.777	—	.487 (.024)	.389 (.011)	.370 (.027)	.428	
20	.716	—	.400 (.022)	.302 (.011)	.313 (.046)	.400	
10	.675	—	.337 (.023)	.236 (.015)	.287 (.075)	.407	
0	.657	—	.302 (.027)	.191 (.016)	.271 (.087)	.397	
−10	.661	—	.293 (.034)	.162 (.011)	.228 (.090)	.358	
−20	.684	—	.309 (.045)	.154 (.019)	.161 (.090)	.292 (.098)	
−30	.725	—	.351	.179 (.041)	.110 (.031)	.204 (.105)	

E

Reference fault: Hosgri Reference Center: 34°55.0'N 120°44.3'W
k = 1.750 2L = 90 C = 25
Bands Used: IX, VIII, VII–VI, V–IV
Upper Values: CP Lower Values: s.d.$_{CP}$

S \ T	−30	−20	−10	0	10	20	30
30	.744	—	.469 (.016)	.393 (.015)	.411	.495	
20	.686	—	.391 (.013)	.324 (.025)	.393	.513	
10	.648	—	.335 (.013)	.276 (.034)	.402	.532	
0	.629	—	.301 (.015)	.238 (.038)	.383	.518	
−10	.627	—	.285 (.020)	.201 (.032)	.336 (.087)	.472	
−20	.641	—	.286 (.030)	.172 (.017)	.265 (.092)	.401	
−30	.672	—	.309 (.042)	.164 (.015)	.178 (.090)	.311	

F

Reference fault: Hosgri Reference Center: 34°55.0'N 120°44.3'W
k = 1.750 2L = 100 C = 25
Bands Used: IX, VIII, VII–VI, V–IV
Upper Values: CP Lower Values: s.d.$_{CP}$

S \ T	−30	−20	−10	0	10	20	30
30	.720	.581 (.021)	.465 (.010)	.417 (.041)	.479		
20	.667	.519 (.021)	.398 (.010)	.370 (.041)	.501		
10	.631	.476 (.021)	.352 (.010)	.341 (.053)	.512		
0	.610	.450 (.023)	.318 (.009)	.309 (.057)	.491		
−10	.603	.438 (.027)	.295 (.010)	.265 (.053)	.440		
−20	.610	.439 (.033)	.283 (.016)	.218 (.040)	.368		
−30	.630	.456 (.041)	.287 (.027)	.182 (.021)	.281 (.096)		

TABLE 18.—*Calculated parameters for the Lompoc earthquake using modified "observed" intensities*

A

Reference fault: Hosgri Reference Center: 34°55.0'N 120°44.3'W
k = 1.750 2L = 50 C = 25
Bands Used: IX, VIII, VII–VI, V–IV (MODIFIED)
Upper Values: CP Lower Values: s.d.$_{CP}$

S \ T	−30	−20	−10	0	10	20	30
30	1.154	—	.756	.562	.398	.317 (.096)	.360 (.073)
20	1.108	—	.696	.498	.332 (.116)	.233 (.122)	.258 (.081)
10	1.084	—	.661	.458	.290 (.112)	.192 (.118)	.190 (.105)
0	1.085	—	.653	.445	.274 (.112)	.173 (.118)	.166 (.120)
−10	1.111	—	.676	.464	.288 (.117)	.183 (.122)	.167 (.125)
−20	1.162	—	.732	.521	.343 (.125)	.231 (.130)	.201 (.133)
−30							

B

Reference fault: Hosgri Reference Center: 34°55.0'N 120°44.3'W
k = 1.750 2L = 60 C = 25
Bands Used: IX, VIII, VII–VI, V–IV (MODIFIED)
Upper Values: CP Lower Values: s.d.$_{CP}$

S \ T	−30	−20	−10	0	10	20	30
30	1.003	—	.589	.391	.244	.209 (.048)	.284 (.035)
20	.958	—	.530	.322	.148	.101 (.039)	.186 (.025)
10	.937	—	.497	.284	.107 (.108)	.016 (.024)	.107 (.014)
0	.940	—	.493	.275	.097 (.085)	.044 (.027)	.052 (.019)
−10	.968	—	.521	.301	.128 (.068)	.076 (.013)	.021 (.051)
−20	1.019	—	.579	.361	.175 (.119)	.087 (.038)	.023 (.114)
−30	1.090	—	.663	.451	.269 (.130)	.147 (.135)	.102 (.139)

C

Reference fault: Hosgri Reference Center: 34°55.0'N 120°44.3'W
k = 1.750 2L = 70 C = 25
Bands Used: IX, VIII, VII–VI, V–IV (MODIFIED)
Upper Values: CP Lower Values: s.d.$_{CP}$

S \ T	−30	−20	−10	0	10	20	30
30	.886	—	.469	.280	.168 (.036)	.178 (.012)	.267
20	.843	—	.398	.187 (.083)	.068 (.013)	.121 (.071)	.199
10	.824	—	.368	.144 (.100)	.041 (.105)	.151 (.110)	.168
0	.830	—	.369	.142 (.101)	.070 (.049)	.161 (.110)	.176
−10	.859	—	.402	.174 (.106)	.088 (.023)	.138 (.111)	.163
−20	.909	—	.461	.237 (.113)	.095 (.022)	.098 (.073)	.117
−30	.978	—	.543	.326	.138 (.124)	.059 (.012)	.040

TABLE 18.—*Calculated parameters for the Lompoc earthquake using modified "observed" intensities*–Continued

D

Reference fault: Hosgri Reference Center: 34°55.0'N 120°44.3'W
k = 1.750 2L = 80 C = 25
Bands Used: IX, VIII, VII–VI, V–IV (MODIFIED)
Upper Values: CP Lower Values: $s.d._{CP}$

S \ T	−30	−20	−10	0	10	20	30
30	.791	—	.379	.211	.153	.212	
			(.069)	(.043)	(.020)	(.060)	
20	.744	—	.298	.113	.137	.251	
			(.074)	(.035)	(.107)		
10	.725	—	.256	.043	.173	.290	
			(.090)	(.036)	(.102)	(.107)	
0	.733	—	.261	.026	.173	.294	
				(.099)	(.103)	(.108)	
−10	.763	—	.297	.063	.138	.263	
				(.103)	(.094)	(.112)	
−20	.812	—	.356	.127	.100	.201	
				(.110)	(.057)	(.119)	
−30	.877	—	.435	.213	.075	.110	
				(.117)	(.013)	(.114)	

E

Reference fault: Hosgri Reference Center: 34°55.0'N 120°44.3'W
k = 1.750 2L = 90 C = 25
Bands Used: IX, VIII, VII–VI, V–IV MODIFIED
Upper Values: CP Lower Values: $s.d._{CP}$

S \ T	−30	−20	−10	0	10	20	30
30	.717	—	.316	.179	.199	.306	.352
			(.052)	(.014)	(.077)		
20	.668	—	.235	.108	.257	.377	.392
			(.052)	(.023)	(.104)		
10	.646	—	.186	.086	.290	.415	.435
			(.059)	(.097)	(.100)		
0	.650	—	.174	.076	.283	.413	.441
			(.075)	(.098)	(.104)		
−10	.679	—	.205	.035	.242	.375	.411
			(.098)	(.101)	(.104)		
−20	.726	—	.263	.029	.173	.307	.349
			(.102)	(.091)	(.111)	(.116)	
−30	.788	—	.339	.112	.098	.216	.263
			(.108)	(.114)	(.075)	(.124)	

F

Reference fault: Hosgri Reference Center: 34°55.0'N 120°44.3'W
k = 1.750 2L = 100 C = 25
Bands Used: IX, VIII, VII–VI, V–IV MODIFIED
Upper Values: CP Lower Values: $s.d._{CP}$

S \ T	−30	−20	−10	0	10	20	30
30	.654	.455	.275	.186	.307		
			(.034)	(.026)	(.109)		
20	.608	.396	.203	.167	.371		
		(.058)	(.030)	(.082)			
10	.584	.362	.158	.186	.399		
		(.061)	(.030)	(.097)			
0	.582	.354	.136	.173	.388		
		(.068)	(.038)	(.096)			
−10	.601	.371	.138	.130	.342		
		(.079)	(.058)	(.099)			
−20	.642	.413	.091	.067	.273		
		(.094)	(.091)	(.104)	(.107)		
−30	.700	.478	.244	.014	.187		
			(.105)	(.068)	(.115)		

TABLE 19.—*Calculated parameters for the Lompoc earthquake using midpoint of Byerly's (1930) "observed" intensity bands*

A

Reference fault: Hosgri Reference Center: 34°55.0'N 120°44.3'W
k = 1.675 2L = 50 C = 25
Bands Used: IX, VIII, VII–VI, V–IV
Upper Values: CP Lower Values: $s.d._{CP}$

S \ T	−30	−20	−10	0	10	20	30
30	.745	.607	.480	.387	.354	.389	
20	.693	.543	.404	.304	.281	.329	
			(.025)	(.011)	(.028)		
10	.664	.504	.351	.241	.226	.290	
			(.028)	(.011)	(.040)		
0	.661	.495	.331	.206	.186	.262	
			(.035)	(.014)	(.046)		
−10	.684	.516	.347	.208	.163	.226	
			(.045)	(.026)	(.029)		
−20							
−30							

B

Reference fault: Hosgri Reference Center: 34°55.0'N 120°44.3'W
k = 1.675 2L = 60 C = 25
Bands Used: IX, VIII, VII–VI, V–IV
Upper Values: CP Lower Values: $s.d._{CP}$

S \ T	−30	−20	−10	0	10	20	30
30	.695	.567	.457	.395	.409	.477	
		(.022)	(.012)	(.017)			
20	.643	.504	.385	.327	.371	.462	
		(.023)	(.011)	(.024)			
10	.613	.464	.334	.274	.353	.458	
		(.026)	(.012)	(.031)	(.091)		
0	.605	.450	.309	.237	.324	.434	
			(.016)	(.030)			
−10	.620	.461	.312	.217	.267	.384	
		(.037)	(.023)	(.019)	(.095)		
−20							
−30							

C

Reference fault: Hosgri Reference Center: 34°55.0'N 120°44.3'W
k = 1.675 2L = 70 C = 25
Bands Used: IX, VIII, VII–VI, V–IV
Upper Values: CP Lower Values: $s.d._{CP}$

S \ T	−30	−20	−10	0	10	20	30
30	.670	.551	.459	.431	.498	.595	
		(.015)	(.011)	(.034)			
20	.620	.492	.395	.384	.502	.611	
		(.015)	(.012)	(.046)			
10	.590	.454	.350	.347	.492	.605	
		(.016)	(.013)	(.057)			
0	.579	.437	.322	.309	.457	.574	
		(.020)	(.011)	(.058)			
−10	.586	.439	.312	.269	.396	.518	
		(.025)	(.011)	(.047)			
−20							
−30							

TABLE 19.—*Calculated parameters for the Lompoc earthquake using midpoint of Byerly's 1930 "observed" intensity bands*–Continued

D
Reference fault: Hosgri Reference Center: 34°55.0'N 120°44.3'W
k = 1.675 2L = 80 C = 25
Bands Used: IX, VIII, VII–VI, V–IV
Upper Values: CP Lower Values: $s.d._{CP}$

S \ T	−30	−20	−10	0	10	20	30
30							
	.658	.550	.478	.491	.616	.729	
20		(.010)	(.018)	(.051)			
	.611	.497	.426	.468	.630	.747	
10		(.010)	(.023)	(.067)			
	.582	.462	.386	.445	.616	.737	
0	(.020)	(.010)	(.024)	(.079)			
	.568	.441	.356	.403	.575	.700	
−10	(.023)	(.012)	(.021)	(.081)			
	.568	.435	.334	.347	.511	.637	
−20		(.016)	(.015)	(.071)			
−30							

TABLE 20.—*Calculated parameters for the Lompoc earthquake using modified "observed" intensities*

A
Reference fault: Hosgri Reference Center: 34°55.0'N 120°44.3'W
k = 1.675 2L = 50 C = 25
Bands Used: IX, VIII, VII–VI, V–IV (MODIFIED)
Upper Values: CP Lower Values: $s.d._{CP}$

S \ T	−30	−20	−10	0	10	20	30
30							
20	.752	.564	.380	.224	.148	.174	
	.719	.519	.319	.143	.073	.141	
10				(.059)	(.032)		
	.717	.512	.302	.102	.063	.159	
0				(.100)	(.110)		
	.743	.536	.324	.120	.051	.150	
−10					(.090)	(.120)	
	.792	.588	.378	.175	.031	.104	
−20				(.118)	(.011)	(.120)	
−30							

B
Reference fault: Hosgri Reference Center: 34°55.0'N 120°44.3'W
k = 1.675 2L = 60 C = 25
Bands Used: IX, VIII, VII–VI, V–IV (MODIFIED)
Upper Values: CP Lower Values: $s.d._{CP}$

S \ T	−30	−20	−10	0	10	20	30
30							
	.638	.457	.290	.179	.199	.288	
20			(.042)	(.010)	(.075)		
	.598	.403	.218	.110	.227	.326	
10			(.045)	(.021)	(.106)		
	.586	.380	.178	.070	.238	.341	
0			(.057)	(.066)	(.107)		
	.604	.394	.180	.041	.218	.326	
−10			(.079)	(.107)			
	.649	.442	.226	.024	.162	.276	
−20			(.106)	(.054)			
−30							

TABLE 20.—*Calculated parameters for the Lompoc earthquake using modified "observed" intensities*–Continued

C
Reference fault: Hosgri Reference Center: 34°55.0'N 120°44.3'W
k = 1.675 2L = 70 C = 25
Bands Used: IX, VIII, VII–VI, V–IV (MODIFIED)
Upper Values: CP Lower Values: $s.d._{CP}$

S \ T	−30	−20	−10	0	10	20	30
30							
	.568	.396	.251	.204	.335	.439	
20		(.044)	(.020)	(.043)			
	.526	.341	.185	.194	.372	.478	
10		(.046)	(.016)	(.098)			
	.509	.314	.144	.197	.378	.488	
0		(.053)	(.018)	(.100)			
	.519	.317	.129	.166	.351	.466	
−10		(.063)	(.031)	(.105)			
	.553	.349	.146	.106	.391	.410	
−20			(.056)	(.111)			
−30							

D
Reference fault: Hosgri Reference Center: 34°55.0'N 120°44.3'W
k = 1.675 2L = 80 C = 25
Bands Used: IX, VIII, VII–VI, V–IV (MODIFIED)
Upper Values: CP Lower Values: $s.d._{CP}$

S \ T	−30	−20	−10	0	10	20	30
30							
20	.520	.360	.246	.285	.467	.576	
	.478	(.031)	(.018)	(.097)			
10		.309	.196	.316	.502	.615	
	.460	(.031)	(.018)	(.097)			
0		.282	.161	.312	.501	.619	
	.463	(.035)	(.021)	(.098)			
−10		.277	.137	.276	.468	.589	
	.487	(.043)	(.014)	(.102)			
−20		.294	.128	.215	.405	.529	
−30			(.015)	(.108)			

plots or equivalent minima for several 2L values, results from the limited azimuth of observation of intensity values for this quake. Little more than 120° is subtended by all stations from the center of the fault. Thus, given somewhat noisy observations, several statistically equivalent solutions are possible, particularly when any model parameters are incorrectly set. This is the identical phenomenon observed when trying to locate earthquake epicenters with data from too limited range and azimuth and a slightly incorrect traveltime curve.

For the parameters used in table 12B (k = 1.6875, 2L = 60), the lowest determined CP and R.M.S. values are as follows:

S	*T*	*RMS*	*CP*
10	20	.690	.402
10	−10	.626	.218
10	0	.632	.110

10	−10	.692	.178
0	0	.637	.070
0	10	.695	.238
−10	−10	.658	.180
−10	0	.667	.041

Thus, minimum CP and RMS values are associated with nearly the same parameter values. We should point out that RMS values as low as those given above are found for 2L values of 70 and 80 km. However, these RMS values are associated with higher CP values (tables 12C and D). Since we consider the CP to be a more critical estimator of proper event parameters, we regard the solution based on a 2L of 60 km as superior to those based on 70 and 80 km.

The conclusion seems clear that, if we accept the general applicability of the model, the intensity data for the Lompoc earthquake require a location on or very near the Hosgri fault. Any location even a few kilometers farther west is rejected at high confidence. The tendency of the analysis based on k=1.675 to achieve a sharper minimum is interpreted to mean a more correct estimate of the k value. Thus, we conclude that the most probable parameters for this earthquake are a 2L of about 60 km centered at or a bit south of the lat 34°55.0′ N., long 120°44.3′ W. Solutions as long as 75 km or so cannot be rejected. However, if such lengths are correct, k = 1.750 is more appropriate. Whatever the k value or 2L, the model requires that the fault break was very near the Hosgri fault. It seems to us that there is little doubt that the intensity and geologic data together require a location on the Hosgri fault.

An issue engendering much heated debate in recent years has been the seismic risk associated with the Diablo Canyon reactor (approximate coordinates lat 35°13.5′ N., long 120°22′ W.). The site is within a few miles of the trace of the Hosgri fault opposite a part of the fault that probably broke in 1927 (fig. 23). If that be true, the site experienced in 1927 the maximum intensity that it will have to endure, because there is no evidence of a major fault nearer the site. We predict that the site would experience an intensity of 9.2 (R/F) if it were on thick saturated alluvium. However, the site is actually on Miocene shale of the Monterey Formation, a formation for which the predicted intensity would be 1.5 units less than that for saturated alluvium. Therefore, we predict that the site would experience a maximum intensity of 7.5–8.0 (R/F) or 7(M/M) for a repeat of the Lompoc earthquake. An even longer break would cause only a small increase in predicted intensity at the reactor site. According to the seismic-gap theory, the next earthquake on the Hosgri fault would not include the 1927 break but would break northward from the end of the 1927 break. Such an earthquake with 2L comparable to that of 1927 would give essentially the same predicted intensity at the site as predicted for the 1927 earthquake.

EARTHQUAKES OF EASTERN UNITED STATES (EUS, K=1 AND 1¼)

Several earthquakes in eastern North America have been studied via their published intensity contours and the graphic technique described on pages 4 and 5. Of particular interest is the Timiskaming earthquake of November 1, 1935, which is important because it is the largest earthquake (felt in much of eastern Canada and the U.S.) for which there are S-P data from several near stations. These data allow us to determine the earthquake's origin time unambiguously and thus to obtain a close estimation of depth of focus. Average estimated O.T. from use of S-P data of 5 stations is 06 h 03 m 37.4 s G.m.t. Analysis of the teleseismic ($\Delta \geq 22°$) data of the ISC with this restrained O.T. gives a depth of 10 km. The recalculated epicenter coordinates are lat 46.98° N., long 78.99° W., D = 10 km. Therefore, there is no doubt that the wide spacing of isoseismals is an attenuation phenomenon.

The estimated 2L and A_{VI} values for this and a few other Eastern United States earthquakes are given in table 21. It is of interest to point out that, when radii of intensity zones for the Cornwall/Massena quake were measured along the St. Lawrence River, the solution required a k value of 1¼ if essential agreement between all data was to be obtained. This is just another example of the reality of the k=1¼ zone shown along the St. Lawrence River on plate 2.

The M_0 values published by Herrmann, Cheng, and Nuttli (1978) for the Eastern United States earthquakes are included in table 21. The seemingly unusual pairing of calculated 2L and M_0 values are discussed in a following section entitled "Length of Break Versus Moment Versus k Value Throughout the United States and Suggested Interpretation."

FAULT LENGTH VERSUS MOMENT, MAGNITUDE, AND ENERGY RELEASE VERSUS K REGION

It was pointed out previously (Evernden, 1975) that there is no direct correlation between size of intensity contours and energy release for earthquakes distributed throughout the U.S. The impact of differing rates of attenuation is so severe that totally erroneous conclusions have been drawn when this factor has been unappreciated or ignored. We will illustrate this fact in two ways.

TABLE 21—*Observed and estimated parameters for selected earthquakes in the Eastern United States*

Earthquake	Date YR.MO.DY	Latitude	Longitude	M	I(MX)	2L km	A_{VI} 10^{14} cm^2	[1]M_o 10^{24} dyne-cm
Grand Banks[2]	1929.11.18	44.5°N	55° W	____	____	1.3 (1)	20	63
East Missouri[2]	1965.10.21	37.9°N	91.1°W	5.2	VI	.03–.04 (1)	56	0.1
Cornwall/Massens	1944.09.05	45.0°N	74.8°W	____	VIII	1.0 (1¼)[3]	6.4	2.5
Illinois[2]	1968.11.09	38.0°N	88.5°W	5.3	VII	.08 (1)	4.8	1.0
New Hampshire[4]	1940.12.20	43.8°N	71.3°W	____	VII	.016 (1)	0.78	1.0
						.16 (1¼)	1.2	1.0
Timiskaming[2]	1935.11.01	46.8°N	79.2°W	____	VII	.11 (1)	6.8	3.2
Missouri[2]	1963.03.03	36.7°N	90.1°W	4.5	VI	.022 (1)	1.1	0.1

[1]Herrmann, Cheng, and Nuttli (1978).
[2]Earthquakes used in figures 23 and 24.
[3]k=1 not permitted by data. Result in agreement with Evernden (1975) and plate 2.
[4]k=1¼ solution in agreement with local magnitude but earthquake in k 1 region of plate 2. Uncertain interpretation.

First, it is frequently assumed that energy release in earthquakes in the Eastern United States (EUS) is comparable to that in California, a conclusion based on the occurrence of three great historical earthquakes in EUS (Cape Ann, Mass., Charleston, S. Car., and New Madrid, Mo.,) and three in California (Fort Tejon, San Francisco, and Owens Valley, the last sometimes described as larger than the 1906 San Francisco quake). Table 22 lists calculated 2L and implied approximate E_0 values (total energy released) for numerous earthquakes studied in one or more papers of this series (energy vs. 2L as in Everden, 1975, p. 1290). The earthquake often considered the largest and greatest U.S. earthquake—December 16, 1811, New Madrid—was in fact the smallest earthquake studied if energy released in intensity-relative frequencies is the primary measure of size. The earthquake classed by Wood (1933) as simply a large local earthquake—March 10, 1933, Long Beach—released approximately 100 times as much elastic energy at such frequencies as did the New Madrid earthquake. As the Cape Ann earthquake was no larger than the Charleston earthquake, the total energy released in these "great" EUS earthquakes was of the order of 5×10^{21} ergs, while the three great California earthquakes released about 3×10^{24} ergs, the Owens Valley earthquake (March 26, 1872) providing less than 1/100 of this energy. Therefore, the intraplate region of EUS has released no more than about one thousandth the energy released in the three cited California earthquakes. According to the historical record, there have been other great California earthquakes since the Cape Ann event, so the contrast in energy release between EUS and California is even greater than here calculated. If these numbers are converted to ergs/km^2/year, the results are:

for US east of long 100° W.3.9 $\times 10^{12}$ ergs/km^2/yr,
for California _____6.2 $\times 10^{16}$ ergs/km^2/yr,

a contrast in energy-release rates of 1/15,000. There simply is no comparison between release rates of elastic energy (at frequencies relative to intensity data) by earthquakes in intraplate areas of U.S. and in California.

The second point we wish to emphasize is the clear correlation between observed seismic moments and the regional k factor, a relation indicating either correlation of stress drop and attenuation factor or the influence of regional characteristics subsumed under our k factor on observed seismic moments. To begin, we illustrate the correlation of calculated and observed 2L values and observed and calculated seismic moments in regions of k 1½ and k 1¾.

TABLE 22.—*2L, "E_0, and "M" values for selected earthquakes in the United States*

Earthquake	k	2L	log"E_0"[1]	"M"[2]
San Francisco 1906	1¾	400	24.2	8.25
Fort Tejon 1857	1¾	320	24.0	7.98
Long Beach 1933	1¾	22	21.4	6.48
Seattle 1949	1½	75	22.6	7.98
Owens Valley 1872	1½	60	22.4	7.85
Kern County 1952	1½	60	22.4	7.85
Charleston 1887	1¼	20	21.4	7.92
New Madrid 1811–12	1¼	20	21.4	7.92
	1	5	20.2	7.83

[1]log "E_0" = 18.7 + 2.11(log 2L), (p. 51–54 and Evernden, 1975).
[2]"M" by formulas of page 41.

Hanks, Hileman, and Thatcher (1975) illustrated the general correlation between observed seismic moment and area included within the intensity VI contour (A_{VI}) by either MM or RF intensities and in either k 1½ or k 1¾ regions. They found that use of such a mix of data types still yielded A_{VI} vs. M_0 data points that showed a general correlation over a large range of M_0 values.

Because A_{VI} values are strongly influenced by k value and intensity scale, we have reanalyzed the data used by Hanks, Hileman, and Thatcher (1975) while adding a few additional events, the intent being to normalize all intensity data to the same scale and to separate data from different k regions. In addition, we have compared observed and calculated 2L values and plotted observed M_0 against calculated/observed 2L values rather than against A_{VI} values.

All observed and calculated quantities are given in table 23. The "observed" 2L values are those actually observed or calculated on the basis of high-frequency spectral data or short-period seismograms. All calculated 2L values are obtained by use of observed intensity data and formulas of this and the previous report (Evernden, 1975).

A few comments on the data of table 23 and the calculated values used in the subsequent discussion are required. In addition to use of A_{VI} values for estimating 2L and M_0, some events were analyzed by using the full set of intensity contours and our graphic technique. If the graphic technique was used, we always chose to accept the 2L values obtained from it, but we applied it only when the 2L and M_0 estimates differed markedly from those obtained from the A_{VI} data. Such discrepancies were found for only a few events for which A_{VI} values were in the 10^{13} cm^2 range, that is, small A_{VI} areas. An aspect of the total intensity data included in table 23 is the maximum shaking intensity. Note that agreement between observed maximum shaking intensity and calculated I(MX) is much better for graphic estimates of 2L than for several A_{VI} values, again supporting use of the 2L and M_0 values calculated from total intensity data. The values of 2L in table 23 that are used in figure 22 and the subsequent discussion are followed by an asterisk.

Table 23 illustrates that the mode of analysis followed here and originally presented in Evernden (1975) leads to estimates of 2L that are in essential agreement with observed breakage or with 2L values estimated by use of short-period seismograms or strong-motion records. This agreement is independent of whether the earthquake is in a region of k 1½ or k 1¾, the 2L calculations for earthquakes in k 1½ assuming an energy density equivalent to an earthquake of equal 2L in k 1¾.

As an additional test of whether the 2L values determined for k 1½ earthquakes are meaningful, we analyzed the published intensity data on all events of the region for which there is documentary evidence of length of surficial cracking or displacement (data provided by M.G. Bonilla of the U.S. Geological Survey). The graphic technique described earlier was used to make the analysis.

Table 24 shows reported and calculated 2L values for the earthquakes studied.

The only additional comments required are:

(a) The 2L value calculated for the Manix earthquake seems to be in serious disagreement with observed values of I (MX) and M_L but in excellent agreement with the M_0 values of 1.4×10^{26} reported by Hanks and Thatcher (1972). (See figure 24 and note that, in k 1½, 2L of 10 implies an M_0 of 1.25×10^{26} dyne-cm.) Perhaps the low value for I (MX) is to be explained by a low water table, and the low M_L value by the fact that it was measured at Pasadena (that is, although the earthquake occurred in a region where k=1½, the path to the Pasadena station was mostly through a region in which k=1¾).

(b) The intensity VI (5.5) dimension for the Oroville earthquake was not used because it is so small (see discussion above). The ground condition in the Oroville area probably accounts for the small area mapped as intensity VI.

(c) The intensity data for the Hebgen Lake earthquake indicate that the attenuation region surrounding the epicenter is not uniform. They imply (via our model) an attenuation factor of k=1½ in the area to the south (toward a region in which we know k to be 1½ on the basis of several earthquakes) but between k 1½ and k 1¼ to the north and east. If a k value of 1.35 is used to the north and east, we obtain a 2L value similar to that for the data from the area to the south and k 1½.

(d) The Fort Sage Mountains and Galway Lake intensity data are grossly inconsistent with reported lengths of fracture. All Fort Sage Mountains data agree on a 2L of 1.0 km (versus reported 8.8 km), while all the Galway Lake data imply a 2L of well under 1 km (versus reported 6.8 km of surficial breakage). Because the 2L values we calculate are for the equivalent k 1¾ earthquake to provide the energy required to develop the observed k 1½ intensity pattern, these very short calculated 2L values suggest one of three conditions: stress drops were abnormally low, high-frequency energy was released from a short piece of the break (as at Parkfield), or observed surficial fracturing was influenced by factors other than rupture length at depth. Whatever the condition, the short calculated 2L values imply, if anything anomalous, that less energy is re-

TABLE 23.—*Observed*

Earthquake	No.	In.	Reg.	Date YR.MO.DY
Hemet	01	MM	7	1963.09.23
Lytle Creek	02	MM	6	1970.12.09
Coyote Mountain	03	MM	7	1969.04.28
Parkfield	04	MM	7	1966.06.28
Desert Hot Springs	05	MM	7	1948.04.12
Long Beach	06	MM	7	1933.03.11
Santa Rosa Mt.	07	MM	7	1934.03.19
San Fernando	08	MM	7	1971.02.09
Borrego Mt.	09	MM	7	1964.04.08
Imperial Valley	10	MM	7	1940.05.18
San Francisco	11	RF	7	1906.04.18
Santa Barbara	12	RF	7	1925.06.29
Lompoc	13	RF	7	1927.11.04
Fort Tejon	14	RF	7	1857.01.09
Wheeler Ridge	15	MM	6	1954.01.12
Truckee	16	MM	6	1966.09.12
Bakersfield	17	MM	6	1952.08.22
Fairview Peak	18	MM	6	1954.12.16
Kern County	19	MM	6	1952.07.21
Oroville	20	MM	6	1975.08.01
Pocatello Valley	21	MM	6	1975.03.28

and calculated parameters of earthquakes in regions of k=1¾ and k=1½, California and Idaho

Observed Values						A_{VI} Calculations						Intensity calculations				
Mag.	Mom.	A_{VI}	2L	I(MX) SHKG	Mom. N,7	A_{VI} RF,7	2L	Mom. RF,7	Mom. MM,6	M_L 7	I(MX)	2L RF,7	Mom. MM,6	Mom. 7	M_L	I(MX)
5.3	0.02	0.24		VI		0.48	1.2	.018		4.7	6.2					
5.4	0.10	0.22		VII		0.44	1.1	.015		4.7	6.2	1.1		0.09	5.6	7.1
5.9	0.50	0.61		VII		1.2	3.6	0.19		5.4	6.9					
5.5	1.3	0.54	3	VII		1.0	3.1	0.12		5.3	7.4					
6.5	1.0	2.6		VII		4.7	27	6		6.6	8.2	10	1		6.0	7.6
6.3	2.0	1.2		VIII		2.1	9	0.8		5.9	7.5	22	3.4		6.5	8.1
6.2	4	2.3		VI		3.9	23	4		6.5	8.1					
6.4	4.7	2.3	16	IX		3.9	23	4		6.5	8.7	19	3		6.4	8.6
6.5	6	3.4		VII		5.6	38	10		6.8	8.5					
7.1	20	3.3		IX		5.4	37	9		6.8	8.5	60	20		7.1	8.8
8.2	850	16	400	IX			130	150				400	1500		8.3	9+
6.3	20	4.4		IX								40	11		6.9	9
7.3	6.5			IX								70	31		7.2	9
8	900		320	IX								320	900		8.1	9+
6.6	0.33	1.75		VII+	.026	0.65	1.8	0.04	0.5	4.9	7.5					
6.4	0.5	1.61		VII	.04	0.60	1.6	0.03	0.41	4.9	7.4					
5.8	0.55	0.32		VIII	.023	0.11	0.33	.000	.007	3.6	6.1	2.1		0.54	5.1	7.6
7.0	90	14	40	VIII	6.0	4.8	31	6.7	100	6.7	10					
7.7	170	17	60	IX	11	5.8	40	11	170	6.9	8.8	60	23	241	7.1	9.1
5.9	0.2	0.48	1.5	VII	.017	0.18	0.36	.002	.018	4.0	6.4	1.5		0.35	4.8	7.4
6.0	0.65	1.4	3	VIII	.053	0.52	1.4	.023	0.28	4.8	7.3	3.0		1.13	5.3	7.8

Notes: "In." = Intensity type of published data. "MM" = Modified Mercalli. "RF" = Rossi Forel. "Reg." = k region. "6" = 1¼. "7" = 1¾. "Mom." = Seismic Moment in 10^{25} dyne-cm. "N" = Moment of Region 6 (1½) earthquake normalized to Region 7 (1¾). "A_{VI}" = Area in 10^{24} cm² included in intensity VI contour. "Observed A_{VI}" values are in intensity and regional units of columns 3 and 4. "M_L" = Local Magnitude. "Observed" magnitude values in all regions are calculated with Richter formula for southern California (Reg. 7). "Calculated I(MX)" is maximum predicted shaking intensity and is in units (MM or RF) of observations. "In. Calculations" are based on full pattern of intensity observations. "2L" values followed by an asterisk are those used in figure 22. For event No. 17, Mom.(RF,7) entry under A_{VI} Calculations is 0.0004.

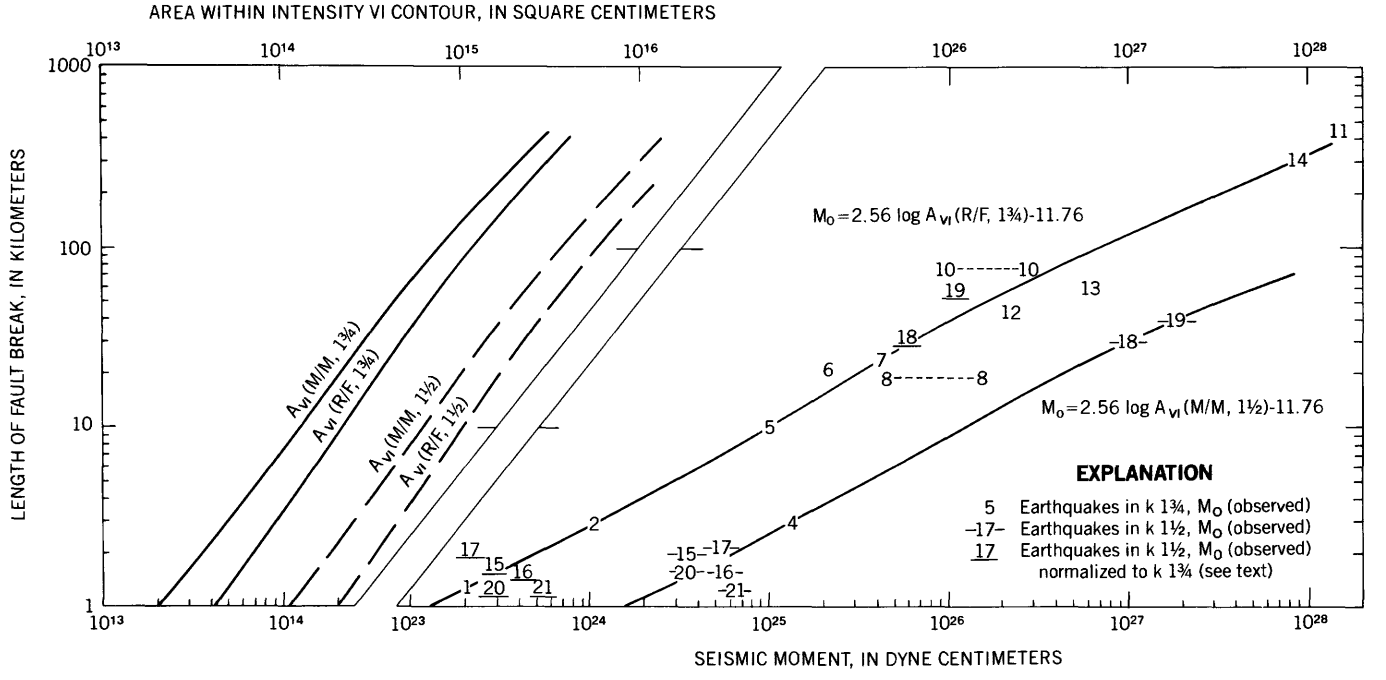

FIGURE 22.—Length of fault break (2L) as a function of seismic moment (M_o; right) and area within R/F and M/M intensity VI contours (A_{VI}; left) for k = 1¾ and k = 1½.

leased by the k 1½ quakes than by k 1¾ earthquakes of equivalent 2L.

Thus all available data seem to indicate that 2L values for k 1½ earthquakes as calculated by means of our model are quite accurate estimates of actual break lengths and, thus, that energy released in the intensity pass-band of k 1½ earthquakes is essentially identical to that of k 1¾ earthquakes of the same 2L.

For our discussion of seismic moment (M_o), we first consider events occurring in regions where k=1¾. The left side of figure 24 indicates the theoretical relations between A_{VI} and 2L for both M/M and R/F and k 1½ and k 1¾. The equivalent areas for the same 2L are determinable and are shown to increase by about a factor of ten from A_{VI} (M/M, 1.75) to A_{VI} (R/F, 1.50). In order to relate A_{VI} or 2L to M_o, an empirical relation must be established as done by Hanks, Hileman, and Thatcher (1975). On separating data of different k regions and intensity scales, we find a different scaling law of A_{VI} and M_o than found by them. The relation found appropriate to k 1¾ data (normalizing A_{VI} (M/M, 1.75) values to A_{VI} (R/F, 1.75) values by figure 22) is:

$$\log M_o = 2.56 \log A_{VI}(R/F, 1.75) - 11.76$$

This curve, drawn on the right side of figure 22, is expressed as a relation between 2L and M_o via the A_{VI} (R/F, 1.75) vs 2L curve of the left side of figure 22. The non-underlined numbers plotted along the curve are calculated or observed 2L vs observed M_o values for k 1¾ earthquakes. In most cases, there is excellent agreement with the empirical curve over the entire range of M_o values. This agreement implies that, for most k 1¾ earthquakes, both short- and long-period energy derive from the same fault length according to a single spectral scaling law.

Two events show marked disagreement with the curve. Event No. 4, Parkfield, is of particular interest because it has been described extensively in the literature. Numerous investigations of long-period data of this earthquake find an M_o value of 10^{25} and observed surface breakage of 30 km or more. However, the strong-motion data indicate that the high-frequency energy came from a 3–4 km length of the fault (Lindh and Boore, 1981). In addition, the intensity VII contour is only 22 km long, a value that is totally anomalous for a normal California earthquake with a 2L of 20 km or more. As shown in table 22, the intensity data imply a 2L of 3 km. The Parkfield quake clearly was abnormal for California because the high-frequency energy was derived dominantly from a short piece of the fault at normal California stress levels, while the long-period energy was derived from failure of a much longer, slowly breaking fault segment. On the basis of other analyses, discordance of the Parkfield datum point with the empirical curve of figure 22 should have been expected. Inadequate analysis has been done on event No. 3 (Coyote Mountain) to ascertain whether a similar explanation applies to that datum point.

As regards event No. 5 (Desert Hot Springs), the agreement with the curve shown on figure 22 would not have resulted from use of the A_{VI} value reported by Hanks, Hileman, and Thatcher (1975). The reported intensity data for that quake show some remarkable inconsistencies in distribution of M/M VI values. These were reported as far away as Los Angeles but were interspersed with many much lower values. The 2L value of 27 km deriving from the A_{VI} area used by Hanks and his coworkers predicts epicentral intensities that are too high and a felt area much too large.

The "Limit of Detection" (L.O.D.) boundary drawn in "U.S. Earthquakes" is usually near intensity 3.0. A 2L value of 10 km for the Desert Hot Springs earthquake places the 3.0 boundary inside the outer lobes of the L.O.D. In addition, a 2L of 10 km or less is required to predict intensities of only VII at Desert Hot Springs and only IV at Death Valley and Needles. Without ignoring the anomalous M/M VI values reported for this earthquake, but for purposes of making a 2L estimate most consistent with intensity observations, we use a

TABLE 24.—*Observed and calculated 2L values for selected earthquakes*

Earthquake	YR	MO	DY	LAT(N)	LONG(W)	M(OB)	2L(OB)	2L(PRED)
Cedar Mountain, Nev.	32	12	20	38.8	118.0	7.2	61	66
Excelsior Mountain, Nev.	41	01	30	38.0	118.5	6.3	1.4	3.5
Hansel Valley, Utah	34	03	12	41.5	112.5	6.6	8	10
Manix, Calif.	47	04	10	35.0	116.6	6.4	4	10
Fort Sage Mountains, Calif.	50	12	14	40.1	120.1	5.6	8.8	1
Kern County, Calif.	52	07	21	35.0	119.0	7.7	[1]60	60
Rainbow Mountain, Nev.	54	07	06	39.4	118.5	6.6	18	18
Rainbow Mountain, Nev.	54	08	23	39.6	118.4	6.8	31	36
Fairview Peak, Nev.	54	12	16	39.3	118.2	7.1	48	40
Hebgen Lake, Mont.	59	08	17	44.8	111.1	7.1	24	[2]28
Galway Lake, Calif.	75	05	31	34.5	116.5	5.2	7	1
Pocatello Valley, Idaho	75	03	28	42.1	112.6	6.0	[3]3	3
Oroville, Calif.	75	08	01	39.4	121.5	5.7	[3]4(1.5)	1.5

[1]33 kilometers of fracture in bedrock. However, epicenter was about 30 kilometers away under Quaternary deposits. See text.
[2]By use of data to south of epicenter. See text.
[3]2L values as determined from short-period seismograms. See text.

2L value of 10 km, which yields a calculated M_0 (1¾) of 1.0×10^{25} dyne cm, M_L of 6.0, and I(MX) of 7.6.

Note again that a formula relating A_{VI} and M_0 serves very well to predict most observations (fig. 22 and table 23). The point of greatest relevance here is one mentioned only in passing above. If observed M_0 values for earthquakes in k 1½ regions are "normalized" to k 1¾ by the ratio of moments predicted via A_{VI} (R/F, 1¾) and A_{VI} (M/M, 1½) values calculated for the 2L value found by observation or analysis of intensities, one obtains normalized M_0 values that agree with predicted M_0 values for earthquakes of this 2L (underlined numbers in fig. 22) in k 1¾ regions. This correlation strongly suggests that observed M_0 values of k 1½ earthquakes are not directly comparable with observed M_0 values of k 1¾ earthquakes insofar as implying relative levels of long-period energy release but are probably correlated with details of the relevant relaxation and radiation phenomena. The explanation of the high M_0 values for k 1½ earthquakes certainly is not a simple regional difference in Q attenuation. The absence of such regional differences in Q is demonstrated by the fact that for nuclear explosions, and thus for point sources, the M_S versus yield curve is independent of k region (Evernden and Filson, 1971).

Now note the reported and calculated M_L values in table 23, wherein all calculated values are for equivalent 2L earthquakes in k 1¾ regions. In Evernden (1975), the relation:

$$M_L = (\log 2L + 3.2667)/0.711$$

was empirically developed on the basis of data from k 1¾ earthquakes. The validity of this relation with regard to the earthquake studied is shown by the fact that the average observed M_L value for k 1¾ earthquakes of table 23 is equal to the average M_L calculated via the above formula when 2L is either observed or obtained from analysis of intensity data.

The next point to note is the marked disagreement between reported M_L values for k 1½ earthquakes and the M_L for an earthquake of equivalent 2L in k 1¾. The average reported M_L of studied k 1½ earthquakes is 6.5, while the average calculated M_L for the equivalent 2L earthquakes in k 1¾ is 5.5, a difference of 1.0. This difference is an average measure of the inconsistencies routinely occurring in M_L estimates of k 1½ earthquakes. If magnitude estimates were used only as originally intended by Richter (1955), that is, as a scheme for ordering earthquakes of a region according to a generalized size parameter, the only error in the present calculations would be an incorrect attenuation formula for k 1½ earthquakes. However, since M_L estimates are considered by many as measures of energy release, moment, and other parameters, a major inconsistency in present practice is to apply a formula developed in k 1¾ regions to earthquakes in all regions. We should be using a set of formulas of the following type:

Region	*Formula*
k 1¾	$M_L = \log A + 1.75 \log (D/100)$
k 1½	$= \log A + 1.50 \log (D/100) - a_1$
k 1¼	$= \log A + 1.25 \log (D/100) - a_2$
k 1	$= \log A + 1.00 \log (D/100) - a_3$

The formula for k 1¾ is inconsistent with Richter (1958, p. 342), because it predicts a value for M_L at 600 km that is 0.5 lower than would be predicted from the data in Richter's table. It is interesting to note that the University of California at Berkeley often reports M_L values about 0.5 M_L greater than does California Institute of Technology, Pasadena, for southern California earthquakes (T. V. McEvilly, oral commun., 1979). A possible explanation for the differing M_L values is that the data used to establish Richter's curve may have been contaminated by multiprovince paths.

Using the formulae of Evernden (1975) and normalizing the set of equations so that earthquakes of the same high-frequency energy, and thus fault length, are given the same M_L, it follows that $a_1 = 0.5$, $a_2 = 1.0$, and $a_3 = 1.5$. Universal use of the k 1¾ formula for estimating M_L leads to errors for stations at about 200 km of 0.6, 1.2, and 1.8 in k 1½, k 1¼, and k 1 regions, respectively. There are other possible schemes of scaling, and there are reasons why the scaling used in Evernden (1975) may not be directly convertible to maximum amplitudes versus distance. The disagreement between 1.0 and 0.6 suggests that additional factors may be influencing maximum amplitude.

The important point is that the high M_L values presently assigned to earthquakes on faults with small 2L in k 1½ areas indicate that an invalid formula was used for calculating M_L, not that stress drop was higher for these quakes than for k 1¾ earthquakes of equivalent 2L. We suggest that the following formulae be used until more detailed work has been done:

Region	*Formula for M_l*
1¾	$\log A + 1.75 \log (D/100)$
1½	$\log A + 1.50 \log (D/100) - 0.75$
1¼	$\log A + 1.25 \log (D/100) - 1.50$
1	$\log A = 1.00 \log (D/100) - 2.25,$

where A is amplitude in micrometers, D is epicentral distance in kilometers, and amplitudes are as measured on standard Wood-Anderson seismometers. A suggested pattern of k values for the United States is to be found on plate 2. Corrections for multiregional paths must be made.

CRUSTAL CALIBRATION AS FUNCTION OF REGION

To elaborate further on the theme of the last paragraphs, one of the major continuing errors in estimating seismological parameters is the use of invalid calibration formulas. The routine m_b values presently published by USGS use a B(Δ) term in the distance range 0°–20° that was demonstrated to be invalid years ago (Evernden, 1969). The M_L B(Δ) term (in M_L = log A + B(Δ)) used universally is the one empirically determined by Richter (1955) as being appropriate to southern California. It is certainly invalid (that is, does not yield consistent estimates of M_L) in regions of different attenuation.

A recent example of the use of such methods to calculate m_b and M_L is seen in the data for the earthquake of March 28, 1975, in Pocatello Valley on the Idaho-Utah border. The published parameters for this quake (Arabasz and others, 1981) are

A_{VI} (M/M, 1.50) = 1.4×10^{14} cm^2
M_L = 6.0
I(MX) = VIII M/M
2L = 3.0 km (analysis of short-period seismograms)
M_o = 6.5×10^{24} dyne-cm.

The m_b values are as calculated and published by the USGS. One anomaly in these data is that values of 6.6 to 7.0 are listed in the 8°–9° range; that is, an incorrect calibration curve for m_b is still being used in this distance range. In Evernden (1969), the incorrect shape of the B(Δ) curve routinely used in the Western United States was extensively discussed and the resultant errors in estimation of m_b were illustrated. The m_b values reported for stations in the distance range 0°–20° for this earthquake should be ignored.

Secondly, the mean m_b value reported for stations in the range 20°–54° is 5.8, while the mean m_b value reported for stations in the range 65°–83° is 6.1. It was pointed out in Evernden and Clark (1969) that the Gutenberg B(Δ) curve for P waves is inconsistent with modern observational data, as this curve yields m_b values that are 0.4 higher in the range 65°–83° than values in the 20°–54° range. If calibration is made against the nearer stations, the reported m_b for this earthquake becomes 5.8, and all reported values within this range fall at or between 5.5 and 6.1

Finally, how does this magnitude compare with that expected for the same event occurring in western California and recorded at low-amplitude stations (Evernden and Clark, 1969; Evernden, 1977)? The source calibration is assessed to be in the neighborhood of 0.25 m_b unit (Evernden, 1969). Nearly all stations in the 20°–54° range are in shieldlike areas, that is, EUS-type crustal structure, a condition that leads to an expected difference of 0.5 m_b unit relative to low-amplitude stations (Evernden and Clark, 1969). Therefore, when compared with the magnitudes used in other reports by this author, the m_b value for this event would have been m_b 5.0 if it had occurred in western California and been recorded at low-amplitude stations.

Next, consider the reported M_L value of 6.0. The B(Δ) curve used by the USGS and by Arabasz, Richins, and Langer (1978) in converting Wood-Anderson data to estimates of M_L is the curve established by Richter (1955) for southern California. In other words, a calibration curve appropriate for a region of k 1¾ is being used in a region of k 1½, a procedure that is almost certain to lead to gross errors if M_L values in k 1½ are to be both independent of distance and correlative in some way with M_L values of events in k 1¾ regions.

Ignoring all USGS M_L values because of the great distance of the stations used, consider only the two M_L values reported by Arabasz, Richins, and Langer (1981), that is, 5.9 at 210 km and 5.8 at 310 km. We assume that these values indicate an average value of 5.8–5.9 in the range 200–300 km. If the value for k is assumed to be 1¾ while it is actually 1½, magnitudes in the 200–300 km range may be overestimated by 0.6–0.9 M_L unit. Therefore, a calibrated M_L value for this event would have been about 5.0–5.3.

The reported A_{VI} (M/M, 1.50) value of 1.4×10^{10} cm^2 leads to a predicted 2L value of 1.35 km and a predicted M_o (1.50) of 2.8×10^{24} dyne cm, while our graphic technique predicts a 2L of 3 km and an M_o of 1.1×10^{25} dyne cm. Both values of M_o are to be compared with the reported value of 6.5×10^{24} dyne cm, which would predict a 2L of 2.0 for an earthquake in a region of k 1½. All of these values are probably indistinguishable from the 2L of 3 km calculated on the basis of short-period seismograms. A 2L of 3.0 implies an earthquake of M_L 5.3 for a region fo k 1¾. Thus, the intensity data, M_L data, and m_b data imply that this event was much smaller than usually considered (about M_L 5¼ if in k 1¾), and all the data agree with the 2L estimate based on high-frequency data. In addition, the 2L value of 3.0 km for a k 1½ earthquake is predicted to be associated with an I_{MAX} (M/M) of 7.8. This value is consistent with the observed value of VIII in a very small area. All these observations appear to establish that this earthquake was of small dimension (2L of 1.5 to 3.0 km) and that its energy output in the pass-band typical of intensity values and M_L values (approximately 0.5–3 Hz) was equivalent to that of an earthquake of equivalent 2L in western California.

LENGTH OF BREAK VERSUS MOMENT VERSUS K VALUE THROUGHOUT THE UNITED STATES AND SUGGESTED INTERPRETATION

A point that probably requires reemphasis is just how meaningful, in a physical sense, are the 2L values we calculate from the intensity data. The procedure for calculating these 2L values must be reiterated. Given the appropriate k value for a region, the intensity data are then used to calculate the energy required at the focus to create the observed quantitative pattern of intensities. Then, we determine the 2L value required in a region where k=1¾, that is the region of calibration for 2L versus energy, to supply the calculated energy requirements. To evaluate whether these calculated 2L values in each region are meaningful, we compare them with other data that establish actual lengths of break for earthquakes for which we have such estimates. Where k=1¾, we should and do get nearly correct values because this is the region of calibration. The data in tables 23 and 24 prove that the procedure described above serves successfully to estimate the 2L values of earthquakes in regions where k=1½. All k 1½ events with known or presumably known 2L values are included in these tables, which show that the agreement between observed and calculated 2L values extends over at least the 2L range from 1 to 60 km.

As for 2L estimates in regions further east, we stress again (as was done in Evernden, 1975) the agreement the calculated 2L (20 km) of the 1886 Charleston earthquake and the size of the high-intensity isoseismal for that quake. In addition, we point out that locations of presently occurring small earthquakes in the Charleston area cluster along a 20-km zone exactly placed to fit within the high-intensity contour of the 1886 earthquake (Arthur C. Tarr, written commun., 1979). Finally, master-event locations by James Dewey (oral commun., 1979) of all historical and instrumentally locatable earthquakes in the Charleston area are along this same 20-km zone. Several earthquakes originally placed offshore can be proven to have occurred in this 20-km zone. Thus, all seismic activity in the Charleston area for the past several decades has consisted of aftershocks of the 1886 earthquake. In other words, there is only one seismic locus in the region, and it seems certain to have been the locus of the 1886 earthquake.

There are no other earthquakes in the Eastern United States for which unequivocal demonstrations of length of break exist. On the basis of geologic and seismologic evidence, Frank McKeown (written commun., 1979) has concluded that there are no fault segments longer than 10 to 20 km in the New Madrid area. To quote from his letter addressing this point:

> I believe that source dimensions of so-called New Madrid earthquakes are small, e.g., not more than 10–20 km in length. The basis for this opinion is that faults in the postulated New Madrid fault zone of Heyl and Brock, as mapped in the Illinois-Kentucky fluorspar district, are of such dimensions (see Heyl and McKeown, 1978). Also, about that time, I started thinking about an apparent relationship of mafic instrusives to earthquake source zones in eastern U.S. This resulted in a speculative paper (McKeown, 1978) which would be different if I were to write it today, but short fault lengths were postulated based upon some circuitous reasoning. I still don't think the ideas in the paper are all wrong, but more emphasis should have been made of the evidence of intraplate rifts and associated rocks. As you know, evidence of a rift and associated structures and intrusives has been accumulating. Hildenbrand, Kane and Stauder (1977) show pretty clearly a rift-like structure that appears to be terminated by northwest-trending structure of some kind near New Madrid. Prior to the aeromagnetic and gravity data, the presence of alkalic mafic intrusives in the subsurface of the embayment and surface around the embayment was indicative of rifting. Evidence for short faults in the New Madrid area can be inferred from the seismicity pattern, focal mechanisms, and reflection profile data. The subsurface structure near New Madrid must be very complex with no apparent through-going long faults, as indicated by diverse epicenter trends and differing focal mechanisms. South of Caruthersville, Mo., the seismicity trend appears to be in the center of the riftlike structure. One can infer that it is related to a fault or fault zone about 100 km long. If, however, a typical east-African type of intraplate rift is present in the subsurface, I cannot believe that the seismicity is along a single long fault. Rifts do not have such faults according to the maps and literature that I have examined. A rift contains numerous parallel-to-subparallel normal faults that apparently result from the tensional stress across a broad arch that preceded formation of the rift. Perhaps if the seismicity were confined to one side of the rift, a long fault zone could be postulated, but even the bounding faults of rifts are commonly en echelon.

Our estimate of a 2½- to 5-km 2L value for this earthquake (k=1, Evernden, 1975) may or may not be consistent with these field observations. Because we do not know the correct k value (anything between 1 and 1.25 being permissible on the basis of the available data), we cannot deny the possibility that the fault is as much as 10 km long.

There is positive evidence that our technique for estimating 2L values yields accurate results in several k regions (k 1¾ to k ¼), there is no reason why the technique should fail in regions of k=1, and available data in the New Madrid area indicate that, indeed, it does not fail but yields accurate 2L estimates.

The conclusion that one must draw from these results is that the fault zones in all regions of the United States are very similar. Asperities must be of essentially equal strength and equal mean distribution on fault surfaces in all regions. Whatever the effective stress conditions are in one region, they are duplicated in all others. The inhomogeneity in stress on fault surfaces in k 1¾ regions (San Andreas fault), expressed by asperities with stress drops of several hundred bars while average stress drop is a few tens of bars, is now common knowledge. What is new here is that this pattern is probably similar in all regions of the United

States. The mean stress can rise somewhat without affecting high-frequency energy but cannot rise an order of magnitude.

Given the validity of our estimates of 2L and its associated implications, the next point to note is the strong dependence of the 2L vs M_0 relation on k value. All of the data of tables 22 and 23 are plotted on figure 23. It is obvious that the relation between moment (M_0) and 2L is not fixed across the United States. Moment actually increased by a factor of about a thousand for the same 2L from k 1¾ to k 1. Because 2L is estimated from high frequencies (~1 – 4 Hz), while M_0 is measured on the basis of long periods (20 seconds to infinity), figure 23 can be considered as a plot of short-period energy versus long-period energy, and the plot implies a thousandfold increase in long-period energy relative to short-period energy from k 1¾ to k 1.

As a point of interest, the correlative A_{VI} versus M_0 data for the earthquake of figure 23 (plotted in fig. 24) show a similarity between the M_0 versus A_{VI} relations for regions k 1¾ and k 1½, while the relations of 2L versus M_0 for these two regions are markedly different. This insensitivity of A_{VI} versus M_0 to change from k 1¾ to k 1½ is why Hanks, Hileman, and Thatcher (1975) were able to get a common curve for A_{VI} versus M_0 when they mixed the data of earthquakes from regions of 1¾ and k 1½.

The question, then, is how to explain the 2L versus M_0 relation of figure 25. To be specific, how is it possible for an M_0 value of 10^{26} dyne-cm to be associated with a 2L value of 1 km, the paired values on the k=1 curve of figure 23? No permissible association of μ, L, D, and H in a uniform half-space could possibly explain these values. There must be another operative inhomogeneity. We suggest that earthquakes of the Eastern United States are along fault zones that constitute soft inclusions in an otherwise highly rigid and strong crust.

Following Eshelby (1957), we consider the following situations:

(a) uniform elastic medium of shear modulus μ_0

(b) soft inclusion (sphere) of shear modulus μ_1 im-

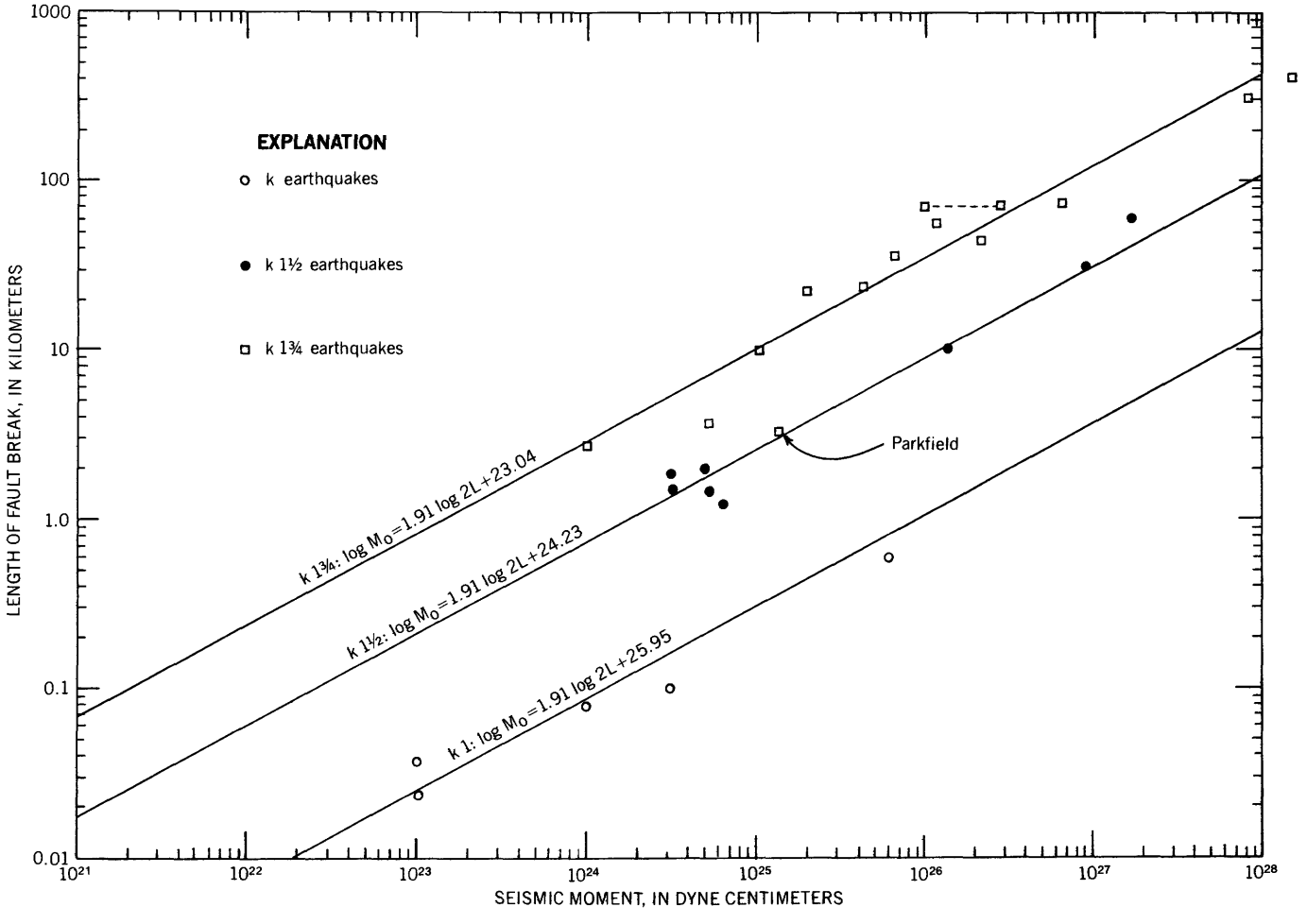

FIGURE 23.—Length of fault break (2L) as a function of seismic moment (M_0) for all k regions of conterminous United States.

bedded in an otherwise uniform elastic medium of shear modulus μ_0.

Presuming shear stress to be applied at distances that are large compared with dimensions of the soft inclusion, we investigate shear stress, τ_I, at the center of the space and at the center of the sphere in terms of the remotely applied shear stress, τ_A.

In case (a), $\tau_I = \tau_A$

In case (b), $\tau_I = \tau_A \mu_1 / [\mu_0 - \beta(\mu_0 - \mu_1)]$

where $\beta_0 = 0.1333\,(4 - 5\nu_0)/(1 - \nu_0)$, and ν_0 = Poisson's ratio outside the inclusion.

For $\nu_0 = 0.25$, $\beta = 22/45 \cong \frac{1}{2}$

Then, we find the following relations:

μ_1/μ_0	1	0.50	0.10	0.05	0
τ_I/τ_A	1	0.67	0.18	0.10	0

Thus, the stress within the soft inclusion is less than the distantly applied stress. Or, in order to achieve a given level of shear stress on a fault within the inclusion, it will be necessary to apply a greater distant shear stress. If μ_1 is one-tenth of μ_0, the externally applied stress must be 5.5 times the stress required on the fault surface. If μ_1 is one-twentieth of μ_0, the externally applied stress must be ten times that required on the fault surface. Thus, if mean shear stress required for failure is 100 bars, regional stresses outside the inclusion must be 550 to 1,000 bars, that is, a low-stress-drop quake in a highly stressed regional environment.

Now, consider the comparative changes in strain energy associated with fault-zone failure at shear stress τ_I. Since strain energy change is a measure of moment, this analysis will be relevant to figure 23.

Consider the following situations, assuming total stress drop on the fault:

(a) As before, that is, uniform space;

$$\Delta E_a = 8r^3\tau_I^2/7\mu_0$$

where r=radius of circular fault patch.

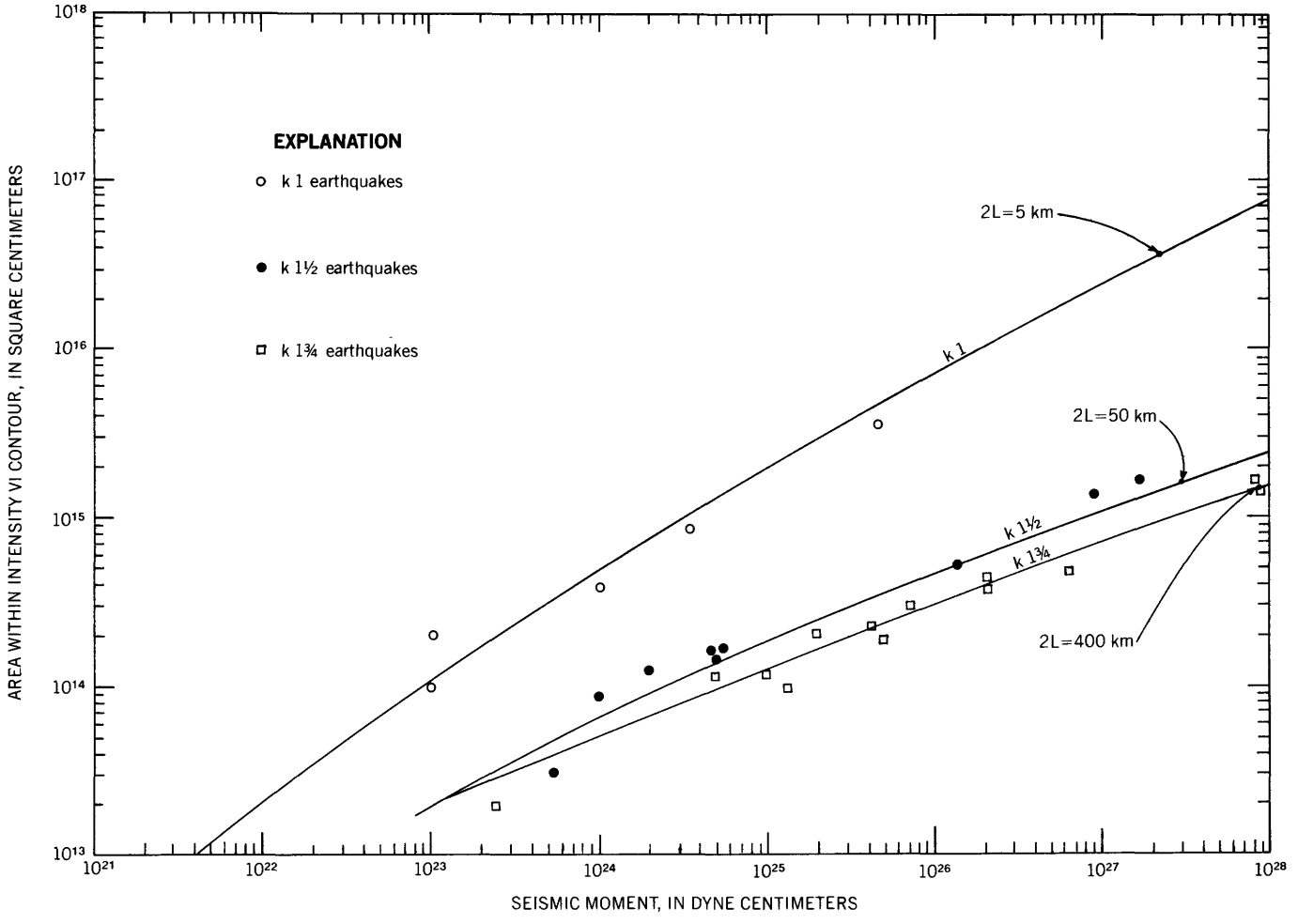

FIGURE 24.—Area within intensity VI contour (A_{VI}) as a function of seismic moment (M_0)for fault lengths (2L) of 5, 50, and 400 km in all k regions of conterminous United States.

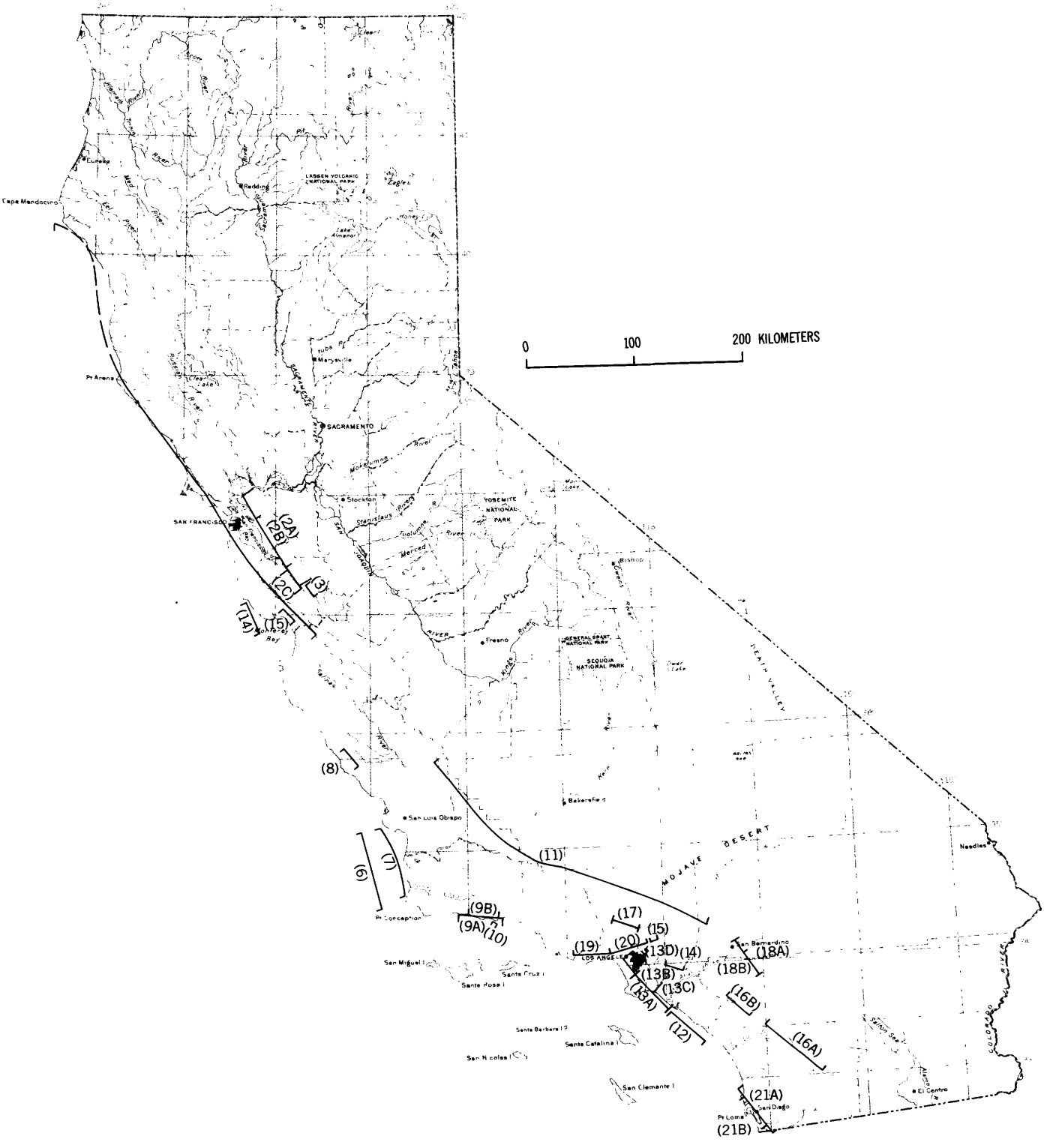

FIGURE 25.—Fault breaks used in models for estimating replacement value of damaged wood-frame construction.

(b) there exists a soft region with radius R and shear modulus μ_1;

$$\Delta E_b = 8r^3\tau_I^2/7\mu_1 \text{ ,r} << \text{R:}$$

(c) same conditions as (b) except that total stress drop is presumed to take place within the entire volume of the soft inclusion;

$$\Delta E_c = \pi R^3(\mu_o + \mu_1)\tau_I^2/3\mu_o\mu_1 \text{ , for } \beta = \tfrac{1}{2}.$$

We then obtain the following values:

μ_1/μ_o		1	0.5	0.10	0.05	0
E_b/E_a	--	1	2	10	20	∞
E_c/E^a	R/r= 2.5	29	43	157	300	∞
E_c/E^a	R/r= 5	229	343	1250	2405	∞
E_c/E_a	R/r=10	1832	2749	10079	19242	∞

It is apparent that nearly any desired ratio of 2L and M_o is possible in concept. The asperities on the fault surface provide nearly all the high-frequency energy, while inhomogeneous relaxation of much lower average stress level can provide the long-period energy. The questions that arise are:

1—Why should one hypothesize total volume relaxation?, and

2—What are reasonable values of R (given a satisfactory answer to 1)?

The basis for a total-volume-relaxation hypothesis is founded on:

(a) The conclusion, based on intensity and 2L data, that all fault zones are similar and thus strongly conditioned and weakened.

(b) The suggestion in observations that dilatancy may occur in the Eastern United States, such dilatancy implying extensive fracturing and weakening of the volume surrounding the fault.

(c) The fact of high values of measured ambient stress in many Eastern United States rocks along with the fact of pervasive fracturing of rocks in the epicentral region of the New Madrid earthquake (Frank McKeown, oral commun., 1977).

This highly fractured mass may then relax partially or entirely with release of the fault surface (and may keep on relaxing for decades, as at Charleston?).

We suggest that the difference between the environments of earthquakes of the Western United States and Eastern United States is mostly the differences away from the fault zone, everything being "soft" in regions where k=1¾, while only the inclusions are "soft" where k=1. We must hypothesize that the relevant μ_1 is not that associated with propagation of shear waves through the inclusion but a μ_1 related to stress storage, that is, a pseudo-μ related to nonlinear deformation of a highly fractured mass.

An increase in M_o of probably no more than a factor of 100 is required to overcome the limitations of standard models for estimation of M_o. Thus, given a μ_1/μ_0 ratio of 0.1, only very limited volumes of total relaxation are required, or only partial relaxation in a larger volume is needed. The required dimensions do not seem to be denied by any available data.

A point that we address only qualitatively is that of the corner-frequency effects noted by investigators of Eastern United States earthquakes and the implication of these effects regarding 2L values within conventional models. We suggest that rapid fault breakage followed by a slower rate of relaxation in an appreciable volume of soft inclusion leads to a spectral shape uninterpretable by homogeneous models.

Some interesting relations are suggested. A major implication is that one should seek sites of potentially damaging Eastern United States earthquakes by seeking zones of low ambient stress. High stress implies high rigidity and little or no chance of fault failure. Low ambient stress and extensive fracturing, possibly associated with evidence of fluid movement from depth, should typify seismic zones in the Eastern United States.

Another interesting possibility is that high deformation associated with relaxation in a finite volume (radius of 1 to several kilometers) would provide the environment in which detectable small strains could be seen many kilometers from the epicenter. If an inclusion deformed premonitorily before an earthquake with small 2L, there should be concomitantly detectable deformation in the strong region surrounding the weak inclusion. Thus, there may be a mechanism for effecting measureable strains at distances inconceivable under a model based upon a homogeneous elastic model.

MAPS OF PREDICTED INTENSITY PATTERNS

As illustrations of the use of our programs for predicting expected intensity patterns for earthquakes anywhere in the conterminous U.S., we include several plates, all of which are in the pocket on the rear cover. Plate 2 consists of two maps:

Digitized geology of the United States (see table 3 for correlation of geologic and ground-condition units and table 4 for designated relative intensities for ground-condition units of plate 2) and the pattern of 4k values presently in our program.

Plate 3 consists of two maps:
Composite Predicted Intensities on Saturated Alluvium:

(1) San Francisco 2L = 400 km, k = 1¾, C = 25
(2) Wasatch fault 2L = 60 km, k = 1½, C = 25
(3) Cape Ann 2L = 10 km, k = 1¼, C = 40

Composite Predicted Intensities Corrected for Ground Condition:

(1) San Francisco 2L = 400 km, k = 1¾, C = 25
(2) Wasatch fault 2L = 60 km, k = 1½, C = 25
(3) Cape Ann 2L = 10 km, k = 1¼, C = 40

Plate 4 consists of two maps:
Composite Predicted Intensities on Saturated Alluvium:

(1) Charleston 2L = 15 km, k = 1¼, C = 40
(2) Owens Valley 2L = 60 km, k = 1½, C = 25

Composite Predicted Intensities Corrected for Ground Condition:

(1) Charleston 2L = 15 km, k = 1¼, C = 40
(2) Owens Valley 2L = 60 km, k = 1½, C = 25

Plate 5 consists of 2 maps:
Composite Predicted Intensities on Saturated Alluvium:

(1) New Madrid 2L = 20 km, k = 1¼, C = 40
or (2L = 5 km, k = 1, C = 40)
(2) Seattle 2L = 40 km, k = 1½, C = 65
(3) Fort Tejon 2L = 320 km, k = 1¾, C = 25

Composite Predicted Intensities Corrected for Ground Condition

(1) New Madrid 2L = 20 km, k = 1¼, C = 40
or (2L = 5 km, k = 1, C = 40)
(2) Seattle 2L = 40 km, k = 1½, C = 65
(3) Fort Tejon 2L = 320 km, k = 1¾, C = 25

We estimate that the earthquake models used to produce these maps represent almost the maximum credible earthquakes in each area.

It should be remembered that the grid size on the U.S. map is 25 km by 25 km. Therefore, nearly all river beds, that is, sites of saturated poor ground, will not constitute the dominant ground condition in hardly any grid element and will thus not be sensed on the maps corrected for ground condition. Those maps are useful, therefore, only for indicating intensities to be expected on bedrock.

The New Madrid earthquake was modeled as if it were in a region of k = 1¼ rather than one of k = 1. It was pointed out in Evernden (1975) that this earthquake can be modeled either way because only in the epicentral region (50 km) at most does k = 1¼.

The southwestward projection of intensity V on plate 3 for the Cape Ann earthquake results from calculational problems concerned with the grid size and proximity of the irregular boundary between k = 1 and k = 1¼ to the hypothetical epicenter. The implied pattern is probably erroneous.

For all k regions except k = 1¾, the program takes account of k boundaries and changes attenuation rates in accordance with plate 2. Adequate documentation to justify all details of plate 2 does not now exist.

The regional contrasts in length of break (energy release) and size of felt areas are apparent on all of the maps.

ESTIMATE OF DOLLAR LOSS FOR INDIVIDUAL POTENTIAL EARTHQUAKES

As a guide to relative risks associated with different faults and potential earthquakes on these faults, we have developed a simple program to estimate expected replacement value for wood-frame construction. We know of most of the inherent dangers in such estimates, but we believe that it is important to have the capability to make rapid estimates of relative potential damage from different potential earthquakes, even if the estimates are too large or too small by a factor of two.

The procedure followed closely parallels that used in Blume and others (1978). Because we have made some changes from their procedures and because their report is not in the hand of many potential readers of this report, we will briefly outline the technique. It has been implemented for cities in California, and it could be implemented for any region.

Data sets required:

(a) List of all California cities and unincorporated areas with populations of greater than 950 in 1977, including county, population, latitude and longitude, and ground condition;
(b) List of all ½′ by ½′ latitude and longitude points in California;
(c) Estimated dollar value of wood-frame construction in a city of 75,000 in California (1977)—$1.06 billion (population/75,000) (Blume and others, 1978);
(d) Table of percentage of damage (P) expected to wood-frame construction versus Rossi-Forel intensity (RFI), based on values given in Freeman (1932), Association of Bay Area Governments (1978), and Blume and others (1978);

(i)	if RFI < 5.9	P=0
(ii)	5.90 ≤ RFI < 6.00	P=(RFI−5.90)
(iii)	6.00 ≤ RFI < 6.80	P=(RFI−6.00)×0.25+0.1
(iv)	6.80 ≤ RFI < 7.40	P=(RFI−6.80)×50+0.3
(v)	7.40 ≤ RFI < 7.85	P=(RFI−7.40)×1.11+0.6
(vi)	7.85 ≤ RFI < 8.25	P=(RFI−7.85)×2.25+1.1
(vii)	8.25 ≤ RFI < 8.70	P=(RFI−8.25)×3.33+2.0
(viii)	8.70 ≤ RFI < 9.05	P=(RFI−8.70)×7.14+3.5
(ix)	9.05 ≤ RFI < 9.50	P=(RFI−9.05)×6.67+6.0
(x)	9.50 ≤ RFI < 10.00	P=(RFI−9.50)×6.00+9.0
(xi)	10.00 ≤ RFI	P=12;

(e) Parameters of each hypothesized earthquake – 2L and coordinates of points on fault, k value, and C value. We virtually ignore character of fault motion (see below).

For the time being, we assume that ground conditions at all sites are one intensity unit less than appropriate for saturated alluvium. Most communities are in alluviated valleys, and in most of these valleys, the water table is at least 10 m deep today. The program can use any or all of three specified ground-condition values. We now calculate and list loss estimates for J (saturated alluvium), J-1, and A (granite) for all sites. For this paper, we tabulate relative losses based on J-1.

The procedure of calculation is as follows (given earthquake parameters):

(a) For each community:
  i—calculate expected RFI (J, J-1, and A) by normal formulas;
  ii—calculate expected percentage of damage, P, to wood-frame construction (table under (d) above);
  iii—calculate expected replacement value for wood-frame construction for J, J-1, and A (population/75,000) × 1.06 × P; answer in billions of dollars.

(b) For each county:
  Sum expected replacement values for all communities in county.

(c) For state:
  Sum expected replacement value for all counties.

(d) For each ½° by ½° grid point and for center and ends of fault, calculate expected RFI (J, J-1, A) and expected percentage of damage.

The results of such calculations (through step c above) for several potential earthquakes are given in table 25. Figure 25 and table 25 show all fault breaks modeled for estimates of replacement value of damaged wood-frame construction. The numbers on figure 25 refer to equivalently numbered earthquakes in table 25.

Because the San Fernando earthquake is the only one for which we have relevant damage data, a few comments on the models used for that earthquake are in order. Most California earthquakes modeled would occur on vertical strike-slip faults. For these, we placed our line source along the surface trace and used a C value of 25, such a C value having been appropriate for such earthquakes by study of the 1906 San Francisco quake (Evernden and others, 1971). Within our simple model, radiation pattern as well as depth of focus are subsumed under a "best fit" C value.

For the San Fernando earthquake, we used a 2L of 19 km (appropriate for M 6.4), placed the epilocus of the hypothetical line source 6 km in the downdip direction from the surface trace of the fault (halfway between the surface trace and the epicenter), and applied C values of 25 and 20. A C value of 25 predicted intensities that were too low very near the fault (maximum predicted value on saturated alluvium of 8.6), while a C value of 20 gave satisfactory near-field intensities (9.2) but did not affect far-field values. Calculation of damage to wood-frame construction in southern California changed from $190 million with C=25 to $260 million with C=20, and most of this increase was, of course, in San Fernando and nearby parts of Los Angeles. Following Blume and others (1978), and using the data from the San Fernando earthquake as a basis, we doubled this figure to obtain an estimate of total replacement value and obtained values of $380 million and $520 million. These values are to be compared with the reported value of $498 million (Steinbrugge and Schader, 1973). Thus, both peak intensities and dollar damage suggest that a C value of 20 is more appropriate than one of 25 for this thrust-generated earthquake. Therefore, for the several thrust faults modeled, we placed the epilocus of the line source 6 km in the downdip direction from the surface trace of the fault and give the dollar-loss estimates relative to C values of 20 and 25. All strike-slip earthquakes are modeled with the epilocus along the surface trace and a C value of 25.

The first earthquake for which estimates are given in table 25 is for a repeat of the 1906 San Francisco earthquake on the San Andreas fault. Evernden and others (1971) showed the necessity of extending the 1906 break to Cape Mendocino in order to explain the observed isoseismals in northern California. The second earthquake of the table is for a fault break from Richmond to San Jose on the Hayward fault. The ground condition for all communities on the east side of San Francisco Bay is treated as J-1 but several of them include areas in which the water table is very near the surface. Dollar losses rise by a factor of three (R/F 8.5 to R/F 9.5 in most cases) if the J ground condition is used. However, the ground condition in parts of the East Bay may be J=1.5 or more, and intensities in areas east of Highway 101 on the San Francisco peninsula will probably be appropriate to the J ground condition (9.8–10). Losses there would be higher than assumed in the calculations. Thus, we consider it probably true that losses to wood-frame construction will be greater for a repeat of 1906 than for an M7 earthquake on the Hayward fault. The shorter hypothesized breaks shown for the Hayward fault represent the central part of the big break and a 30-km break opposite San Jose. Losses from the former are predicted to be twice as high as those from the San Fernando earthquake, while damage from the latter is predicted to

equal about half that caused by the San Fernando earthquake.

We disagree with estimates by Wesson and others (1975) that a potential M7+ earthquake might occur on the "Zayante fault," because the character of the mapped surface trace of that "fault" (fortuitous coalescing of short, apparently separate failure zones) seems to deny the possibility of a simultaneous break along all the features that they assumed to be part of it.

The 4-km Santa Barbara break is intended to simulate the recent earthquake (1972); the east end of the break was placed at the epicenter of the main shocks and the length was constrained to predict no greater than an M 5.4 quake. All losses are predicted to be in Santa Barbara County, and almost all the damage would be in Santa Barbara. The aftershock zone is more than 4 km long (Lee and others, 1978), and whether a 2L of more than 4 for the main earthquake is appropriate is unknown.

The 320-km break on the central San Andreas fault is for a repeat of Fort Tejon 1857. The predicted losses are well below those for the two large earthquakes in the San Francisco Bay area, yet this earthquake is commonly considered to pose the greatest threat of damage to southern California. As seen in table 25, our estimate of the replacement value of damaged structures is \$1.2 billion (2 × 0.61), a value in essential agreement with the \$1.3 billion estimated by Blume and others (1978). The high attenuation rates in southern California and the distance between the fault and the most heavily urbanized areas will lead to far lower losses than normally assumed (J-1 intensities predicted for the city of Los Angeles range from R/F 7.5 to 6.3 or M/M 6.8 to 5.7).

Table 25 clearly illustrates the existence of potential threats to southern California nearly as great or greater than that posed by the San Andreas fault. A break (13B of table 25) of 22 km (M 6.5) immediately north of the part of the Newport-Inglewood fault that broke in 1933 will cause losses comparable to those of an 1857 repeat (M 8.1), while a long break of 42 km (M 6.9) (13D of table 25) along the same fault is predicted to cause shaking damage 1⅔ times greater than a repeat of 1857. A 20-km break on the Whittier fault (M 6.4) will cause greater losses than did San Fernando and about half the losses to be expected from an 1857 repeat. Even a 31-km (M 6.7) break on the Malibu Coast fault will cause losses amounting to half as much

TABLE 25.—*Predicted replacement value of wood-frame construction (and all construction) damaged by potential earthquakes in California*

No.	Fault	2L	M	Lat[1] N	Long[1] W	Lat[2] N	Long[2] W	Predicted replacement value (J-1) Wood-frame construction	Total
1	San Andreas (1906)	400	8.3	36°51.00′	121°33.10′	40°15.90′	124°27.20′	$1.72B	$3.44B
2A	Hayward (1836?)	100	7.4	38°00.61′	122°22.92′	37°11.76′	121°44.62′	1.14	2.28
2B	Hayward	50	7.0	37°48.89′	122°13.73′	37°24.46′	121°54.58′	.54	1.08
2C	Hayward	20	6.4	37°27.53′	121°52.28′	37°11.76′	121°44.62′	.11	.22
3	Calaveras (1911)	11	6.1	37°09.10′	121°34.90′	37°14.20′	121°39.90′	.02	.04
4	Palo Colorado—San Gregorio	30	6.7	37°05.68′	122°18.31′	36°50.47′	122°10.47′	.04	.08
5	Zayante	15	6.3	37°02.43′	121°53.64′	36′56.55′	121°47.03′	.03	06
6	"Hosgri"	80	7.3	34°29.90′	120°54.50′	35°12.20′	121°05.90′	.01	.02
7	Hosgri (1927)	70	7.2	34°36.00′	120°38.80′	35°11.90′	120°54.50′	.02	.04
8	Nacimiento (1952)	20	6.4	35°44.20′	121°07.70′	35°52.10′	121°16.90′	<.001	----
9A	Santa Barbara (1925?)	40	6.9	34°28.20′	120°04.80′	34°25.70″	119°39.10′	.023	.046
9B	Santa Barbara (1925?)	29	6.7	34°27.70′	120°00.10′	34°25.90′	119°41.40′	.015	.030
10	Santa Barbara (1978?)	4	5.4	34°22.20′	119°43.00′	34°23.34′	119°45.44′	.003	.006
11	San Andreas (1957)	320	8.1	34°18.30′	117°31.50′	35°45.10′	120°17.80′	.61	1.22
12	Laguna Beach-New Clemente	40	6.9	33°34.05′	117°56.10′	33°18.65′	117°36.92′	.16	.32
13A	Newport-Inglewood	45	6.9	33°54.50′	118°17.40′	33°36.30′	117°58.80′	.90	1.80
13B	Newport-Inglewood	22	6.5	33°54.50′	118°17.40′	33°45.50′	118′08.10′	.53	1.06
13C	Newport-Inglewood (1933)	22	6.5	33°45.40′	118°08.10′	33°36.30′	117°58.80′	.33	.66
13D	Newport-Inglewood	42	6.9	34°02.69′	118°25.77′	33°45.50′	118°08.10′	1.05	2.10
14	Whittier	20	6.4	33°58.99′	118°00.00′	33°55.14′	117°47.80′	.35	.70
15	Raymond Hill	10(C=20) (C=25)	6.0	34°12.18′	118°01.95′	34°10.35′	118°07.80′	.26 .17	.52 .34
16A	Elsinore (south)	70	7.2	33°25.80′	117°00.00′	33°00.00′	116°27.00′	.04	.08
16B	Elsinore (north)	30	6.7	33°40.54′	117°22.93′	33°29.19′	117°09.27′	.03	.06
17	San Fernando (1972)	19(C=20) (C=25)	6.4	34°22.78′	118°30.31′	34°18.62′	118°16.55′	.26 .19	.52 .38
18A	San Jacinto	30	6.7	34°03.04′	117°11.80′	33°51.89′	117°02.44′	.06	.12
18B	San Jacinto	38	6.8	34°08.96′	117°16.76′	33°51.89′	117°02.44′	.09	.18
19	Malibu Coast	31(C=20) (C=25)	6.7	34°06.10′	118°56.44′	34°05.10′	118°33.17′	.38 .28	.76 .56
20	Santa Monica	32(C=20) (C=25)	6.7	34°06.10′	118°33.17′	34°10.01′	118°09.27′	1.14 .71	2.28 1.42
21A	Rose Canyon	51	7.0	32°53.11′	117°18.05′	32°30.41′	116°58.79′	.28 (J-1) .07 (J-2)	.56 (J-1) .14 (J-2)
21B	Rose Canyon	32	6.7	32°48.85′	117°14.44′	32°34.67′	117°02.40′	.23 (J-1) .06 (J-2)	.46 (J-1) .12 (J-2)

[1]Coordinates at one end of break.
[2]Coordinates at other end of break.

or more than the damage associated with an 1857 repeat. The greatest apparent threat in southern California, however, is the Santa Monica fault, for which we predict a total replacement value of \$1.5–2.3 billion ($2 \times (0.7–1.14)$) as the result of an M 6.7 (2L = 32 km) earthquake. However, this calculation illustrates the danger of calculating dollar loss without considering recurrence time. Evidence in hand, from marine terraces along the southern California coast and from geodetic measurements in the general region, indicates that significant displacements on the Santa Monica fault have been extremely rare in recent millenia and that the major active thrusts today are much farther north. Therefore, return times for an earthquake such as we have modeled may well be many hundreds to thousands of years. Combining a very long expected return time with an estimate of potential damage as high as we have calculated leads to a predicted annual loss that is very low.

Though the San Jacinto fault is the most active fault in southern California today, its location and the apparently limited size of earthquakes that occur on it render it a minimal regional threat, although it certainly is of great significance to San Bernardino and environs (18A and 18B). Because the earthquakes hypothesized for the San Jacinto fault are assumed to be related to breakage along the northern 30 or 39 km of the fault, even doubling of that length by extension southward would not greatly increase the predicted losses.

The two modeled breaks on the Elsinore fault are probably larger than expectable. The 70-km break on the Elsinore fault was hypothesized to be the greatest earthquake that can have impact on San Diego. Predicted replacement value of wood-frame construction from such an M 7.2 earthquake is only \$40 million. We did not know the appropriate dimensions to attach to a potential earthquake on the Rose Canyon fault. If a break of a few tens of kilometers can develop on this fault, damage in San Diego would greatly exceed \$40 million. Because San Diego is built largely on bedrock or marine terraces, and because reported intensities are frequently two units less than on saturated alluvium, we included replacement values of the earthquakes on the Rose Canyon fault (21A and 21B) for both J-1 and J-2.

Table 25 clearly indicates that the California earthquakes with comparatively short return times that will cause the greatest damage are maximum expectable earthquakes on the Hayward fault and the northern section of the San Andreas fault. A repeat of the San Francisco 1906 is predicted to cause damage for which the replacement value would be nearly three times that of a repeat of Fort Tejon 1857. Even a 50-km break on the central Hayward fault is predicted to cause losses comparable to those of a Fort Tejon repeat.

Although other fault breaks could have been modeled, the examples that we have cited illustrate that numerous possibilities exist for extensive damage from earthquakes in southern California. Our calculations indicate, however, that losses to wood-frame construction amounting to more than 5 times the damage caused by the San Fernando earthquake are not likely. An important point to keep in mind is that all damage estimates given above are based on damage due to shaking. Potential losses from dam failure and consequent inundation, rupturing of dikes, extensive fires, and other hazards are not included, nor are indirect costs resulting from disruption of a variety of services and industries.

MATHEMATICAL DETAILS OF MODEL FOR PREDICTING INTENSITIES

A long curved fault (k=1¾) is assumed to be a series of uniform point sources as closely spaced as desired. The formula used is

$$a = A \left[\frac{10^{11.8+1.5M}}{n}\right]^{1/\gamma} \left[\sum_{i=1}^{n} (R_i + C)^{-k\gamma}\right]^{1/\gamma} \quad (1)$$

(effectively, equation (7) of Evernden, Hibbard, and Schneider (1973) with $\gamma = 4$ and the coefficient of M = 0.864 rather than 0.80) and

$$I = 3(0.5 + \log a) \qquad \text{(Richter, 1958)} \quad (2)$$

where

a = "acceleration"

I = intensity (Rossi-Forel) = I(R/F)

M = local magnitude = $M_L \cong M_S$

n = number of equally spaced subevents used in the model to achieve nearly uniform release of energy along the fault break

$\epsilon = 10^{11.8+1.5M}$ = energy (ergs) released by earthquake of magnitude M (Richter, 1958, p. 366).

R_i = distance, in kilometers, from point i of n points on fault to point of observation

C = pseudo-depth term chosen so as to give proper near-range die-off of intensities. Intensity values beyond 50 to 100 km are nearly insensitive to variation in expected values of C for earthquakes in the United States.

k = term controlling rate of die-off of a ($a \propto \Delta^{-k}$) and thus effectively of I

γ = log [energy arriving at point]/a or a = [energy arriving at point]$^{1/\gamma}$

A = 0.779 = arbitrary leading coefficient selected so

as to give correct intensity values at a uniform ground condition for a particular earthquake. Once set for the normalizing earthquake, it cannot be changed. The value given above is set to give identical short-range I values as given by equation (7) of Evernden, Hibbard, and Schneider (1973) with $\gamma = 4$.

The points of the "fault" are distributed over a length (2L) appropriate to the M value (or an M value is used appropriate to the length of break 2L). See below.

When shorter faults in other regions are considered, equation (1) is slightly altered in order to simplify analysis and manipulation and to escape the multipoint aspect of energy release. Replace $(R_i + C)$ by $(R_i^2 + C^2)^{1/2}$ and convert equation (1) into an integral expression of uniform energy concentration along the break (using "energy concentration along the break" as a semantic device while recognizing that the source of energy is not the fault but the strained volume of rock).

$$a = 0.779 \left[\frac{10^{11.8+1.5M}}{2L} \int_{-L}^{+L} \frac{dl}{(R^2 + C^2)^{4k/2}} \right]^{1/4} \quad (3)$$

where definitions are as in the sketch below.

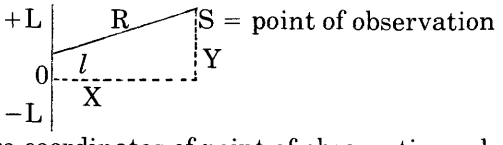

X, Y are coordinates of point of observation relative to the center of break with the Y axis oriented along the line of break.

$$R^2 = X^2 + (Y - l)^2$$

$$a = 0.779 \left[\frac{10^{11.8+1.5M}}{2L} \left(\frac{1}{(X^2 + C^2)^{(4k-1)/2}} \right) \int_{\theta_S}^{\theta_N} \cos^{4k-2}\theta \, d\theta \right]^{1/4} \quad (4)$$

where

$$\rho = (X^2 + C^2)^{1/2}, \quad \theta_N = \tan^{-1}\frac{Y + L}{\rho}, \quad \theta_S = \tan^{-1}\frac{Y - L}{\rho}$$

Now, we discuss the role of the various parameters in controlling predictions.

(a) *L and M.*—As equation (4) stands, L and M are entered as separate quantities. A one-unit change in M with no change in L results in a 1.1-unit change in I for $\gamma = 4$ or 0.8 for $\gamma = 6$, while a tenfold change in L with no change in M causes a 0.75-unit change in I($\gamma = 4$) or 0.50 ($\gamma = 6$) plus an effect from the integral, the influence of this term being dependent upon position.

As a matter of fact, it appears from empirical California data that there is a general correlation between L and M. In all that follows, M is eliminated from the equation by assuming an L, M relation of a form designed to agree approximately with California L, M data

$$2L = 10^{\alpha} \times \delta M$$

so that

$$2L = 10 \text{ km for } M = 6,$$

and

$$2L = 400 \text{ km for } M = 8.25$$

leading to

$$2L = 10^{0.711M - 3.2667}$$

$$M = (3.2667 + \log 2L)/0.711.$$

If

$$\epsilon_D = \frac{10^{11.8 + 1.5 M}}{2L} \text{ (ergs per kilometer of break),}$$

we obtain the results shown in table 26.

TABLE 26—*Magnitude (M) Relative to length of break (2L) and energy density (ϵ_D)*

[2]M	2L	logϵ_D	[2]M	2L	logϵ_D	[2]M	2L	logϵ_D
4	0.4	18.2	6	10	19.8	8	265	21.4
4½	0.9	18.6	6½	23	20.2	8¼	400	21.6
5	2	19.0	7	50	20.6	8½	600	21.8
5½	4.5	19.4	7½	116	21.0	9	1350	22.2

[1]Laws relating L and M are given in text.
[2]M, Local magnitude of California earthquakes.

(b) *The C parameter*—The C parameter plays the role of depth in calculations. Although C must have a definite relation to depth of focus, the exact value does not agree with depths expected from travel-time analysis. Influence of uncertainty in C on estimation of k values can be largely eliminated by considering I values observed at distances of 50 km or more from the epicenter. Observations indicate that C values less than 25 do not seem to be appropriate for large U.S. earthquakes, and values greater than 60 or so seem irrelevant. Failure to achieve agreement between C value and probable depth of focus may well arise from the fact that the dominant energy influencing intensity is in trapped modes, whereas amplitudes of such modes show a complicated relation to depth of focus.

Calculated intensity values from equations (4) and (2) (I values reduced by 1.05 for reasons to be described below) are given in table 27. It appears that uncertainty as to whether C should be 25 or 50 will cause confusion in the estimation of k by less than ¼ when using I data from 50 km. If the earthquakes used are large enough to give valid estimates of intensities to distances of more than 400 km, estimates of k can be based on intensity data from 100 km and more, thus eliminating any confusion in k estimates arising from uncertainties in C. If appropriate values of C are sug-

TABLE 27—*Influence of variations in L and C on predicted intensity values ($\gamma = 4$, $Y = 0$)*

k	L	C	Δ (km) 0	50	100	400	800
1¾	50	25	9.5	7.9	6.6	3.6	2.0
1¾	50	40	8.6	7.6	6.5	3.6	2.0
1¾	50	50	8.1	7.4	6.4	3.6	2.0
1½	50	25	10.6	9.3	8.1	5.5	4.2
1½	50	40	9.8	9.0	8.1	5.5	4.2
1½	50	50	9.4	8.8	8.0	5.5	4.2
1¾	10	25	8.8	7.0	5.6	2.5	0.9
1¾	10	40	7.7	6.7	5.5	2.5	0.9
1¾	10	50	7.2	6.4	5.4	2.5	0.9
1½	10	25	9.8	8.3	7.1	4.4	3.1
1½	10	40	7.9	8.0	7.0	4.4	3.1
1½	10	50	8.5	7.8	6.9	4.4	3.1

gested by other data, confusion is eliminated. Also, peak intensities and estimates of L from field observations place very severe limits on permissible k values. Therefore, uncertainties in C have no serious impact on estimates of k from moderate or larger earthquakes.

Table 27 shows that the behavior of intensity values at short ranges will lead to clear predictions of appropriate C values, subsequent to setting of k and L values.

(c) *k and* γ. Equation (4) would suggest that k and γ values might be strongly correlated. For a fixed k value, however, the γ value influences primarily the ϵ_D factor (a factor not a function of k) and has minimal effect on $(X^2 + C^2)^{(k\gamma-1)/2}$ for γ variation from 4 to 6 (the probable range requiring consideration); in addition the change in value of the integral is small for such changes in γ. Table 28 illustrates these points. The I values for k = 1½, γ = 6 are normalized to give the same I value at L = 200, Δ = 0 as for k = 1½, γ = 4. The (γ = 6, k = 1½) I values are between those of (γ = 4, K = 1½) and (γ = 4, k = 1½), and they yield a rate of decay with distance more similar to (γ = 4, k = 1¼) than (γ = 4, k = 1½). The actual predicted I values do not fall as rapidly with decreasing L for γ = 6 as for γ = 4. Study of U.S. intensity data as reported in Evernden (1975) has shown the appropriateness of using a γ value of 4.

(d) *Leading coefficient.*—This coefficient is completely arbitrary and can be set once for a given ground condition. The coefficient used will be considered as that appropriate for predicting I values on saturated alluvium, that is, the ground condition with the zero correction factor in Evernden, Hibbard, and Schneider (1973), and has been chosen to give the correct I values for the San Francisco earthquake of 1906.

(e) *Problem of energy to be summed for very long fault breaks.*—For long fault breaks such as the one produced by the San Francisco earthquake of 1906, a question can arise as to whether the integration in equation (4) should include energy from the entire length of the break or energy arising in a time window around the time of arrival from the nearest part of the fault. Since the intent is to have one formula that is applicable over the scale from long breaks to short ones, this factor should be considered. The mode of analysis is to set the time window, then calculate from it which part of the fault would produce arrivals at the point of observation within the time window (assuming velocity of break of 3.5 km/s and velocity of wave propagation of 3.5 km/s). The next problem is how to select the appropriate time window. One second is certainly too short, and 100 s seems certainly too long. The windows considered are ±5 and ±10 s around the time of arrival of the peak increment (from the nearest point of the break). Throughout the study, it is assumed that the phasing of arrivals is not critical because the general prevalence of earth inhomogeneities is adequate to confuse phasings. Because all intensity values reported for the San Francisco 1906 earthquake were shown by Evernden, Hibbard, and Schneider (1973) to be explainable on the basis of short-period data, this assumption does seem appropriate.

TABLE 28—*Influence of variations in γ and k on predicted intensity values ($C = 25$, $Y = 0$)*

L	γ	k	Δ (km) 0	100	400	800	δI^{100} 800
200	4	1½	11.1	8.8	6.4	5.1	3.7
	6	1½	11.1	9.0	6.8	5.6	3.3
	4	1¼	12.2	10.4	8.4	7.3	3.0
10	4	1½	9.8	7.2	4.4	3.1	4.1
	6	1½	10.3	7.9	5.5	4.3	3.6
	4	1¼	10.9	8.6	6.4	5.3	3.4
1	4	1½	8.3	5.6	2.9	1.5	4.1
	6	1½	9.3	6.8	4.4	3.2	3.6
	4	1¼	9.3	7.1	5.0	3.7	3.4

Table 29A gives predicted I values for I_T (total energy independent of window length), I_5 and I_{10} (energy in time window ±5 and ±10 s around peak arrival) for the San Francisco 1906 event. It is seen that $I_5(7)$ and $I_{10}(7)$ ($I_5(7)^{NORM}$ and $I_{10}(7)^{NORM}$ also) are indistinguishable. $I_5(7)$ and $I_5(8)$ are I values for kγ of 4 × 1.75 and 4 × 2.0, respectively. The superscript NORM signifies I values normalized to give $I_T(8)$ at an epicentral distance of zero. $I_5(7)$ has essentially the same rate of decay with Δ as does $I_T(8)$. The formula for $I_T(8)$ is the exact one used for the San Francisco 1906 event by Evernden, Hibbard, and Schneider (1973). The Δ versus I data for the same earthquake (Y = 0) are as in table 30.

Thus, the I (observed), $I_T(8)$, and $I_{5/10}(7)^{NORM}$ are nearly indistinguishable. Therefore, the rule of using windows 5 to 10 s on either side of peak arrival will be followed. This means that the k factor for the West Coast will be 1¾ instead of 2 as used in Evernden, Hibbard, and Schneider (1973). Data for other smaller California earthquakes where the time-window correction is not required support this change in k value. Since the fundamental setting of equation parameters

TABLE 29.—*Effect of length of time window on predicted intensity*

[Fault Breaks From Center: $V_{FB} = V_S = 3.5$ km/sec]

(A) L = 200, C = 25, Y = 0 (San Francisco, 1906)

X	$I_5(7)$	$I_{10}(7)$	$I_T(8)$	$I_5(7)^{NORM}$	$I_{10}(7)^{NORM}$	$I_5(8)$
0	11.0	11.1	10.0	10.0	10.0	9.9
45	9.5	9.6	8.4	8.5	8.5	8.2
100	7.9	8.2	6.8	6.9	7.1	6.5
200	6.4	6.6	5.2	5.4	5.5	4.7
400	4.8	5.1	3.6	3.8	4.0	2.9
800	3.2	3.4	1.8	2.2	2.3	1.1

(B) L = 30, C = 25; I(6) = I(γ = 4, k = 1½)

Case I, Y = 0			Case III			
X	$I_5(6)$	$I_I(6)$	Y	X	$I_5(6)$	$I_I(6)$
0	10.3	10.4	25	25	9.7	9.7
100	7.7	7.9	50	50	8.6	8.6
800	3.7	3.9	100	100	7.3	7.3
			400	400	4.5	4.6

Case II, X = 0; Y, Variable;
$I_5(6) = I_I(6)$.

Key: V_{FB} = velocity of fault break, V_S = velocity of shear waves. $I_5(7)$ = I based on energy arriving ±5 sec re peak arrival (γ = 4, k = 1¾). $I_{10}(7)$ = I based on energy arriving ±10 secs re peak arrival (γ = 4, k = 1¾). $I_5(8)$ = I based on energy arriving ±5 secs re peak arrival (γ = 4, k = 2). $I_5(8)$ = I based on total calculated energy (γ = 4, k = 2). $I_5(7)^{NORM} = I_5(7)$ normalized to give I at Δ = 0 equal to $I_T(8)$. $I_{10}(7)^{NORM} = I_{10}(7)^5$ normalized to give I at Δ = 0 equal to $I_T(8)$.

TABLE 30.—*Observed and predicted intensity values for San Francisco earthquake of 1906*

Δ (km)	0	75	110	160	230	350	500
I(obs)	10	8	7	6	5	4	3
$I_T(8)$	10	7.6	6.7	5.8	5.0	4.0	3.2
$I_5(7)^{NORM}$	10	7.7	6.9	6.0	5.2	4.2	3.4

is accomplished by use of the 1906 San Francisco earthquake, the leading coefficient of equation (4) is changed so that predicted I values are reduced by 1.05 (average difference between (I_5, I_{10}) and (I_5^{NORM}, I_{10}^{NORM}), so the final operative equation is

$$a = 10^{4.29}\left[\frac{L^{1.11}}{(X^2 + C^2)^{(4k-1)/2}}\int_{\theta_S}^{\Theta_N}\cos^{4k-2}\theta d\theta\right]^{1/4} \quad (5)$$

where γ will be set at 4 and k will take values dictated by patterns of isoseismals. It can be shown that, for fault lengths of 60 km or less, I_T can be considered as equivalent to $I_{5/10}$.

Note that the leading coefficients in equations 3, 4, and 5 have been changed from those in Evernden (1975). The values in the earlier paper are incorrect.

DETAILS OF ROSSI-FOREL AND MODIFIED MERCALLI INTENSITY SCALES

ROSSI-FOREL

I. Microseismic shock.—Recorded by a single seismograph or by seismographs of the same model, but not by several seismographs of different kinds; the shock felt by an experienced observer.

II. Extremely feeble shock.—Recorded by several seismographs of different kinds; felt by a small number of persons at rest.

III. Very feeble shock.—Felt by several persons at rest; strong enough for the direction or duration to be appreciable.

IV. Feeble shock.—Felt by persons in motion; disturbance of movable objects, doors, windows; cracking of ceilings.

V. Shock of moderate intensity.—Felt generally by everyone; disturbance of furniture, beds, etc., ringing of some bells.

VI. Fairly strong shock.—General awakening of those asleep; general ringing of bells; oscillation of chandeliers; stopping of clocks; visible agitation of trees and shrubs; some startled persons leaving their dwellings.

VII Strong shock.—Overthrow of movable objects; fall of plaster; ringing of church bells; general panic, without damage to buildings.

VIII. Very strong shock.—Fall of chimneys; cracks in the walls of buildings.

IX. Extremely strong shock.—Partial or total destruction of some buildings.

X. Shock of extreme intensity.—Great disaster; ruins; disturbance of the strata, fissures in the ground; rock falls from mountains.

MODIFIED MERCALLI (ABRIDGED)

I. Not felt except by a very few under especially favorable circumstances. (I Rossi-Forel scale)

II. Felt only by a few persons at rest, especially on upper floors of buildings. Delicately suspended objects may swing. (I to II Rossi-Forel scale.)

III. Felt quite noticeably indoors, especially on upper floors of buildings, but many people do not recognize it as an earthquake. Standing motor cars may rock slightly. Vibration like passing of truck. Duration estimated. (III Rossi-Forel scale.)

IV. During the day felt indoors by many, outdoors by few. At night some awakened. Dishes, windows, doors disturbed; walls make cracking sound. Sensation like heavy truck striking building. Standing motor cars rocked noticeably. (IV to V Rossi-Forel scale.)

V. Felt by nearly everyone; many awakened. Some dishes, windows, etc., broken; a few instances of cracked plaster; unstable objects overturned. Disturbance of trees, poles, and other tall objects sometimes noticed. Pendulum clocks may stop. (V to VI Rossi-Forel scale.)

VI. Felt by all; many frightened and run outdoors. Some heavy furniture moved; a few instances of fallen plaster or damaged chimneys. Damage slight. (VI to VII Rossi-Forel scale.)

VII. Everybody runs outdoors. Damage negligible in buildings of good design and construction; slight to moderate in well-built ordinary structures; considerable in poorly built or badly designed structures; some chimneys broken. Noticed by persons driving motor cars. (VIII– Rossi-Forel scale.)

VIII. Damage slight in specially designed structures; considerable in ordinary substantial buildings with partial collapse; great in poorly built structures. Panel walls thrown out of frame structures. Fall of chimneys, factory stacks, columns, monuments, walls. Heavy furniture overturned. Disturbs persons driving motor cars. (VIII+ to IX– Rossi-Forel scale.)

IX. Damage considerable in specially designed structures; well-designed frame structures thrown out of plumb; great in substantial buildings, with partial collapse. Buildings shifted off foundations. Ground cracked conspicuously. Underground pipes broken. (IX+ Rossi-Forel scale.)

X. Some well-built wooden structures destroyed; most masonry and frame structures destroyed with foundations; ground badly cracked. Rails bent. Landslides considerable from river banks and steep slopes. Shifted sand and mud. Water splashed (slopped) over banks. (X Rossi-Forel scale.)

XI. Few, if any (masonry) structures remain standing. Bridges destroyed. Broad fissures in ground. Underground pipe lines completely out of service. Earth slumps and land slips in soft ground. Rails bent greatly.

XII. Damage total. Waves seen on ground surfaces. Lines of sight and level distorted. Objects thrown upward into the air.

REFERENCES CITED

ABAG, 1978, Earthquake intensity and expected cost in the San Francisco Bay Area: Association of Bay Area Governments, Hotel Claremont, Berkeley, Calif.

Agnew, A. C., and Sieh, K. E., 1978, A documentary study of the felt effects of the great California earthquake of 1857: Seismological Society of America Bulletin, v. 68, p. 1717–1729.

Algermissen, S. T., 1973, A study of earthquake losses in the Los Angeles, California area: Department of Commerce, Washington, D. C.

Arabasz, W. J., Richins, W. D., Langer, C. J., 1981. The Idaho-Utah border (Pocatello Valley) earthquake sequence of March-April, 1975: in press.

Benioff, N., 1938, The determination of the extent of faulting with application to the Long Beach earthquake: Seismological Society of America Bulletin, v. 28, p. 77–84.

Blume, J. A., Scholl, R. E., Somerville, M. R., and Honda, K. R., 1978, Damage prediction of an earthquake in southern California: Final Technical Report Contract No. 14-08-0001-15889, U. S. Geological Survey.

Bolt, B. A., and Miller, R. D., 1975, Catalogue of earthquakes in northern California and adjacent areas; 1 January 1910–31 December 1972: Seismographic Stations, University of California, Berkeley, California, 567 p.

Borcherdt, R. D., 1970, Effects of local geology on ground motion near San Francisco Bay: Seismological Society of America Bulletin, v. 60, 29–61.

Byerly, P., 1925, Notes on the intensity of the Santa Barbara earthquake between Santa Barbara and San Luis Obispo: Seismological Society of America Bulletin, v. 15, p. 279–281.

———1930, The California earthquake of November 4, 1927: Seismological Society of America Bulletin, v. 20, p. 53–56.

Coffman, J. L., and von Hake, C. A., Earthquake history of the United States: Publication 41–1, Revised Edition (through 1970), NOAA, Washington, D.C.

Eshelby, J. D., 1957, The determination of the elastic field of an ellipsoidal inclusion and related problems: Proceedings of Royal Society, London, ser. A, p. 241, 376–396.

Evernden, J. F., 1969, Magnitude estimates at regional and near-regional distances in the United States: Seismological Society of America Bulletin, v. 59, p. 591–639.

———1975, Seismic intensities, "size" of earthquakes, and related phenomena: Seismological Society of America Bulletin, v. 65, p. 1287–1315.

———1976, A reply: Seismological Society of America Bulletin, v. 66, p. 339–340.

———1977, Adequacy of routinely available data for identifying earthquakes of m_b 4.5: Seismological Society of America Bulletin, v. 67, p. 1099–1151.

Evernden, J. F., and Clark, D., 1969, Study of Teleseismic P, Part II: Physics of Earth and Planetary Interiors, v. 4, p. 24–31.

Evernden, J. F., and Filson, J., 1971, Regional dependence of surface-wave versus body-wave magnitudes: Journal of Geophysical Research, v. 76, p. 3303–3308.

Evernden, J. F., Hibbard, R. R., and Schneider, J. F., 1973, Interpretation of seismic intensity data: Seismological Society of America Bulletin, v. 63, p. 399–422.

Freeman, J. R., 1932, Earthquake damage and earthquake insurance: New York, McGraw-Hill, 904 p.

Gawthrop, W., 1978, The 1927 Lompoc, California earthquake: Seismological Society of America Bulletin, v. 68, p. 1705–1716.

Hanks, T. C., 1979, The Lompoc, California earthquake (November 4, 1927; M = 7.3) and its aftershocks: Seismological Society of America Bulletin, v. 69, p. 451–462.

Hanks, T. C., Hileman, J. A., and Thatcher, W., 1975, Seismic moments of the larger earthquakes of the southern California region: Geological Society of America Bulletin, v. 86, p. 1131–1139.

Hanks, T. C., and Thatcher, W., 1972, A graphical representation of seismic source parameters: Journal of Geophysical Research, v. 77, no. 23 p. 4393–4405.

Herrmann, R. B., Cheng, S., and Nuttli, O. W., 1978, Archeoseismology applied to the New Madrid earthquakes of 1811–12: Seismological Society of America Bulletin, v. 68, p. 1751–1759.

Heyl, A. V., and McKeown, F. A., 1978, Preliminary seismotectonic map of the central Mississippi valley and environs: U.S. Geological Survey miscellaneous field studies, map MF–1011, scale 1:150,000.

Hildenbrand, T. G., Kane, M. F., and Stauder, W., 1977, Magnetic and gravity anomalies in the northern Mississippi embayment and their spacial relation to seismicity: U.S. Geological Survey miscellaneous field map studies, map MF–914, scale 1:1,000,000 (1978).

Hileman, J. A., Allen, C. R., and Nordquist, J. M., 1973, Seismicity of the southern California region: California Institute of Seismol-

ogy, Pasadena, California.
Jackson, E. L., Public response to earthquake hazard: California Geology, v. 30, no. 12, p. 278–280.
Lawson, A. C., 1908, Report of the State earthquake investigation commission upon the California earthquake of April 18, 1906: Carnegie Institute of Washington, no. 87, 2 vols.
Lee, W. H. K., Johnson, C. E., Henyey, T. L., Yerkes, R. F., 1978, A preliminary study of the Santa Barbara earthquakes of August 13, 1978 and its major aftershocks: U.S. Geological Survey Circular, 11 p. (1979).
Lindh, A., and Boore, D. M., 1981, Parkfield revisited: Seismological Society of America Bulletin.
McAdie, A. G., 1911, San Francisco, *in* Notes on the California earthquake of July 1, 1911: Seismological Society of America Bulletin, v. 1, no. 3, p. 112.
McKeown, F. A., 1978, Hypothesis: many earthquakes in the central and southeastern United States are causally related to mafic intrusive bodies: Journal of Research of the U.S. Geological Survey, #6, no. 1, Jan.–Feb., p. 41–50.
Medvedev, S. V., 1961, Determination of earthquake intensities, Chap. 4, Earthquakes in the U.S.S.R.: Moscow, Academia Nauk Press, (in Russian).
———1962, Engineering Seismology: Moscow, Academia Nauk Press, translated into English by Israel Program for Scientific Translations, Jerusalem 1965, 260 p.
———1968, The international scale of seismic intensity, Chapt. 9 in Seismic zoning of the U.S.S.R.: Moscow, Academy of Sciences, available in translation from Department of Commerce, National Technical Information Services, Springfield.
Milne, W. G., 1977, Seismic risk maps for Canada: Proceedings VI World Conference of Earthquake Engineering, New Delhi, v. 1, 930 p.
Milne, W. G., and Davenport, A. G., 1969, Distribution of earthquake risk in Canada: Seismological Society of America Bulletin, v. 59, no. 2, p. 729–754.
Mitchell, G. D., 1928, The Santa Cruz earthquakes of October, 1926: Seismological Society of America Bulletin, v. 18, p. 152–213.
Murphy, L. M., and Cloud, W. K., 1954, United States earthquakes—1952: Washington D. C., U.S. Coast and Geodetic Survey, ser. 773.
Murphy, L. M., and Ulrich, F. P., 1951, United States earthquakes—1949: Washington D.C., U.S. Coast and Geodetic Survey, ser. 748.
Neumann, F., 1931, United States earthquakes—1929: Washington D. C., U.S. Coast and Geodetic Survey, ser. 553.
———1935, United States earthquakes—1933: Washington D. C., U.S. Coast and Geodetic Survey, ser. 579.
Nuttli, O. W., 1951, The western Washington earthquake of April 13, 1949: Seismological Society of America Bulletin, v. 41, p. 21–28.
Richter, C. F., 1955, Foreshocks and aftershocks, Bulletin 171 (Earthquakes in Kern County California during 1952): Part II, Division of Mines, State of California, p. 177–197.
Steinbrugge, K. V., and Schader, E. E., 1973, Earthquake damage and related statistics; San Fernando, California, earthquake of February 9, 1971: Washington D. C., U.S. Department of Commerce, v. 1, part B, p. 691–724.
Templeton, E. C., 1911, The central California earthquake of July 1, 1911: Seismological Society of America Bulletin, v. 1, p. 167–169.
U.S. Department of Commerce, 1968, United States earthquakes 1928–1935, U.S. Government Printing Office, Washington, D.C. 20402, variously paged.
Wesson, R. L., Helley, E. J., Lajoie, K. R., and Wentworth, C. M., 1975, Faults and future earthquakes: *in* Borcherdt, R. D., Studies for seismic zonation of the San Francisco Bay Region: U. S. Geological Survey Professional Paper 941–A, p. A5–A30.
Wood, N. O., 1911, On the region of origin of the central California earthquakes of July, August, and September, 1911: Seismological Society of America Bulletin, v. 2, p. 31–39.
———1933, Preliminary report on the Long Beach earthquake (California), Seismological Society of America Bulletin: v. 23, p. 43–56.

GPO 792-179/1001